CHEMICAL REVIEWS

pubs.acs.org/CR Review

Iontronic Devices from Biological Nanopores to Artificial Systems: Emerging Applications and Future Perspectives

Published as part of Chemical Reviews special issue "Sequencing and Nanopore Technologies".

Jiabei Luo,[‡] Antoine Remy,[‡] and Yujia Zhang*

Cite This: *Chem. Rev.* 2025, 125, 11840−11877 Read Online

ABSTRACT: Inspired by the ion transport mechanisms in biological systems, ionic technologies have emerged as a transformative field that bridges biology and electronics. Unlike electrons, ions not only transmit electrical signals but also convey chemical information and exhibit ion-specific transport behaviors. At the center of iontronic devices lie ion channels, highly selective and efficient structures that control ion transport. These ion channels, whether biological nanopores or artificial nanofluidic channels, fundamentally determine the properties of the devices. Therefore, understanding, engineering, and integrating versatile ion channels into artificial systems are critical to advancing the field. This Review provides a comprehensive overview of iontronic devices and systems, mainly covering advances after 2010, beginning with the principles of ion transport in both biological and artificial ion channels. We then examine fabrications and characterizations, with a focus on how material and structural design influence ionic properties. Device architectures are summarized and compared across multiple dimensions and scales. We highlight emerging applications in bioiontronics, neuromorphic computing, energy harvesting, water treatments, and environmental sustainability. Despite significant advancements, we propose that challenges remain in achieving the desired ion selectivity, efficient ionic signal transduction, and seamless integration of iontronics with electronics and biology.

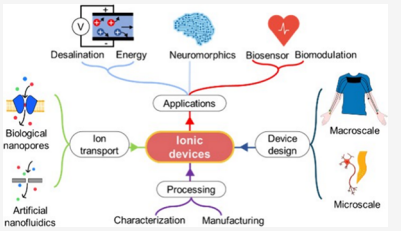

CONTENTS

Received: July 9, 2025
Revised: November 15, 2025
Accepted: November 18, 2025
Published: December 1, 2025

https://doi.org/10.1021/acs.chemrev.5c00579
Chem. Rev. 2025, 125, 11840−11877

1. INTRODUCTION

In recent decades, electronics have emerged as the cornerstone of modern technology, fundamentally transforming fields such as computation,[1−4] sensing,[5−7] communication,[8−10] and healthcare.[11−13] Driven by continuous advancements in semiconductor technologies, electronics have enabled the development of increasingly compact, powerful, and intelligent devices.[14−18] These innovations have not only shaped the digital world but have also laid the foundation for complex systems that power our everyday lives. However, despite these remarkable achievements, conventional electronics face inherent limitations in mimicking the complex functionalities of biological systems.[19−22] One of the fundamental challenges lies in the binary nature of electronic signals, which contrasts with the continuous, dynamic, and analogue ionic signals in living organisms.[23−27] Additionally, deficient biocompatibility, low energy efficiency, and the inability to operate in soft, hydrated environments hinder the integration of conventional electronics with biological systems.[28−32] As our technological aspirations move toward more biointegrated and adaptive systems,[33−35] it becomes crucial to explore new paradigms that seamlessly bridge the gap between electronic circuits and the delicate, fluid nature of biological environments.[36−39]

In this context, iontronic devices have emerged as a promising solution, offering a fundamentally different approach by using ions as charge carriers rather than electrons.[40−44] In biology, ions are fundamental to a wide range of physiological processes, from neural signals and synaptic plasticity to metabolic energy conversion.[45−49] The adoption of ions is closely associated with biological evolution, resulting in intelligent, energy-efficient, and adaptive control.[50−53] Inspired by these natural processes, iontronic devices leverage the principles of ion transport to develop technologies with enhanced biocompatibility, energy efficiency, and dynamic responsiveness.[54−59] By shifting the focus from electrons to ions, iontronic devices represent not just a technical modification but a fundamental paradigm shift. This transition opens up new possibilities for creating devices that could more naturally integrate with biological systems, moving beyond the limitations of conventional electronics and paving the way for next-generation biointegrated technologies.[60−65]

In the early 1970s, the term "ionic device" began to be used to broadly describe systems that incorporate ions as signal carriers for communication, storage, or output. However, with the rapid development of the field and its diversifying applications, attention has shifted toward devices designed to actively control ion transport in response to external stimuli, including ion-electron coupling, chemical gradients, light, and mechanical gating. In this context, the term "iontronic device" has become more precise, as it reflects both the active regulation of ion dynamics and their integration with other systems for various applications. While some ionic devices may exhibit ion transport behaviors, iontronic devices are specifically engineered to harness such transport for functional outcomes. For instance, nanofluidic iontronic transistors based on carbon nanotubes can actively regulate ion movement through voltage gating, a result of the ion-electron coupling effect.[66] Another example is an ultrathin solid-state iontronic power source that harnesses ion-electron coupling in graphene oxide nanochannels for energy applications.[67] In comparison, an example of an ionic device is conventional ionic conductive electrodes for recording electrophysiological signals, which involve ion movements at biointerfaces to transduce biological activities but lack mechanisms for actively differentiating different ions. Resistive ionic sensors are typically classified as ionic devices, as their resistance changes result from alterations in ion-conductive pathways under mechanical deformation. Nevertheless, under certain conditions, mechanical strain can induce ion convection or modulate electrical double layers (EDLs) at ionic−electronic interfaces, showing an active control of ion transport. Therefore, the classification of "ionic device" or "iontronic device" should require a case-by-case consideration based on their working principles. Through these examples, we propose a distinctive use of "ionic device" and "iontronic device" to clarify the general understanding of iontronic technology.[68] We expect it to be refined into precise technical definitions by professional societies and regulatory agencies according to the needs and perspectives of their stakeholders.

1.1. Review Briefing

The Review examines the development path and future application prospects of iontronic devices, with a primary focus on progress over the past 15 years and the transition from natural biological nanopores to artificial iontronic systems. The Review begins by introducing the fundamental concepts and research significance of iontronic devices, emphasizing that the core of this field lies in the precise regulation of ion transport processes. It highlights that the development of iontronic devices not only addresses fundamental scientific questions but also has significant implications for breakthroughs in various cutting-edge interdisciplinary fields, including energy, information processing, and biomedical technologies. The Review then delves into the role of biological nanopores in regulating ion transport, focusing on the structural characteristics and functional differences among natural protein nanopores, modified protein nanopores, and peptide nanopores. It also selects representative iontronic devices based on these different biological nanopores to illustrate their similarities and differences. Chapter 2 showcases the inherent molecular recognition and channel regulation capabilities of biological nanopores and provides bioinspired insights for the design of subsequent artificial systems. Following this, the Review shifts its focus to the advancements in artificial iontronic systems. Chapter 3 covers the development of solid-state nanofluidic channels, macroscale iontronic devices and systems, and miniaturized iontronic devices, including microscale dropletronics, fibers, and thin films. This comprehensive coverage illustrates how engineering design at various scales can replicate and even surpass biological systems, enabling a wide range of device functionalities and controllability. The Review then compares biological nanopores and artificial systems in Chapter 4, summarizing the natural advantages of biological nanopores, such as selectivity and sensitivity, while also highlighting the advancements of artificial systems, in terms of structural stability, manufacturability, and integration capabilities. Moreover, it discusses the standard fabrication methods and measurement techniques applicable to both systems, thereby establishing a theoretical and technical foundation for constructing biological-artificial hybrid iontronic devices.

https://doi.org/10.1021/acs.chemrev.5c00579
Chem. Rev. 2025, 125, 11840−11877

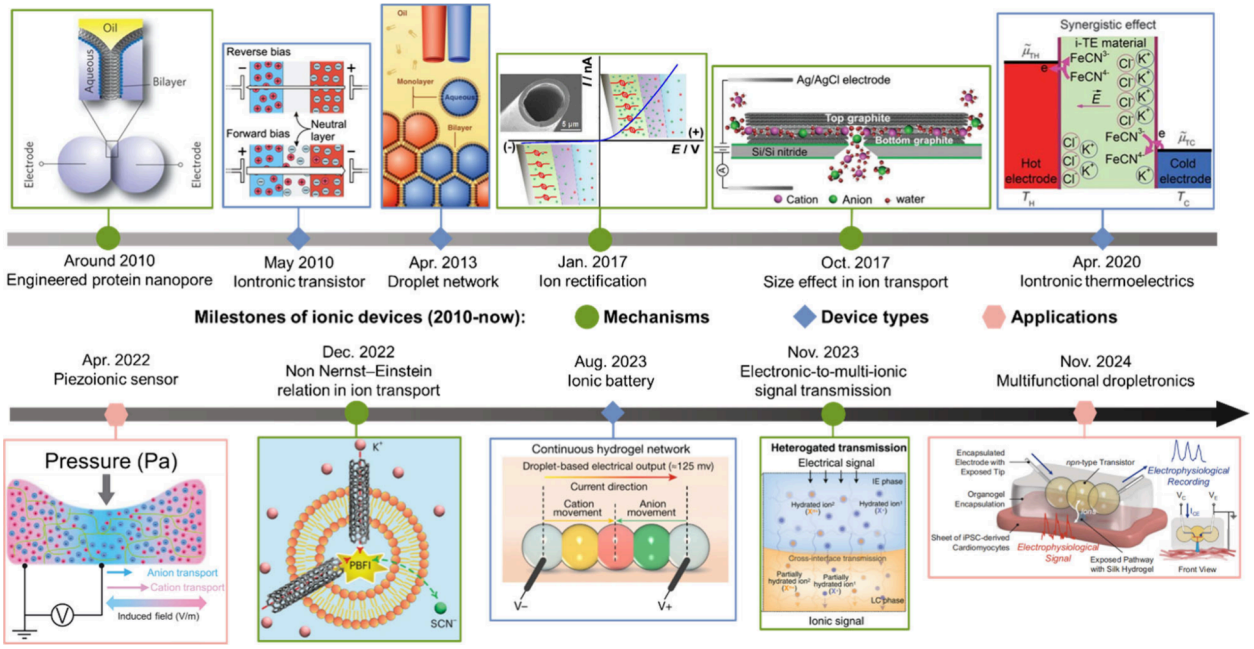

Figure 1. Milestones of iontronic devices in the last 15 years. The journey began around 2010 with protein pore exhibiting diode-like behaviors.[69] In 2010, iontronic transistors enabled gate-controlled ion movements.[74] In 2013, droplet networks incorporating membrane proteins opened pathways to complex iontronic circuits.[75] In January 2017, polyimidazolium-modified micropipettes were proposed to allow for micrometer-scale ion current rectification.[70] In October 2017, angstrom-scale slits revealed steric effects and ion selectivity beyond hydrated diameters.[71] In 2020, iontronic thermoelectrics was developed to harvest energy from room-temperature gradients.[76] In April 2022, structured piezoionic hydrogels enabled self-powered artificial nerves for pressure sensing and neuromodulation.[78] In December 2022, single-file water chains in carbon nanotube porins were found to disrupt the Nernst−Einstein relation via ion−water cluster transport.[72] In August 2023, lipid-supported hydrogel droplet networks enabled the development of microscale iontronic power sources for neuromodulation.[77] In November 2023, cascade-heterogated biphasic gels enabled the selective transmission of multi-ionic signals at biointerfaces.[73] In 2024, surfactant-assisted hydrogel droplets were assembled into modular iontronic circuits with biointerface capabilities, marking a new era of multifunctional, miniaturized iontronics.[79] Reproduced with permission from ref 69. Copyright 2009 Springer Nature. Reproduced with permission from ref 74. Copyright 2010 United States National Academy of Sciences. Reproduced with permission from ref 75. Copyright 2013 American Association for the Advancement of Science. Reproduced from ref 70. Copyright 2017 American Chemical Society. Reproduced with permission from ref 71. Copyright 2017 American Association for the Advancement of Science. Reproduced with permission from ref 76. Copyright 2020 American Association for the Advancement of Science. Reproduced with permission from ref 78. Copyright 2022 American Association for the Advancement of Science. Reproduced with permission from ref 72. Copyright 2022 Springer Nature. Reproduced from ref 77. Available under a CC-BY 4.0 license. Copyright 2023 Springer Nature. Reproduced with permission from ref 73. Copyright 2023 American Association for the Advancement of Science. Reproduced with permission from ref 79. Copyright 2024 American Association for the Advancement of Science.

Next, the Review concentrates on the diverse emerging applications of iontronics in Chapter 5, including implantable or wearable biomedical devices compatible with biological interfaces (biointerfaces), neuromorphic computing systems that mimic synaptic functions, energy harvesting and storage devices, and water treatment platforms for desalination and water purification. These applications highlight the huge potential of iontronic devices. In Chapter 6, the Review concludes by summarizing the current achievements and discussing the challenges and future directions in the field. The authors emphasize that achieving more efficient and controllable iontronic devices requires continuous breakthroughs in material innovation, interface engineering, and system integration. A particular focus is placed on promoting the fusion of biological and artificial systems to develop new "abiotic−biotic" iontronic interfaces (termed bioiontronics), which are seen as a critical direction for future progress. Overall, the Review covers the theoretical foundations and practical advancements of iontronic devices, highlighting the importance of interdisciplinary integration. We aim to provide readers with a comprehensive and forward-looking view of the promising future of iontronic devices.

1.2. A Brief Chronology of the Evolution of Iontronic Devices: The 2010s to Present

While this Review mainly focuses on the developments over the last 15 years, earlier studies of nanopores in solid substrates laid critical groundwork for recent advances in iontronic devices. For example, a synthetic conical nanopore was shown to produce different ion currents depending on the direction of concentration gradients, due to the nanopore's shape and surface charge.[69] In another case, DNA-modified nanopores were able to mimic biological gating by closing at low pH and reopening under voltage control.[70]

From 2010, iontronic devices have evolved from a limited research area into a multidisciplinary field that bridges electronics, nanofluidics, and bioinspired systems. This evolution has been marked by significant milestones in mechanisms, devices, and applications (Figure 1).

Fundamental discoveries in ion transport have driven new mechanisms. The journey began around 2010 with the engineering of protein nanopores that showed diode-like properties, laying the foundation for droplet-based iontronic devices, termed dropletronics.[69] The discovery of ionic current rectification in symmetric electrolyte solution in 2017 further

https://doi.org/10.1021/acs.chemrev.5c00579
Chem. Rev. 2025, 125, 11840−11877

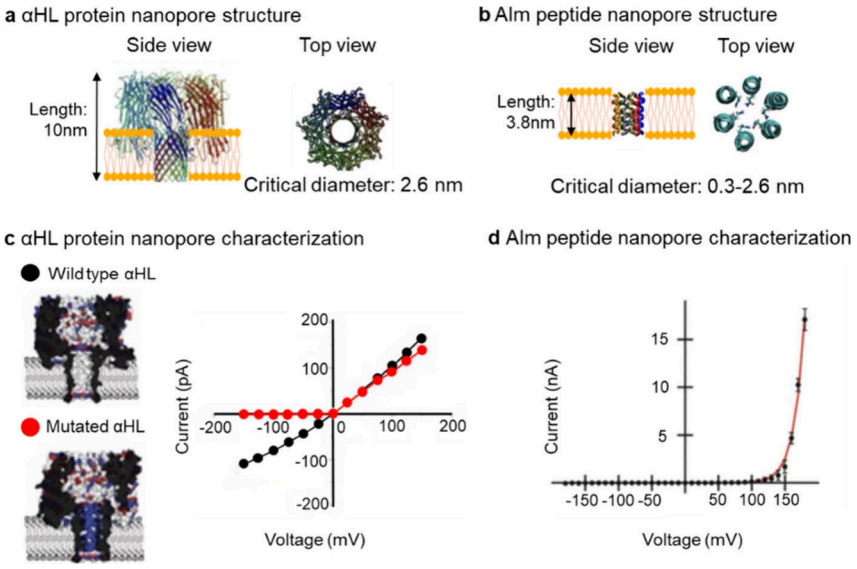

Figure 2. Comparison between protein and peptide nanopores. (a and b) Structural representation of two biological nanopores: the protein nanopore αHL and the peptide nanopore Alm. Lipid bilayers that embed the nanopores are shown in yellow. (a) Side (left) and top (right) views of αHL highlighting its total length of ∼10 nm and critical inner pore diameter of ∼2.6 nm.[101] Reproduced from ref 101. Copyright 2017 American Chemical Society. (b) Side (left) and top (right) views of the hexameric form of Alm nanopore with a total nanopore length of ∼3.8 nm and the critical inner diameter ranging from 0.3 to 2.6 nm, depending on the oligomeric state.[102] (c and d) Ionic characterization of αHL and Alm nanopores. Reproduced with permission from ref 102. Copyright 2023 Elsevier. (c) I−V curves for wild-type αHL (black data-point), displaying a linear behavior, and a mutant variant of αHL (red data-point) exhibiting ionic rectification. Mutation sites responsible for the altered response are highlighted in blue in the bottom-left panel.[69] Reproduced with permission from ref 69. Copyright 2009 Springer Nature. (d) The I−V curve for Alm reveals pronounced nonlinearity. Each data point represents the average value of five consecutive experiments, and the data are fitted to an exponential function.[105] Reproduced from ref 105. Copyright 2011 American Chemical Society.

extended iontronic diodes to the micrometer scale.[70] In the same year, studies on angstrom-scale channels uncovered size-dependent ion transport, highlighting the role of nanoconfinement in modulating ionic mobility.[71] More recently, in 2022, deviations from the Nernst−Einstein relation in carbon nanotube porins showed exotic water transport behaviors and mechanisms, suggesting that quantum physics governs ion dynamics at the nanoscale.[72] In 2023, the electronic-to-multi-ionic signal transmission was achieved by cascade-heterogated biphasic gel iontronics, marking significant advancements for hierarchical and selective ionic signal transmission.[73]

Parallel to these mechanistic insights, iontronic device types have advanced rapidly. The field made a breakthrough in 2010 with the development of the iontronic transistor, which utilized conducting polymers and ion-selective membranes to achieve gated ion flow—a critical step toward the development of iontronic circuitry.[74] In 2013, droplet networks were manufactured, demonstrating the potential for ionic information processing by incorporating functional membrane channels within different droplet compartments.[75] In 2020, iontronic thermoelectric materials showcased the ability to convert temperature gradients near room temperature into ionic currents, opening avenues for energy harvesting.[76] In 2023, a dropletronic power source was developed, which used internal ion gradients to generate ionic current output and induce neuronal modulation.[77]

The above discoveries of mechanisms and device types enabled on-demand control of ion transport, providing new applications of iontronics. In 2022, the piezoionic effect was demonstrated for several applications, including piezoionic skin and peripheral nerve stimulation, demonstrating the possibility of self-powered piezoionic neuromodulation.[78] In 2024, the capabilities of dropletronics were further expanded to include iontronic diodes, npn- and pnp-type transistors, diverse reconfigurable logic gates, and memristive synapses.[79] Notably, the dropletronic transistor was used to record electrophysiological signals from sheets of human cardiomyocytes, paving the way for the development of miniature bioiontronic systems. These advancements suggest a future in which iontronic devices could be seamlessly integrated with biological systems, offering new possibilities for medical diagnostics and therapies. The emerging applications, in terms of biointerfaces, neuromorphic computing, energy harvesting and storage, and water treatment, will be detailed in Chapter 5.[80−89]

2. BIOLOGICAL NANOPORES FOR CONTROLLING ION TRANSPORT

Biological nanopores are naturally occurring protein or peptide structures with nanoscale channels that can be used for ion transport across lipid membranes. These channels are essential for cellular homeostasis, electrochemical signaling, and metabolic regulation.[90−92] In this Chapter, we introduce protein and peptide ion channels embedded in lipid membranes that enable selective ionic conduction. We describe their structural and ionic properties, their classification based on gating mechanism, and their typical voltage−current behavior. Finally, we highlight how biological nanopores are increasingly integrated into iontronic platforms for energy storage, signal processing, and neuromorphic applications.

2.1. Comparison of Natural and Modified Protein Nanopores and Peptide Nanopores

Biological ion channels can be classified according to their gating mechanisms:

- Leaky ion channels remain permanently open, enabling constant passive ion flow across the membrane. For

https://doi.org/10.1021/acs.chemrev.5c00579
Chem. Rev. 2025, 125, 11840−11877

Table 1. Comparison between Commonly Used Biological Nanopores[a]

Nanopore	αHL	Aerolysin	CsgG	MspA	gA	Alm	Melittin	Monazomycin
Natural origin	*Staphylococcus aureus*	*Aeronomas spp*	*Escherichia coli*	*Mycobacterium smegmatis*	*Bacillus brevis*	*Trichoderma spp*	*Apis mellifera*	*A streptomices*
Diameter (nm)	1.5 ± 0.1	1.2 ± 0.2	1.1 ± 0.2	1.1 ± 0.1	0.4	0.3 ± 0.2	3.5 ± 2.5	1.5 ± 0.5
Length (nm)	10	10	9.6	9.6	2.6 (dimer)	3.2	NA	4 ± 1.5
Ionic current at 100 mV (pA)	136	55	115	197	1.4	12−115	NA	NA
Molecular weight (kDa)	34	52	29	20	1.9	0.5−2.2	2.8	1.4
Subunit number	7	7	9	8	2	4−12	4	4−12
Commercial availability	Yes	No	No	No	Yes	Yes	Yes	Yes
References	101, 106−110	101, 107, 109, 110	109−112	110, 113, 114	109, 115−117	102, 105, 118−121	122−126	127−129

[a]Summary of representative biological nanopores, including protein and peptide types. The table compares each nanopore's diameter at the narrowest constriction (critical diameter), pore length, typical ionic current at 100 mV, molecular weight of individual monomers, and oligomeric states (i.e., the number of monomers forming the pore). "Commercial availability" indicates whether the nanopore is available through commercial suppliers (e.g., Sigma-Aldrich, Thermo Scientific) as lyophilized powder.

example, sodium leak channels maintain the resting membrane potential.[93]

- The mechanosensitive ion channels respond to membrane deformation, opening upon membrane bending and closing when the cell recovers its original conformation, enabling mechano-sensation. Examples include Piezo-type mechanosensitive ion channel components 1 and 2 (Piezo 1 and 2).[94]
- The heat-activated ion channels, such as TRPV4, open when the temperature is raised, supporting thermosensation.[95]
- Voltage-gated ion channels, such as voltage-gated potassium channels, open upon changes in membrane potential and trigger neuronal signaling.[96]
- Ligand-gated ion channels, such as the nicotinic acetylcholine receptor,[97] undergo conformational changes upon specific ligand binding, enabling chemical signaling between cells.[98]

Biological ion channels span a wide range of molecular structures, from peptide-based pores, such as gramicidin A (gA, ∼4 kDa, homodimer), to complex multiunit protein assemblies, such as aerolysin (364 kDa, heptamer). Their ion selectivity arises from both geometrical constraints and electrostatic interactions within the pore lumen. For instance, the potassium ion channel employs a narrow selectivity filter lined with carbonyl oxygen atoms arranged in a constrained geometry, precisely coordinating the rapid movement of dehydrated potassium ions while excluding smaller ions such as sodium ions, which cannot be stabilized within the filter.[99,100]

Among natural nanopores, several have been used in research due to their ability to undergo artificial modifications. One key example is alpha-hemolysin (αHL), a protein nanopore derived from the Gram-positive bacterium *Staphylococcus aureus* (Figure 2a). αHL comprises both transmembrane and extracellular domains, and features a critical (minimal) inner pore diameter of approximately 2.6 nm.[101] By contrast, Figure 2b depicts Alamethicin (Alm), a peptide-based nanopore, extracted from the fungus *Trichoderma viride*.[102] By comparison with αHL, Alm lacks an extracellular domain and only contains a transmembrane domain with a narrower and more variable critical diameter ranging from 0.3 to 2.6 nm, depending on the number of monomers forming the pore and the environment.[102]

Ion transport through ion channels is often characterized by ionic conductivity and current−voltage (I−V) characteristics. Channels with high ionic conductivity are often advantageous for applications requiring rapid signal transduction and a high signal-to-noise ratio (SNR). Conversely, channels with low ionic conductivity may benefit systems that require precise control of ion movement, such as molecular detection or DNA sequencing. The shape of the I−V curve, whether linear or nonlinear, offers valuable insights into the functional properties of a nanopore. For example, linear I−V characteristics are commonly used in sequencing technologies for their predictable signal response.[103,104] In contrast, nonlinear I−V behavior often indicates voltage-dependent gating, enabling applications such as neuromorphic computing.[105] Figure 2c, illustrates the I−V characteristics of a wild-type αHL, which displays a linear response. Following protein engineering to incorporate 49 positively charged arginine residues within the lumen, the modified αHL exhibited a rectifying, nonlinear I−V curve, characterized by negligible currents under negative biases (−150 mV) and positive currents under positive potentials (150 mV).[69] Figure 2d shows the I−V curve of an Alm nanopore, which exhibits an exponential increase in current above 100 mV, highlighting its voltage-dependent pore formation.[105]

An overview of commonly used biological nanopores is provided in Table 1, which includes their biological origin, structural features, ionic conductivity, and commercial availability. For channels displaying an Ohmic behavior, the ionic current is described by the linear relationship: $I = V \times G$, where I is the ionic current (A), V is the applied voltage (V), and G is the ionic conductance (S).

Among protein nanopores, αHL and aerolysin insert into lipid membranes following heptameric oligomerization, exhibiting distinct transmembrane and extracellular domains. CsgG assembles as a nonamer comprising transmembrane and periplasmic regions, while MspA forms an octameric channel with both transmembrane and extracellular segments. Peptides, such as gA, Alm, and Melittin, consist solely of transmembrane domains. gA assembles through head-to-head dimerization of short peptides spanning half the membrane, whereas Alm and Melittin form full-length membrane-spanning oligomers. On the ion transport view, protein nanopores and gA generally exhibit linear I−V characteristics. In contrast, Alm, Melittin, and Monazamycin display nonlinear profiles.[130,131] Monazamycin is a voltage-dependent, membrane-spanning antibiotic that oligomerizes to form pores.[132−134]

https://doi.org/10.1021/acs.chemrev.5c00579
Chem. Rev. 2025, 125, 11840−11877

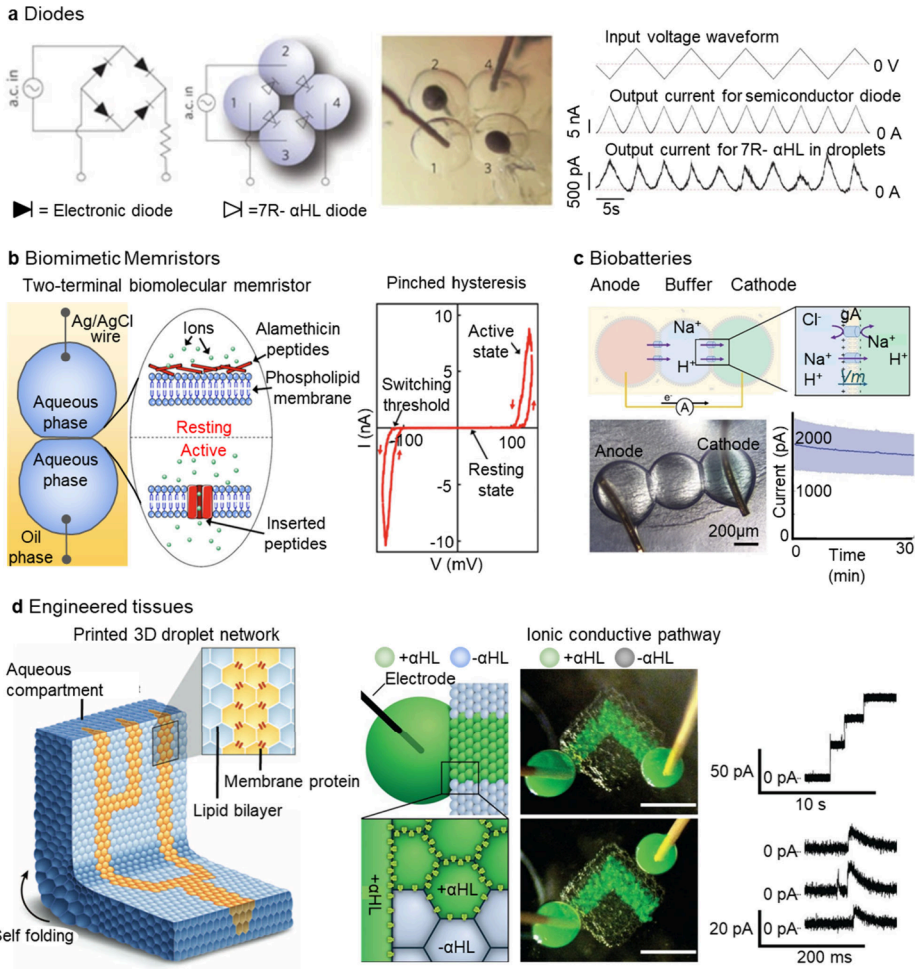

Figure 3. Examples of biological nanopores used in the construction of iontronic devices. (a) Full-wave rectifier based on four iontronic diodes incorporating modified αHL.[69] Left: schematic of a conventional semiconductor rectifier circuit and the droplet counterpart. Center: photograph of the assembled iontronic rectifier. The droplet was around 800 μm in diameter. Right: output current waveforms for both rectifiers in response to a triangular input voltage ranging from ±1.5 V for the semiconductor device and ±100 mV for the droplet system. Reproduced with permission from ref 69. Copyright 2009 Springer Nature. (b) Biomimetic memristors.[136] Left: schematic of the iontronic memristor system, showing the transition between resting and active states. Right: The I−V curve exhibits a pinched hysteresis characteristic of memristive behavior. Reproduced from ref 136. Copyright 2018 American Chemical Society. (c) Biobatteries. Top: Diagram of the droplet-based biobattery developed. Bottom left: image of the assembled biobattery. Bottom right: measured current output over time.[141] Reproduced from ref 141. Available under a CC-BY 4.0 license. Copyright 2024 Wiley. (d) Engineered tissues with ionically connected droplet networks. Left: 3D-printed droplet network incorporating protein nanopores.[75] Right: schematic and fluorescence image of ionic conductive pathways formed by αHL-mediated droplet connections. The upper-right panels show that current is detected when the electrodes are aligned with the ionic conductive path, whereas misaligned electrodes yield only transient capacitive signals. Scale bars, 500 μm. Reproduced with permission from ref 75. Copyright 2013 American Association for the Advancement of Science.

2.2. Iontronic Devices Based on Various Biological Nanopores

Biological nanopores have been used to construct iontronic devices as key components for regulating ion transport. A key capability of biological nanopores is ionic rectification, which has been used to create various iontronic diodes.[69] Maglia et al. engineered mutant αHL nanopores exhibiting a time delayed rectification across a wide concentration range (0.2−3 M potassium chloride (KCl)), which showed a rectification ratio of 60 ± 10 under 50 mV (Figure 2c).[69] Embedding these rectifying nanopores in droplet interface bilayers (DIBs), and applying a sinusoidal voltage waveform, they developed a half-wave rectifier capable of converting alternating current to direct current. Moreover, four droplets were interconnected to form a full-wave rectifier (Figure 3a), where the spatial orientation of the nanopores was critical. The functionality of the network depended on the asymmetric placement of the pores at the droplet interfaces, as reversing their orientation altered the direction and behavior of ion flow through the system. With inputs applied to droplets 2 and 3 and outputs recorded from droplets 1 and 4, the device reproduced the expected waveform profile of a solid-state full-wave rectifier, demonstrating the viability of logic behavior in soft iontronic systems by using nanopores.

Beyond rectification, biological nanopores have been used to build iontronic memristors, which are nonlinear iontronic components whose conductance states depend on prior stimuli.[135] These devices are of particular interest for neuromorphic computing, in terms of mimicking synaptic behaviors and low-power energy storage.[136−138] Najem et al. demonstrated a DIB-based memristor using the voltage-gated insertion behavior of the peptide channel Alm (Figure 3b).[136] In a droplet pair, the voltage-gated insertion produced a pinched hysteresis loop in the I−V curve, a hallmark of memristive behavior.[136]

https://doi.org/10.1021/acs.chemrev.5c00579
Chem. Rev. 2025, 125, 11840−11877

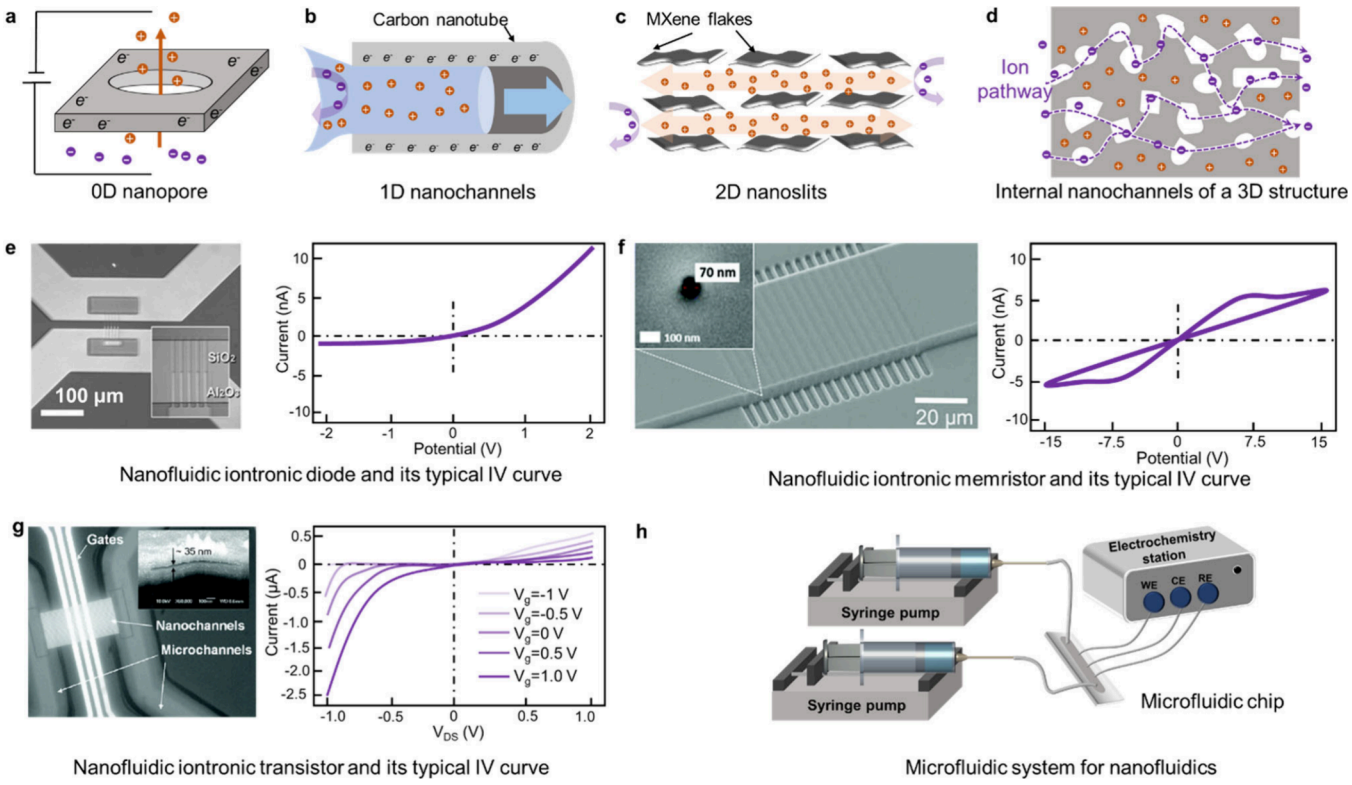

Figure 4. Solid-state nanofluidics. (a) Negatively charged 0D nanopore arrays enable charge-selective separation of cations. (b) The ionic Coulomb drag effect between the ionic movement along the negatively charged 1D carbon nanotubes, which is enabled by the ion-electron coupling at the channel-liquid interface. Reproduced with permission from ref 148. Copyright 2024 Springer Nature. (c) Cation-selective ion separation based on negatively charged 2D MXene flakes.[150] Reproduced from ref 150. Copyright 2023 American Chemical Society. (d) Anion-selective ion separation based on a positively charged 3D porous structure. Reproduced with permission from ref 151. Copyright 2021 Springer Nature. (e–g) Examples of iontronic devices based on solid-state nanofluidics and their typical I–V curves, including a nanofluidic iontronic diode (e),[161] a memristor (f),[162] and a transistor (g).[161,164] Reproduced from ref 161. Copyright 2005 American Chemical Society. Reproduced from ref 162. Copyright 2009 American Chemical Society. Reproduced with permission from ref 163. Copyright 2019 The Royal Society of Chemistry. Reproduced with permission from ref 164. Copyright 2024 American Wiley. (h) Microfluidic systems are often used as a characterization platform for solid-state nanofluidics.

This device mimicked short-term synaptic plasticity, exhibiting both paired-pulse facilitation and depression, where the second response in a stimulus pair was modulated by the first, reflecting dynamic changes in biological synapses.

Biobatteries represent an important class of bioinspired energy systems, offering scalable strategies for converting ionic gradients into usable electrical power. Mayer's group has pioneered several designs in this field. For example, they proposed an electric-eel-inspired biobattery with a scalable stacking approach to enhance power output.[139] In another design, a torpedo-fish-inspired biobattery was developed, providing a scale-up approach for stacking ultrathin sheets (<500 μm) with a tunable surface area to assemble electrically active repeating units.[140] Building upon these concepts, subsequent studies introduced biological nanopores into biobattery architectures, leveraging their intrinsic ion selectivity and gating properties to enhance conversion efficiency and functional control. Liu et al. incorporated the monovalent cation-selective channel gA into nanoliter-scale DIB-based biobatteries (Figure 3c).[141] The droplet biobattery comprised a reduced Nicotinamide adenine dinucleotide/9,10-anthraquinone-2,6-disulfonic acid redox anode droplet and a 2,2′-azino-bis-3(ethylbenzothiazoline-6-sulfonic acid)/laccase enzyme cathode droplet, which generated ionic output currents of up to ∼2000 pA through gA-mediated proton and sodium exchange. The droplet anode and cathode can have multiple electrolyte droplets integrated in between, enabling powered directional molecule transport for drug delivery and biomodulation. These droplet biobatteries illustrated a path toward soft, self-sustained biointerfaces using native bioanalytes as energy sources.[142]

Furthermore, three-dimensional (3D) droplet printing has enabled the assembly of ionic conductive soft matter, mimicking signal transduction in natural tissues (Figure 3d). Villar et al. used a piezo-driven 3D printer to deposit tens of thousands of picoliter droplets in lipid-containing oil, resulting in mm-scale heterogeneous structures.[75] Patterned ionic conduction was achieved by selectively incorporating αHL channels along a continuous droplet path. When silver/silver chloride electrodes were attached to this path, ionic currents could be recorded in response to voltage inputs, confirming successful conduction (Figure 3d, top-right panel). Misalignment disrupted signal transmission, underscoring the importance of pattern design and the incorporation of biological nanopores (Figure 3d, bottom-right panel). Together, these systems harness biological nanopores to create ionic conductive pathways in synthetic tissues and iontronic systems. Owing to their biocompatibility and ability to support patterned ion transport, they enable advanced functions such as directional signal propagation, sensing, and synapse-like behavior. This opens new avenues for neuromorphic systems engineering, implantable bioiontronic interfaces, and dynamic biohybrid materials.

https://doi.org/10.1021/acs.chemrev.5c00579
Chem. Rev. 2025, 125, 11840–11877

Natural nanopore structures inspire the design of synthetic nanochannels and membranes, in which confined geometries and tailored surface chemistries are engineered to mimic biological functions. For instance, conical or asymmetric nanochannels replicate the rectification behaviors of protein pores, enabling diode-like ion transport.[143] Chemical functionalization enables dynamic responses to various stimuli, including pH, voltage, or ligand binding.[144] The adoption of these design principles facilitates controllable ion transport and allows memory effects for various iontronic applications.[145] Nevertheless, performance limitations of biological nanopores (e.g., instability outside native environments), functional requirements for complex logic operations and neuromorphic computing, and further mechanistic understanding of ion transport under nanoconfinement and at ionic-electronic interfaces have collectively motivated the transition of iontronic devices from biological nanopores to artificial systems (Chapter 3).

3. ARTIFICIAL IONTRONIC DEVICES FOR HARNESSING ION TRANSPORT

Artificial iontronic devices can harness controlled ion dynamics within synthetic structures to achieve novel functionalities. There are three main research directions: solid-state nanofluidics, macroscopic iontronics, and miniature iontronics. In this Chapter, we first describe these three directions by showing key device examples and their iontronic properties. We then focus on artificial iontronic devices at various scales and dimensions and compare their advancements and limitations.

3.1. Artificial Iontronic Devices Based on Solid-State Nanofluidic Channels

3.1.1. Classification and Materials. Solid-state nanofluidics focuses on the transport phenomena of ions and water molecules in artificial nanoscale channels.[146] Unlike biological ion channels embedded in soft membranes, artificial ion channels are mainly fabricated based on solid-state substrates and can be classified by the dimensionality of their ion transport pathways: zero-dimensional (0D) nanopores, 1D nanotubes, 2D nanoslits, and 3D nanostructures. 0D nanopores are approximately circular or nearly point-like in geometry (Figure 4a). A 0D nanopore system typically refers to a single pore (diameter ∼0.5 nm−1 μm), or distantly separated pores in a nanopore array.[147] Common substrate materials include graphene, silicon nitride, crystals, and polymers.[148] The intrinsic narrow confinement of 0D nanopores gives rise to size selectivity, allowing for applications in single-molecule sensing and DNA sequencing. 1D nanotubes refer to iontronic devices that confine ion transport along a tube-shaped nanochannel, such as carbon nanotubes (CNTs) and boron nitride nanotubes (Figure 4b).[149] The 1D pathway is characterized by long-range directional confinement, which enables surface−ion coupling and facilitates highly controllable ionic transport. This directional control is essential for mimicking neuron-like conduction, where signal fidelity depends on the guided propagation of ions. 2D nanoslits refer to iontronic devices that have 2D materials with interlayer spaces as ionic conductive channels, such as graphene oxide and MXene (Figure 4c).[150] Ion transport in 2D nanoslits is modulated by the interlayer distance of 2D materials, which dictates the degree of steric hindrance and ion selectivity. The tunability of 2D materials is crucial for ion sieving in water purification and for gating devices, where precise control of interlayer distance enables dynamic regulation of ion transport. 3D nanostructures refer to iontronic devices with interconnected nanochannels and porous networks, which can be found in hydrogels, porous materials, and architectures featuring interconnected nanopore networks (Figure 4d).[151,152] The intrinsic feature of 3D nanostructures is multidirectional ion transport through interconnected channels, which provides both high ionic flux and mechanical robustness. These properties directly support applications in energy storage, in which rapid ion transport across large volumes enhances charge/discharge rates, and soft electronics, in which the combination of ionic conductivity and structural flexibility ensures reliable integration at macroscopic scales. The solid-state nanofluidics can replicate key features of biological ion channels, including ion selectivity by surface functional groups or asymmetrical geometry, rectification behavior by conical or asymmetric pores, and stimuli-responsiveness by functional material modifications.[153−156]

3.1.2. Device Examples. The physical and chemical properties of the ion channel can regulate the ion transport through solid-state nanofluidics.[157−159] The I−V characteristics of artificial ion channels provide direct insights into their ion transport properties, including ionic rectification, selectivity, and conductivity. Typically, symmetric nanochannels exhibit linear I−V curves, indicative of ohmic behavior, whereas asymmetric channels or those with heterogeneous surface charges exhibit nonlinear, rectified curves. These behaviors are often influenced by parameters such as channel geometry, surface charge density, and chemical modification. For example, nanopores functionalized with charged groups demonstrate diode-like behavior, in which ions preferentially move in one direction.[160] Such rectifying I−V curves are essential for designing logic systems based on ion transport.

Based on the above regulations, various iontronic devices based on artificial nanofluidics have been developed, including nanofluidic iontronic diodes, memristors, and transistors (Figure 4e−g).[161−163] As shown in Figure 4e, by utilizing distinct isoelectric points on the surfaces of silicon dioxide (SiO_2) and aluminum oxide (Al_2O_3), and photolithography to define the charge distribution, a nanofluidic iontronic diode with heterogeneously charged surfaces is created. The corresponding I−V curve indicates the ionic rectification outcome. As shown in Figure 4f, a nanofluidic iontronic memristor is developed by using the principle of ion concentration polarization, which is induced through highly ordered cylindrical nanochannels. The I−V curve displays characteristic pinched-hysteresis loops of the nanofluidic iontronic memristor, which are similar to those of its solid-state counterparts. At an increased voltage sweep rate, the nanofluidic iontronic memristor exhibits I−V curves with pinched hysteresis loops that collapse into a straight line. As shown in Figure 4g, a nanofluidic iontronic transistor using two-dimensional silicon dioxide nanochannels is presented. Rapid field-effect control of ionic concentrations and conductance in the nanofluidic confinement is demonstrated. The current−voltage (I−V) characteristics exhibit typical transistor behavior for a nanofluidic iontronic transistor when the gate voltage (V_g) is varied from −1 V to +1 V.[164] Under a negative drain-source bias (V_{DS}) of −1 V, applying a negative gate voltage from 0 V to −1 V progressively decreases the ionic current until it becomes undetectable, indicating the device is in the off state. Conversely, applying a positive gate voltage from 0 V to +1 V increases the ionic current to approximately 2.5 μA, indicating the on state. When a positive drain-source bias (V_{DS}) of +1 V is applied, the transistor exhibits similar gate-controlled switching behavior but

https://doi.org/10.1021/acs.chemrev.5c00579
Chem. Rev. 2025, 125, 11840−11877

Table 2. Dimensions of Representative Macroscopic Iontronic Devices

Device type	Key functional unit	Scale	Device area	Reference
Diode	Asymmetric ion transport interface	Millimeter scale	5−100 mm^2	180, 187−189
Transistor	Gated ion transport channel	Millimeter scale	0.02−100 mm^2	66, 164, 190
Artificial synapse	Ion transport channel coupled with ion reservoirs	Centimeter scale	0.25−0.5 cm^2	191−193
Wearable sensor	Stretchable ion-conductive network	Centimeter scale	1−5 cm^2	182, 184, 185, 194
Energy harvester	Ion-selective transport interface	Macroscopic scale	>5 cm^2	186, 195, 196

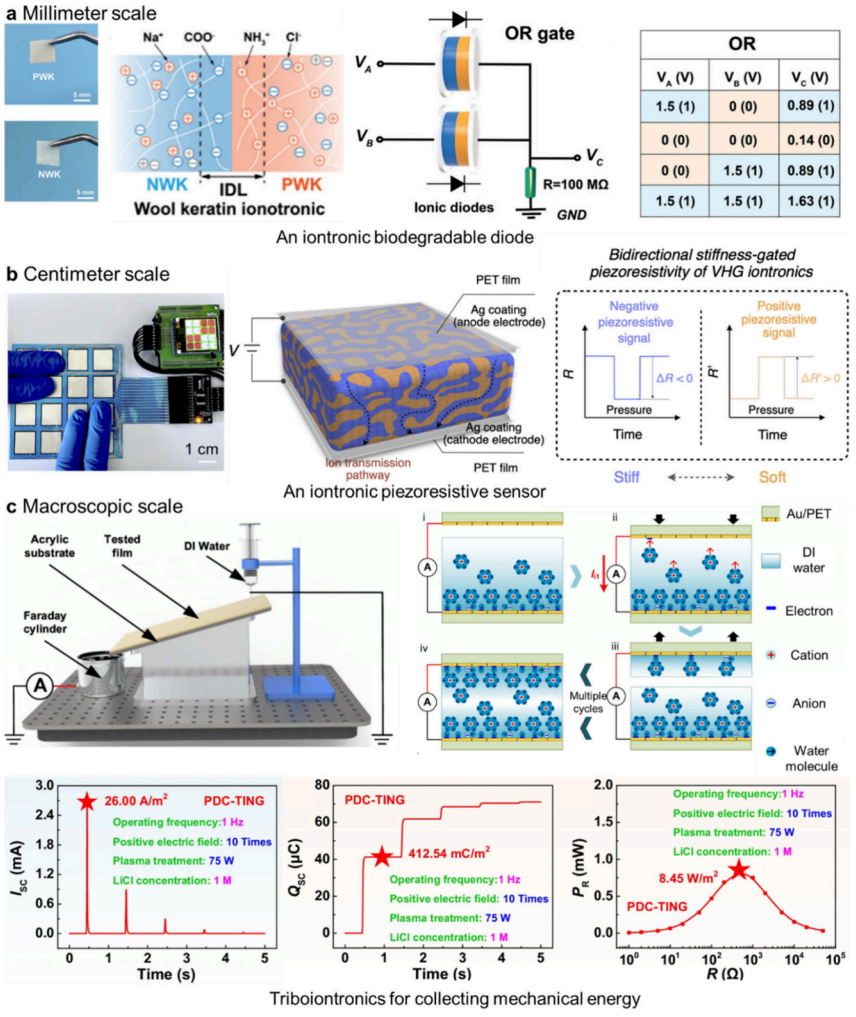

Figure 5. Macroscopic iontronic devices. (a) Left, photographs and schematic of positively charged and negatively charged wool keratins (PWK and NWK) forming a millimeter-scale ionic heterojunction. Right, demonstration of a logic gate based on WK iontronic diodes.[180] Reproduced with permission from ref 180. Copyright 2024 Wiley. (b) Photograph of a centimeter-scale iontronic piezoresistive sensor array (4 × 4 units) (left), and its ion transmission pathway inside (middle). Right, the device shows bidirectional stiffness-gated piezoresistivity.[182] Reproduced from ref 182. Available under a CC-BY 4.0 license. Copyright 2024 American Association for the Advancement of Science. (c) A macroscopic scale triboiontronics for collecting energy carried by deionized (DI) water droplet sliding (top left), the mechanism of triboiontronics with temporal control of EDL formation by controllable ion migration (top right), and the short-circuit current density, transferred charge density, and peak power density of the triboiontronic nanogenerator (bottom).[186] Reproduced from ref 186. Available under a CC-BY 4.0 license. Copyright 2024 Springer Nature.

with reversed polarity; it turns on at $V_g = -1$ V and off at $V_g = +1$ V.

It is worth noting that solid-state nanofluidic channels typically require a significantly larger supporting system for proper functioning and characterization. For example, artificial iontronic devices based on solid-state nanofluidics usually incorporate a microfluidic system for fabrication and functional evaluation (Figure 4h).[165−167] These chips integrate nanoscale ion channels into controllable physicochemical environments, enabling precise control over ion concentration gradients, electric fields, and fluidic dynamics.[168−170] Nevertheless, integration limits the overall miniaturization and portability of the system. While the ion channels themselves operate at the nanoscale, the supporting microfluidic systems and associated components, such as fluid reservoirs and electrode interfaces, often result in a much larger device. This discrepancy between the functional nanoscale channels and the macroscale supporting system not only poses challenges for applications such as tissue implantation and *in vivo* sensing but also undermines the miniaturization advantages offered by nanoscale channels.

https://doi.org/10.1021/acs.chemrev.5c00579
Chem. Rev. 2025, 125, 11840−11877

3.2. Macroscopic Iontronic Devices

3.2.1. Structures and Materials. Macroscopic iontronic devices refer to systems in which ion transport occurs at scales of around one centimeter or larger. Unlike nanofluidics, macroscopic iontronics relies on bulk ion transport and interfacial conversion of ions and electrons. Macroscopic iontronics offers several distinctive characteristics. Their mechanical flexibility and elasticity allow for seamless integration with deformable surfaces, including human skin and internal organs. Biocompatibility is another essential feature, which enables safe and functional interaction with biological tissues. Furthermore, their robustness ensures functional durability under repeated mechanical deformation, making them suitable for long-term and dynamic use.

Macroscopic iontronic devices are usually constructed from multilayer materials, such as layered assemblies of iontronic conductors.[171,172] These structures are designed to maintain functionality under large-scale deformation, environmental exposure, and long-term use, while preserving reliable ion transport and signal transduction. A typical macroscopic iontronic device consists of the following key elements: an ionic conductive layer, which is the functional layer responsible for ion transport; a flexible substrate and an encapsulation layer, which provide mechanical integrity and protects functional layers; interconnection layers, which are designed to incorporate interconnects, microchannels, or patterned microstructures to pattern ion transport or signal collection, especially in devices such as iontronic skins, e-skins, and implantable devices.[173,174]

The performance of macroscopic iontronic devices depends on the materials that support ionic conductivity, mechanical flexibility, and biocompatibility. These materials can be broadly categorized into ionic conductors and support materials. Ideal ionic conductors include hydrogels, ionic liquids, and polyelectrolytes.[175−177] As for the support materials, elastomers, thermoplastics, polyurethanes, hydrophobic layers, and breathable films are common choices.[178,179]

3.2.2. Device Examples. To better define what is "macroscopic" in iontronics, it is helpful to consider the physical dimensions of the reported systems. Macroscopic iontronic devices often range from millimeter-scale components to centimeter-scale systems, and in some cases, even larger, such as body-scale wearable systems (Table 2). This classification refers to the unit's overall functional dimensions, rather than to isolated structural features such as nanopores or nanochannels. For example, as shown in Figure 5a, a millimeter-scale iontronic diode was demonstrated to efficiently rectify alternating current signals.[180] The rectification ratio was ∼9.2 under ±1 V biases, and was improved to nearly 200 when using CNTs electrodes under ±0.02 V biases. The iontronic analogs of p-type and n-type were obtained by subjecting pH-responsive wool keratin to acid and base treatment, respectively. When the two oppositely charged wool keratin membranes adhered, analogous to the formation of a depletion layer at the junction of p-type and n-type semiconductors, the wool keratin heterojunction established an ionic double layer (IDL) at the interface. According to the theory of mixing entropy, the mobile counterions positioned at the interface undergo diffusion toward opposite regions, where they subsequently combine. This process leads to the formation of an IDL, composed of fixed-charge polymer chains at the interface. The presence of IDL gives rise to a drift current that opposes the diffusive movement of counterions, thereby hindering their further diffusion. Once equilibrium was achieved, the wool keratin heterojunction established a built-in electric field. The IDL in heterojunction was critical to the functionality of wool keratin-based iontronic diodes, as it enabled their rectifying and ion-transporting capabilities.

Centimeter-scale iontronic sensors constructed from ion gels and stretchable electrodes have been applied to multimode sensing.[181] These devices are generally defined as centimeter-scale iontronic devices, not because their internal transport pathways are macroscopic, but because the overall functional units are typically fabricated at the centimeter level. While active ion channels, nanopores, or hydrogel networks operate on the nanoscale to the microscale, integration into wearable patches or stretchable sensor arrays requires device dimensions of approximately several centimeters. The centimeter-scale sizes ensure mechanical robustness, stable signal acquisition, and practical interfacing with skin or external hardware. Defining them as centimeter-scale devices thus highlights the scale of operational units, distinguishing them from nano- and microscale components on one side and larger body-scale systems on the other. For example, a centimeter-scale piezoresistive iontronic device with bicontinuous phases was used as a pressure sensor with a high strain performance (Figure 5b).[182] The iontronic phases predominantly dissipated external energy, thereby enhancing the system's impact resistance and toughness. Meanwhile, the bicontinuous interface also served as a critical barrier to crack propagation. As a result, the piezoresistive iontronic device can withstand strains exceeding 1000%. Unlike other piezoresistive systems with unidirectional sensing outputs, such as resistance decrease or increase under input forces, iontronics demonstrated bidirectional stiffness ion gating, coordinately integrating negative and positive piezoresistive signals to enhance the sensor's awareness capabilities. This feature was achieved through a switchable stiffness-gating ion transmission pathway enabled by the bicontinuous structure of the soft iontronic phase and the stiff vitrimer phase, which modulates ion transport efficiency in response to mechanical stimuli to yield both negative and positive piezoresistive signals. Recent advances highlight the versatility of centimeter-scale iontronic devices in bioinspired sensing, transient bioiontronics, and soft robotics. A bioinspired retina based on iontronic hydrogels demonstrates inhibitory and excitatory synaptic functions, enabling contrast regulation for image recognition, motion analysis, and robotic path planning, thereby approaching the natural signal processing of the human eye.[183] Complementing this, fully biodegradable iontronic skins built from natural polyelectrolyte derivatives achieve high ionic conductivity, skin compliance, and complete degradability within days, offering sustainable solutions for electrophysiological monitoring and addressing e-waste concerns in wearable healthcare.[184] In parallel, architected stretchable iontronic sensors fabricated by multimaterial 3D printing of leakage-free polyelectrolyte elastomers exhibit multimodal sensing of tension, compression, shear, and torsion with robust stability.[185] Together, these studies underscore the potential of iontronic devices at the centimeter scale to combine biological inspiration, sustainability, and multifunctionality, paving the way for next-generation interactive and environmentally responsible iontronics.

Iontronic devices have been applied at the macroscopic scale. These iontronic devices are considered macroscopic because their functional units operate on scales sufficiently large to sustain ion flux across extended structures. The macroscopic scale is important for energy harvesting, as large interfacial areas enable the accumulation of asymmetric EDLs, thereby

https://doi.org/10.1021/acs.chemrev.5c00579
Chem. Rev. 2025, 125, 11840−11877

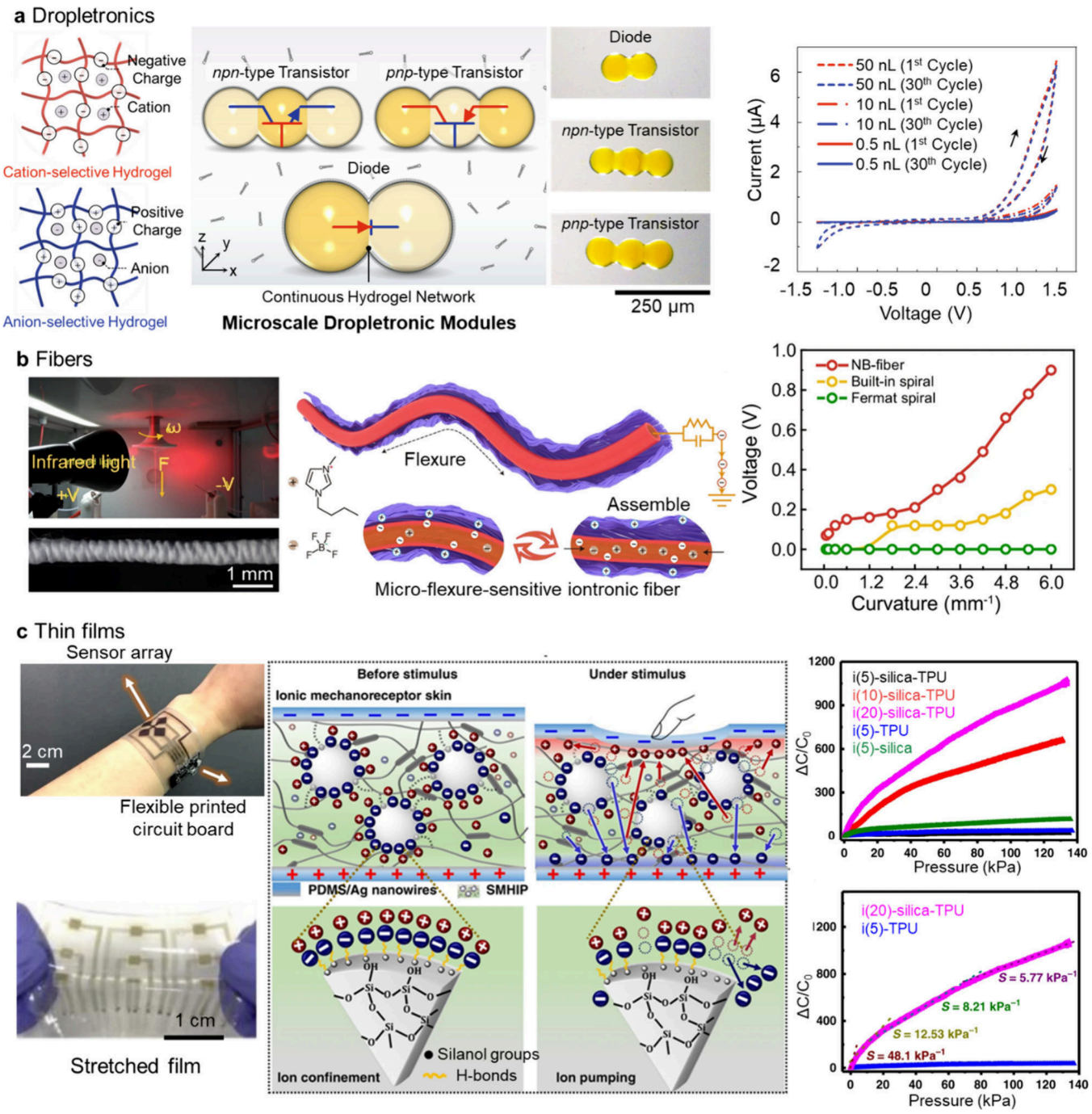

Figure 6. Miniature iontronic devices. (a) Left, chemical structures of the cation- and anion-selective droplet hydrogels. Middle, illustrations and bright-field images of a dropletronic diode and transistors. Right, the dropletronic diodes with different volumes show stable diode performance under multiple cycles.[79] Reproduced with permission from ref 79. Copyright 2024 American Association for the Advancement of Science. (b) Left, the microcurvature-sensitive iontronic fabric with a plain weave structure from a commercial loom. By coupling electronic and ionic conduction in the fiber (middle), the fiber is highly sensitive to microcurvature (right).[211] Reproduced from ref 211. Available under a CC-BY 4.0 license. Copyright 2024 Springer Nature. (c) Left, a transparent, flexible iontronic film as a sensor array coated on a flexible printed circuit board. Middle, the iontronic SMHIP film exhibits pressure-induced disruption of hydrogen bonds between the ion pairs and the silica surfaces, leading to the release and reversible pumping of ions. Right, the interfacial EDL capacitance (C_{EDL}) changes with pressure.[218] Reproduced from ref 218. Available under a CC-BY 4.0 license. Copyright 2019 Springer Nature.

enhancing charge transfer and improving output performance. For instance, a triboiontronic system achieved controllable ion migration by regulating the formation of an asymmetric EDL over lengths exceeding 6 cm (Figure 5c), which produced a transferred charge density of around 410 mC m^{-2}.[186] The establishment of efficient triboiontronics was enabled by the dynamic control of EDL formation at the solid−liquid interface. Initially, a gold (Au) layer was sputtered onto a dielectric polyethylene terephthalate (PET) substrate to act as a charge-collecting layer. In the event of contact between deionized water and the bottom Au/PET layer, direct interaction with the PET substrate may occur through microscopic cracks in the sputtered

https://doi.org/10.1021/acs.chemrev.5c00579
Chem. Rev. 2025, 125, 11840−11877

Au layer. This process can result in solid−liquid contact electrification (CE) and the formation of a stable EDL (Figure 5c.i). Second, as the top Au/PET layer moved downward to contact the water, the initial CE led to the formation of a new EDL, thereby establishing two EDLs with significantly different symmetries (Figure 5c.ii). This established an ion concentration gradient, thereby facilitating electron transfer in the external circuit and generating an ionic current (I_{i1}). Third, the detachment of the top Au/PET layer was found to halt ion migration (Figure 5c.iii). Through repeated cycles of contact and separation, the constructed ion concentration gradient gradually weakened, yet the ion migration persisted until equilibrium was achieved between the two EDLs (Figure 5c.iv). By dynamically managing the asymmetric EDL formation between the dielectric substrate and liquids, the triboiontronic nanogenerator can achieve a short-circuit current of 2.6 mA, a transferred charge of 41 μC, a peak power of 0.85 mW, and an open-circuit voltage of 0.25 V. The transferred charge density and peak power density could reach 413 mC m^{-2} and 8.5 W m^{-2}, respectively.

3.3. Miniature Iontronic Devices

Miniature iontronic devices refer to iontronics with at least one critical dimension that is at the microscale or smaller. In 2007, the first iontronic pump was published, reducing the device to a 50-μm-wide channel and enabling stimulation of individual cells.[197] Over time, advanced micro- and nanomanufacturing has enabled the miniaturization of iontronic devices, including the production of microscale droplets, fibers, and thin films. By comparison with macroscopic devices stated in the previous Section, miniature iontronic devices can retain the fundamental capabilities of ion transport and ionic signal processing, while enhancing interfacial ion dynamics for ultrafast switching and ion selectivity. This provides improved resolution and responsiveness for applications in iontronic logic devices, soft microactuators, and biointerfaces.[198,199]

3.3.1. Dropletronic Device. The earliest phase of dropletronic devices focused on the behavior and control of single droplets as compartmentalized, functional units.[200] In this stage, droplet devices enabled a controllable, rapid mixture of chemical compounds in microscale droplet reactors, and therefore decreased reaction times and required reactant volumes. In conjunction with precise droplet generation and repeatability, droplet-based systems have become potent high-throughput platforms for synthetic biology research and biomedical applications, such as biomolecule synthesis, delivery, and diagnosis.[201] External stimuli, such as electric fields, magnetic fields, or acoustic waves, were employed to manipulate droplet positions, connections, and interfacial properties. Nonetheless, the research at this stage focused mainly on chemical biology perspectives and did not involve much ionic or iontronic throughput.[202]

Based on this background, the second stage introduced a continuous hydrogel dropletronic network, which was a significant advancement toward scalable and programmable iontronic systems. The surfactant-supported assembly of hydrogel droplets was developed to construct a range of dropletronic devices.[79,142,203] In brief, the pregel droplets were deposited in a surfactant-containing oil with a microinjector. The droplets formed interface bilayers (DIBs) within seconds of contact. The DIBs allowed the fabrication of hydrogel assemblies with distinct compartments. This approach produced droplets as small as 0.5 nL, which are less than 100 μm in diameter. After assembly, UV irradiation for 1 min initiated photochemical cross-linking of the hydrogel,[204,205] which ruptured the DIBs, with the constituent surfactants diffusing into the oil phase. The rupture process established ion-conductive pathways, thereby activating the dropletronic devices. The assembly of freestanding microscale hydrogel droplets was used to construct various iontronic modules, circuits, and biointerfaces (Figure 6a). Chemical modifications produced a pair of oppositely charged hydrogels. Microscale assembly of various combinations of hydrogel droplets produced iontronic diodes, npn- and pnp-type transistors, and diverse reconfigurable logic gates. The result was consistent with a model of bipolar membrane heterojunctions (Figure 5a), leading to mobile ion accumulation and high ionic conductivity under forward bias, and ion depletion and low ionic conductivity under reverse bias. Moreover, the dropletronic transistor can serve as a biocompatible sensor to record electrophysiological signals from sheets of human cardiomyocytes, paving a way to the building of miniature bioiontronic systems. Notably, 3D printing can extend droplet fabrication into multilayered architectures.[75] For example, a stacked dropletronic network of 140 droplets was demonstrated as a connected power source.[203] This continuous-stacked transition is conceptually analogous to the transition from 2D to 3D integrated circuits, unlocking higher functional density and computational capability.

3.3.2. Fiber Device. Fiber iontronic device introduces unique advantages in structural flexibility, continuous ion transport, and seamless integration into wearable and textile-based systems.[206] Fiber usually refers to a structure with an aspect ratio greater than 20.[207,208] Fiber iontronic devices have diameters ranging from tens to hundreds of micrometers. They can be fabricated through wet spinning, coaxial printing, or electrospinning, and often incorporate conductive polymers, ion gels, or hydrogels. The flexible morphology enables mechanical compliance and high-aspect-ratio signal delivery, facilitating ionic signal conduction and mechanical stimulus responsiveness. Additionally, the integration of fibers into yarns enables the creation of robust and processable architectures. Further assembling these yarns into fabrics unlocks macroscopic functionality and spatial programmability, such as sensing and energy harvesting. A biomimetic spun silk iontronic fiber was used for intelligent discrimination of motions and tactile stimuli, it can be stretched to 250% without breaking and ionic conductivity remains at 33 mS m^{-1}.[209] When twist or bundle the iontronic fibers, an iontronic yarn was formed, which showed an inherent short-term synaptic plasticity with a memory of ∼6 s, ultralow energy consumption below one femtojoule, and the ability to transduce chemical and optical signals.[210]

Iontronic fabrics can be produced by knitting or weaving thin iontronic fibers. As shown in Figure 6b, a scalable manufacturing process for iontronic fabrics was developed, demonstrating compatibility with modern weaving techniques.[211] The innovative tribo-gap design was responsible for the curvature-sensitive (flexure-sensitive) properties exhibited by the iontronic fabrics. During curvature, a time-varying electric field is generated by ion migration-induced electrostatic induction, producing electrical signals. By combining precise microcurvature detection, this iontronic fabric enabled subtle physiological detection with a sensing limit of 0.1 mm^{-1} curvature, equivalent to a curvature factor of more than 21.8% within a 10° bending range. Notably, by facilitating ion flow through electrostatic induction and tribo-gap design during

https://doi.org/10.1021/acs.chemrev.5c00579
Chem. Rev. 2025, 125, 11840−11877

Table 3. Comparison between Biological Nanopores and Artificial Ion Channels[a]

Parameter	Biological nanopore		Artificial ion channel	
Material	●●	Organic materials	●●●	Inorganic and organic materials
Size control	●	Dependent on the natural structure	●●●	Customizable manufacturing
Voltage range	●	Low (<200 mV)	●●	High (up to several volts)
Current range	●●	pA to nA	●●	pA to μA
Signal quality	●●	High SNR under low operating voltage	●●	High SNR under high operating voltage
Selectivity	●●	Versatile reaction sites in the lumen	●	Mainly by charge and size selection
Modification	●●	Requires single-molecule chemistry	●●	Channel surface modification
Stability	●	Denaturation and membrane rupture	●●	Channel blockage and contamination
Durability	●	Preservation under demanding conditions	●●	Compatible with solid-state encapsulation
Bioenvironment	●●●	Suitable for many biological conditions	●	Limited, requires surface modification
System integration	●●	Platform-based, e.g., droplet networks	●●●	Scalable by solid-state chip manufacturing
Resource availability	●	Needs synthetic biology platforms	●●	Available from multiple suppliers

[a]The number of dots (●) denotes the qualitative strength of a given feature, with examples or relevant metrics denoted for each. Three dots indicate the performance is relatively compatible for practical applications. One dot suggests the feature could be further improved.

flexure, an impressive voltage response of 0.9 V was achieved at a radius of curvature of 6 mm^{-1}. It is worth noting that the structure of iontronic devices is irrelevant to their ion transport pathways. For instance, 2D graphene oxide nanoconfined channels can be produced into flexible fiber devices (~120 μm diameter) for iontronic energy applications.[212]

3.3.3. Thin-Film Device. A thin-film iontronic device features a planar structure that supports multichannel ionic interactions. Thin-film iontronic devices are planar structures with thicknesses typically below 100 μm. These films are often fabricated by spin-coating or layer-by-layer self-assembly, enabling precise control over film thickness, composition, and functionality at the microscale.[213−215] For example, through molecular self-assembly, an iontronic film was developed with controllable thickness, high ionic conductivity of ~14 mS cm^{-1}, and excellent mechanical stretchability exceeding 130% and stability over 700 stretch repetitions.[216] In addition to molecular self-assembly, an iontronic film from flake self-assembly was obtained by using MXene-based films cross-linked by cellulose nanofiber dual networks.[217] The iontronic film showed a high in-plane toughness of 18 MJ m^{-3}, high in-plane and out-of-plane elastic modulus of 0.9 and 3.7 GPa, and conductivity of 1.5 S cm^{-1}. As shown in Figure 6c, inspired by the structural and functional characteristics of biological cellular systems, an iontronic synthetic multicellular hybrid ion pump (SMHIP) film was developed to emulate mechanoreceptor functionality.[218] The SMHIP comprises hydrogen-bonded ion pairs anchored on the surfaces of silica microstructures, which serve as artificial mechanoreceptor cells. The microstructures are embedded within a thermoplastic polyurethane (TPU) elastomer, which acts as an artificial extracellular matrix. Under external mechanical stimuli, the SMHIP exhibits pressure-induced disruption of hydrogen bonds between the ion pairs and the silica surfaces, leading to the release and reversible pumping of ions. This ion movement establishes EDLs at the interface between the SMHIP and the electrodes, resulting in a measurable capacitive response. The capacitance increases proportionally with the contact area, effectively reflecting the magnitude of the applied mechanical pressure. Notably, this iontronic mechanoreceptor film demonstrates exceptional sensitivity from 48 to 5.8 kPa^{-1} across a broad pressure spectrum of 0−135 kPa at an ultralow operating voltage of 1 mV, surpassing the pressure-sensing capabilities of various natural skin mechanoreceptors.

3.4. Advancements and Limitations of Various Artificial Iontronic Systems

Solid-state nanofluidic systems can provide more precise control of ion transport than macroscopic and miniature iontronic devices due to their delicate ion channels. The fabrication of nanofluidic systems can also be scaled up, enabling scalable and reproducible manufacturing.[219−221] However, the mechanical rigidity and limited stretchability of most solid-state materials restrict the integration of nanofluidic devices into soft and deformable systems, which are often required for biomedical and wearable applications. Moreover, the nanoscale confinement, while useful for ionic selectivity, could lead to low ion throughput, necessitating signal amplification and noise reduction approaches. Furthermore, the integration of multiple bulky nanofluidic components into large, multifunctional systems remains complex and costly, limiting their widespread use outside laboratory settings.

By comparison, macroscopic iontronic devices exhibit several advantages, including mechanical flexibility and biocompatibility. Macroscopic iontronic devices allow for seamless integration with soft human tissues, robots, and environmental interfaces. Furthermore, they can be fabricated from cost-effective, soft materials such as hydrogels, ion gels, and elastomers, making them suitable for wearable health monitoring, tactile sensing, ionic actuation, and energy conversion. However, macroscopic systems also face disadvantages that hinder their further development in ion-specific, precision-demanding, or computational scenarios. The low integration density makes it difficult to build complex logic or computing units. The large physical size limits the spatial resolution and response speed of ionic signals. Additionally, the bulky size also restricts the application for confined, implantable bioiontronic devices.

These limitations have driven the development of miniature iontronic devices that retain the ion transport mechanisms of nanofluidic devices but operate at significantly smaller scales than their macroscopic counterparts. From dropletronics to iontronic fibers and thin films, miniature iontronic devices represent the frontier of artificial iontronic systems, showing enhanced functionality, efficiency, and adaptability.[222] Miniaturization of the iontronic device can reduce ionic signal delay and lower power consumption, which are essential for ionic computing. Miniature systems can also allow a close interface to biological tissues for cell-level detection and modulation.[223] This scaling-down trend aligns with the demands of biointerface

https://doi.org/10.1021/acs.chemrev.5c00579
Chem. Rev. 2025, 125, 11840−11877

Table 4. Fabrication Toolbox for Biological Nanopores and Artificial Ion Channels and Systems

	Fabrication	Channel size	Morphology	Material	Reference
Biological nanopores	Recombinant expression	1−5 nm	Determined by protein structure	Engineered variants of natural pores	246−250
Artificial nanopores	Focused electron beam	1−100 nm	Regular (e.g., circular)	Solid-state materials	251−253
	Dielectric breakdown	1−10 nm	Irregularly circular	Insulating materials	254−256
	Etching	2 nm−1 μm	Circular, custom shapes	Metals, semiconductors, ceramics, polymers	257−259
	Atomic layer deposition	10−100 nm	Circular	SiN_x, SiO_2, Al_2O_3	259−261
	Directional-assembly	0.8−15 nm	Regular, periodic pores	Block copolymers, 2D materials	262−264
Artificial iontronic systems	Dry-spinning	nm−mm	Fibers	Conductive polymers, ion-conductive elastomers	209, 265
	Wet-spinning	nm−μm	Fibers	Conductive polymers, silk fibroin, ionic liquid	266−268
	Electrospinning	nm−μm	Porous films	Polymers, composite nanofibers	61, 269−271
	Spin coating	nm−μm	Thin films	Ionic liquid-polymer composites, sol−gels	272−274
	Mold casting	50 nm−10 μm	2.5D structures	Hydrogels, ion elastomers, polymer precursors	275−277
	3D printing	10−100 μm	3D structures	Photocurable polymers, conductive hydrogels, bioinks	77, 79, 142

and biohybrid systems, driving the next generation of intelligent and multifunctional bioiontronics.

4. FROM BIOLOGICAL NANOPORES TO ARTIFICIAL IONTRONIC SYSTEMS

4.1. A Comparison of Biological Nanopores and Artificial Ion Channels

Biological nanopores and artificial ion channels have both been used in single-molecule sensing, ion selection, DNA sequencing, and biomolecular diagnostics. Although both systems fundamentally rely on the detection of ionic current modulations as molecules translocate through nanoscale confinements, they exhibit different physical, chemical, and functional characteristics. A systematic comparison between biological and artificial ion channels is summarized to illustrate their respective advantages, limitations, and applicable scenarios (Table 3).

Biological nanopores show better ion selectivity than artificial ion channels, which is attributed to steric constraints for size exclusion, electrostatic interactions through charged lumen residues, and precise single-molecule chemistry.[99,224,225] These mechanisms enable biological channels to maintain a high ion throughput (10^7−10^8 ions s^{-1}) and selectivity, allowing for extensive applications in biomolecule sequencing.[226,227] Another advantage of biological channels is their low noise level at low frequencies (<100 Hz).[228,229] Wild-type protein channels usually operate at physiological voltages (<200 mV), which is lower than artificial ion channels, resulting in lower signal amplitudes. Moreover, biological nanopores allow precise control over ion transport through lumen modification. Key engineering functionalities include:

- **Ionic rectification**: The strategic placement of charged residues, such as arginine, in the lumen constriction of biological nanopores can create an electrostatic asymmetry, thereby enhancing ionic rectification.[69]
- **Selectivity switching**: Targeted mutagenesis alters coordination chemistry. For example, a single amino acid substitution in the epithelial sodium ion channel can broaden its ion selectivity to include larger species, such as potassium or cesium ions.[230]
- **Conductance tuning**: The insertion of steric elements, such as β-hairpin peptides into the FraC nanopore, can change the channel diameter and modulate its conductance.[231]

In contrast, artificial ion channels show advantages over biological nanopores in other features. First, in terms of material flexibility, artificial ion channels can be fabricated from a wide range of inorganic and organic materials, including silicon nitride, graphene, ion-conducting hydrogel, and glass, enabling tailored properties for specific applications.[232] Their size control is exact, as pore diameters and geometries can be engineered down to the subnanometer scale by using techniques such as focused electron beam and controlled dielectric breakdown, which we will discuss later in the next Section. Additionally, artificial ion channels exhibit superior voltage tolerance, capable of withstanding higher applied voltages than biological nanopores embedded in membranes, thereby facilitating molecular translocation and throughput.[23] In the current range, artificial ion channels can support ionic currents up to microamperes, offering large signals for measurement.[233,234] Artificial ion channels exhibit superior tolerance to operating conditions, thereby enabling the attainment of higher SNR values at high operating voltages and elevated salt concentrations. Furthermore, artificial ion channels are generally more stable than biological nanopores, demonstrating better chemical stability and long-term mechanical durability. They can withstand a range of solvents, pH conditions, mechanical deformations, and degradations, making them suitable for more aggressive or variable operational environments.[235] Their compatibility with system integration, including microfluidic platforms, and solid-state electronic and optical systems, is also a major advantage, promoting the development of compact, scalable sensing devices.[236] Finally, the commercial availability of artificial ion channels has been steadily increasing, making them more accessible for more exhaustive research and industrial use.

Despite these strengths, artificial ion channels face several challenges, including relatively low SNRs under physiologically relevant voltages (<200 mV), limited ion selectivity, and potential toxicity. Signal quality and noise level might be undesirable in artificial ion channels due to intrinsic material defects, surface charge fluctuations, and dielectric noises. To address this, researchers have explored surface passivation techniques, including atomic layer deposition and chemical functionalization, to reduce noise and enhance stability.[237,238] To improve selectivity, artificial ion channels can be modified

https://doi.org/10.1021/acs.chemrev.5c00579
Chem. Rev. 2025, 125, 11840−11877

with chemical groups or hybridized with biomolecules.[239−242] Lastly, solid-state artificial ion channels often require surface modification, such as PEGylation, to improve compatibility with biological samples, whereas biological nanopores can spontaneously insert into biological membranes and function in certain biological conditions.[243−245]

4.2. Common Fabrication Approaches

In this section, we aim to provide a brief overview of the production approaches for biological nanopores and artificial ion channels, and guide our readers through the design and fabrication of artificial iontronic systems. To demonstrate and compare the various areas, we summarized a toolbox of common fabrication approaches in Table 4.

Biological nanopores are mainly synthesized via recombinant expression in microbial hosts, such as *Escherichia coli*. Postexpression, these proteins are purified using affinity chromatography and self-assemble into oligomeric structures upon integration into lipid bilayers or synthetic membranes. To modulate performance, nanopores can be engineered through site-directed mutagenesis or chemical modifications to adjust iontronic properties, including pore size and charge distribution. Droplet networks with DIBs provide an integration platform for biological nanopores to build artificial iontronic systems (see Section 2.2 for more details). Alternatively, in integrated sequencing devices, such as the MinION developed by Oxford Nanopore Technologies, nanopores are embedded in patterned membrane arrays.[103] Each nanopore is individually addressable, allowing for parallel sequencing of multiple DNA or RNA molecules. The incorporation process involves aligning and securing the membrane with embedded nanopores onto electronic platforms that can detect ionic current changes as nucleic acids translocate through the pores.

Artificial nanopores are typically fabricated based on solid-state substrates using approaches to pattern cavities as ion channels.[278] Focused electron beam sculpting uses high-energy electrons, often from transmission electron microscopes, to drill through materials with nanometer precision.[279−281] This method enables atomic-scale control over pore size and shape, which is essential for single-molecule sensing applications. However, the technique is costly, time-consuming, and impractical for scale-up production. In contrast, dielectric breakdown creates pores by applying an intense electric field across a thin insulating membrane, causing a local material breakdown.[282−284] This approach is inexpensive and can be performed *in situ* under aqueous conditions, facilitating real-time control over pore size through feedback mechanisms.[256] Nevertheless, dielectric breakdown often produces pores with irregular geometries and local damage, reducing device reliability. Wet and dry etching offer scalability for material removal and the fabrication of large numbers of nanopores.[285,286] Etching selectively removes material along the tracks from heavy ion irradiation, producing pores with adjustable sizes based on etching time and conditions. Despite its simplicity and scalability, etching is hindered by limited precision, and the requirement for masks further complicates the fabrication process. For fine-tuning existing nanopores, atomic layer deposition is used to deposit conformal thin films layer by layer, enabling atomic-level control over pore size and surface chemistry.[287−289] However, the deposition process is demanding and needs to be applied to prepared nanopores, restricting its use to specialized applications.

Moving beyond nanopores to nanochannels, the fabrication of artificial iontronic systems employs a range of soft-material approaches, including dry spinning, electrospinning, spin coating, mold casting, and 3D printing. Spinning methods may utilize vapor-induced phase separation, wherein exposure of the polymer solution to a nonsolvent vapor, typically water vapor, initiates phase separation. This process leads to the formation of nanopores within the fibers. This results in the formation of artificial nanopores within the fiber. Additionally, the premixing of sacrificial nanofibers into spinning solutions during spinning has also been shown to facilitate the introduction of artificial nanochannels.[290,291] Dry spinning enables the production of continuous polymer fibers by extruding a solution through a spinneret and allowing the solvent to evaporate.[64] It offers reasonable control over fiber diameter but suffers from limitations in material choice and uniformity. Dry spinning produces continuous polymer fibers by extruding a solution through a spinneret and allowing the solvent to evaporate. It offers reasonable control over fiber diameter but is limited in material choice and uniformity. Unlike pure spun fibers, dry-spinning techniques can also be applied as coating techniques to commercial fibers (e.g., silicon rubber) to obtain iontronic fibers.[269] Electrospinning creates fibrous films with nanoscale fibers and interconnected porosity.[292−295] Parameters like voltage, solution viscosity, and collector distance can be adjusted to introduce high surface area and interconnected channels. However, ensuring channel uniformity across large areas can be challenging, and the high fabrication voltage is a limitation for electrochemically active materials. Spin coating forms thin polymer films with controlled thicknesses using centrifugal forces, which is ideal for layering materials uniformly.[296,297] By spin coating nanoparticle-doped solution and removing the sacrificial nanoparticles afterward, artificial nanochannels can be fabricated inside the polymer films. More cost-effective methods, such as scrape coating and freeze-drying, are better suited to larger porous structures than to precise nanochannel fabrication.[298,299] Although scalable, scrape coating struggles with fine control over feature size and uniformity, whereas freeze-drying produces highly porous but heterogeneous structures by removing solvents, which is unsuitable for applications requiring uniform nanochannels. Finally, template method uses predefined porous structures, such as anodized aluminum oxide, to mold nanochannels with high uniformity and aspect ratios.[300−302] The major limitation lies in the fidelity of template removal, which can introduce defects or residual material contamination. 3D printing can offer unprecedented control over complex microscale geometries and can be applied to soft materials, such as droplet 3D printing, which can incorporate nanopores within artificial droplet networks.[79,203] It allows for customizable designs but is hampered by limitations in material printability, production rates, and resolution.

4.3. Key Factors, Computational Methods, and Measurement Techniques

Despite the different device types, the fundamental ion transport behavior can be reflected in the I−V characteristics. The I−V curve shows the relationship between the applied voltage and the resulting ionic current, providing insights into the device's ionic conductance, selectivity for specific ions and molecules, and rectification behavior.[303] These properties are the results of the ion channel's geometry, surface charges, and hydrophobicity profiles.[304] Therefore, the I−V response serves as a primary characteristic to reflect the basic information on the device (also

https://doi.org/10.1021/acs.chemrev.5c00579
Chem. Rev. 2025, 125, 11840−11877

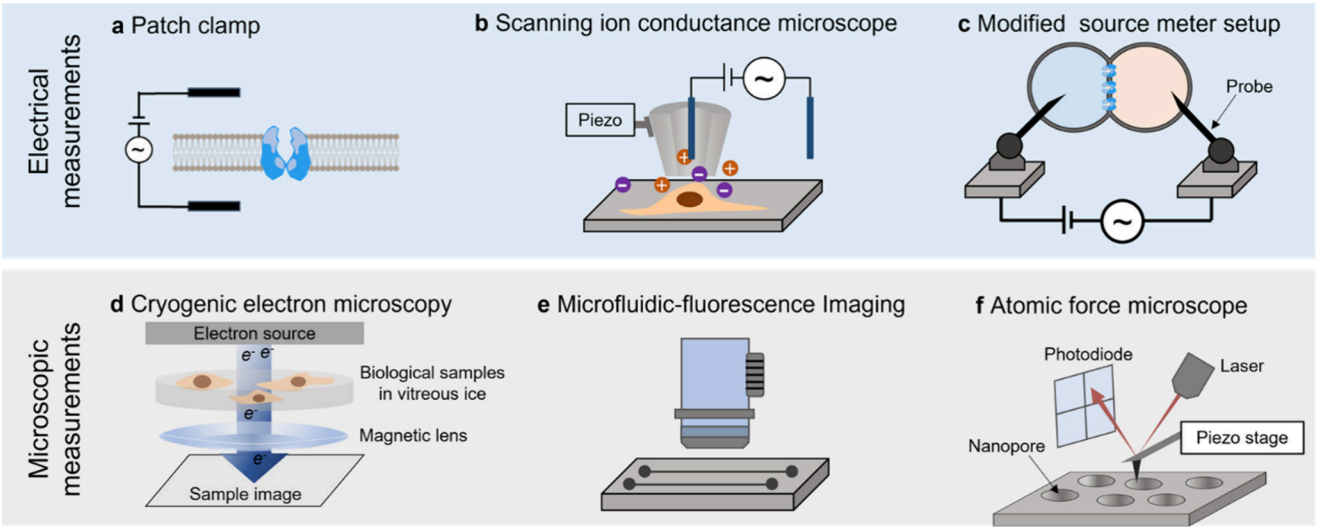

Figure 7. Measurement techniques for nanopore structures and ion transport properties. Electrical approaches include (a) patch clamp for I−V characteristics, (b) scanning ion conductance microscopy for mapping ion transport properties, and (c) a multichannel electrochemical setup for dropletronics. Direct imaging approaches include (d) cryo-EM for characterizing protein nanopore structures, (e) microfluidic fluorescence imaging for studying ion transport properties, and (f) AFM for characterizing size and geometry.

see Section 2.1Section 3.1.2). In biological nanopores, I−V curves are typically linear over moderate voltage ranges, consistent with Ohmic behavior and stable, symmetric pore structures. Deviations from linearity often indicate conformational changes, asymmetric charge distributions, or functionalization-induced gating phenomena. Even angstrom-level modifications in the pore lumen, induced by protein engineering, can significantly alter ion transport properties and the I−V curves. In artificial ion channels, ion transport is influenced by both the channel geometry and its surface charge. Larger variations in channel size due to fabrication inconsistencies can lead to performance variability, resulting in deviations in I−V curves.

In addition to ion transport behavior, mechanical stability and environmental durability, such as resistance to humidity, temperature changes, and chemical exposure, are important factors for the application of various iontronic devices. These factors ensure the operational longevity of iontronic systems, especially under high applied voltages, fluidic flows, or mechanical stress. Biological nanopores require embedding in stable lipid bilayers or polymer supports to maintain integrity. Artificial nanopores, fabricated from more robust materials such as silicon nitride or graphene, exhibit superior mechanical resilience, allowing for use in harsh chemical environments and under high voltages. Artificial systems face a balancing act between maximizing porosity and maintaining structural robustness. Advanced fabrication methods aim to optimize this trade-off, ensuring both high molecular permeability and mechanical durability. While porosity is a key factor for enhancing ion flux and surface area, it is far from the only factor affecting performance. Surface charge density and chemical functionality at nanochannel walls or interfaces can strongly affect ion selectivity, gating behavior, and electroosmotic flow. Likewise, the geometry and confinement scale, such as channel diameter, length, and tortuosity, directly influence ionic mobility and EDL formation.

While the key factors define the fundamental performance of iontronic devices, their optimization increasingly relies on theoretical simulations. Several computational methods have been used to bridge the gap between molecular-scale understanding and device-level functions. For example, (1) density functional theory (DFT) calculations, which captures ion−electron interactions at the quantum level, quantifying adsorption energies, charge transfer, and electronic structures at iontronic interfaces;[305] (2) molecular dynamics (MD) simulations, which serve as a basic yet powerful tool to analyze Ångström-scale channels, offering atomistic insights into ion dehydration, Coulomb interactions, and confinement-induced barriers;[306] (3) finite element modeling (FEM), which operates at the mesoscale to resolve ion and charge transport in complex device geometries, and can extract microscopic parameters such as ionic diffusion coefficients;[307] (4) modified Poisson-Nernst−Planck (mPNP) simulations, which have been used to explain nonlinear ion transport and synaptic plasticity at the function level of neuromorphic iontronic devices;[308] (5) iontronic integrated circuits simulation, which quantifies rectification, leakage, and signal degradation at the circuit level of iontronic computing systems.[309,310]

The key factors mentioned above require accurate measurement techniques for nanopore and nanochannel structures and their ion transport properties.[311−313] Broadly, there are two major categories: electrical measurements (Figure 7, top), which probe ion transport behavior by measuring the temporal change of electrical field signals, and microscopic measurements (Figure 7, bottom), which provide spatial information on ion distribution, channel geometry, and device states.

For electrical measurements, the patch clamp technique is considered the gold standard for nanopore characterization (Figure 7a).[314−316] In this setup, the nanopore separates two electrolyte-filled chambers, and electrodes are placed on either side to apply electrical inputs and measure the outputs. For example, in a voltage-clamp recording, an I−V curve is obtained by sweeping the input voltage over a defined range and recording the output current. Patch-clamp characterization can provide high temporal resolution, from microsecond to millisecond scales, for recording transient translocation events, such as DNA threading and protein binding. The recording can also reveal various nanopore properties, including ionic conductivity, rectification, and gating events. Scanning ion

https://doi.org/10.1021/acs.chemrev.5c00579
Chem. Rev. 2025, 125, 11840−11877

conductance microscopy is another technique that measures ion flux near a nanopore or a porous surface (Figure 7b).[317−320] It operates by positioning a nanopipette filled with electrolyte and a reference electrode close to the sample surface. As the nanopipette scans, changes in ionic current between the pipet and the sample reveal the local ion transport. Scanning ion conductance microscopy enables spatially resolved recording of ion transport behavior across nanopores and mapping of surface charge distributions and conductivity patterns. This method provides a direct localization of ion transport properties, complementing bulk electrical measurements.[321,322] For artificial iontronic systems, such as porous membranes or dropletronic systems, ensemble measurements become more essential for recording the collective behavior of numerous ionic channels. For instance, by incorporating ion channels into droplet interfaces and connecting droplets with external electrodes, the collective ionic currents across the DIBs can be measured. In these setups, a source meter or electrochemical system is connected to the measurement electrodes, which are steered by multiple micromanipulators to insert into the droplets to measure I−V and electrochemical characteristics (Figure 7c).[79,142,203]

For the structural analysis of nanopores, scanning electron microscopy (SEM) and transmission electron microscopy (TEM) were broadly used.[279,323] SEM has been instrumental in visualizing the surface topology of nanopore samples.[243,324] By scanning samples with a focused electron beam and detecting secondary or backscattered electrons, SEM provides detailed images of surface features and pore distribution. TEM, on the other hand, has been a cornerstone in visualizing the internal structure of nanopore samples.[325] By transmitting electrons through ultrathin sections of samples, TEM provides high-resolution images of internal structures.

With the increasing requirements for image resolution and fidelity, cryogenic electron microscopy (Cryo-EM) is now used to determine high-resolution three-dimensional morphologies for the structural analysis, especially for biological nanopores.[326,327] Cryo-EM can resolve conformational states of nanopores under different functional conditions and provide details of oligomeric structures, which are important for understanding translocation behavior and molecular selectivity (Figure 7d).[328] Furthermore, Cryo-EM can be applied to synthetic nanopores to validate structural integrity and assembly, such as DNA origami constructs.[329,330] By preserving the native arrangement of lipids or support membranes, Cryo-EM also enables contextual analysis of nanopore embedding and membrane interactions, offering a near-physiological view of their operational environment. Fluorescence microscopy is commonly used to image ion transport across nanopores or porous membranes.[331,332] Typically, a fluorescent dye sensitive to ionic concentration is included in the system, such as Fluo-4 for calcium ions.[333,334] By tracking changes in fluorescence intensity near and across ion channels, researchers can visualize ion flux patterns, transport rates under different conditions, and localized zones of ion depletion or accumulation (Figure 7e). This method provides a dynamic, real-time view of ion transport phenomena, making it a valuable complement to electrical measurements. However, it often requires careful calibration of fluorescent signals and is prone to signal quenching over time. Atomic force microscopy (AFM), or scanning force microscopy, uses a nanoscale tip to physically scan the sample surface, generating a topographical map with subnanometer vertical resolution.[335] In nanopore research, AFM is beneficial for measuring channel size and morphology, and characterizing surface roughness and near-field properties (Figure 7f).[151,336,337] Unlike the electron microscope, AFM can operate in liquid environments, enabling the imaging of hydrated membranes and ion channels in near-physiological conditions.[338−340]

The measurement techniques for nanopore structures and ion transport can be classified into two categories: direct observation and indirect observation. Direct observation techniques include patch clamp for I−V characteristics, multichannel electrochemical setups for dropletronics, cryo-EM for resolving protein nanopore structures, and AFM for characterizing pore size and geometry. In contrast, indirect observation techniques do not send probes or currents through the nanopore; instead, they monitor changes in the surrounding environment to study ion transport. An example is fluorescence imaging for visualizing ion dynamics, which uses fluorescence signals to reflect changes in ion concentration.

Importantly, when using electrical methods, the choice of electrodes can influence measurement fidelity. This issue becomes critical for miniaturized iontronic devices, for which volume constraints limit the use of bulk electrodes, and interfacial processes, such as Faradaic charge transfer and EDL formation, can influence the measured currents and voltages.[67] Together, integrating both electrical and microscopic measurements, while carefully considering electrode configuration, is essential for reliable characterization of nanopore structures and ion transport properties in iontronic devices.

5. EMERGING APPLICATIONS OF ARTIFICIAL IONTRONIC SYSTEMS

As mentioned in the Introduction, iontronics is an emerging field that leverages the controlled movement and interaction of ions in functional materials to create novel iontronic devices. Unlike conventional electronic systems that rely on electron transport, iontronic systems can harness ion transport to interface with biological systems, perform neuromorphic computing, store energy, and facilitate water treatment (Figure 8).

5.1. Bioiontronics

Iontronics has inherent compatibility with biology through ion movement, opening numerous opportunities for medical diagnostics, therapeutic interventions, and continuous health monitoring. Some of the most exciting and impactful applications of iontronics in this field include implantable biointerfaces, on-skin devices, and wearable systems.[341,342]

Implantable neural interfaces can utilize iontronic transduction mechanisms to facilitate high-fidelity communication with neurons, demonstrating remarkable potential for precise interaction with neural circuits. Traditional metallic electrodes often struggle with high interfacial impedance, mechanical mismatch, and signal degradation over time when implanted in soft neural tissue.[343] In contrast, iontronic systems based on conducting polymers, organic electrochemical transistors (OECTs), and electrolyte-gated interfaces harness ion transport to modulate biological activities with low impedance and high biocompatibility. The ion transport mechanism typically involves volumetric ionic penetration into active materials, which translates ionic neural activity into measurable electronic output or vice versa. These dynamic, reversible ionic processes enable low-voltage operation with high signal transduction fidelity, while the soft, conformable materials reduce immune

https://doi.org/10.1021/acs.chemrev.5c00579
Chem. Rev. 2025, 125, 11840−11877

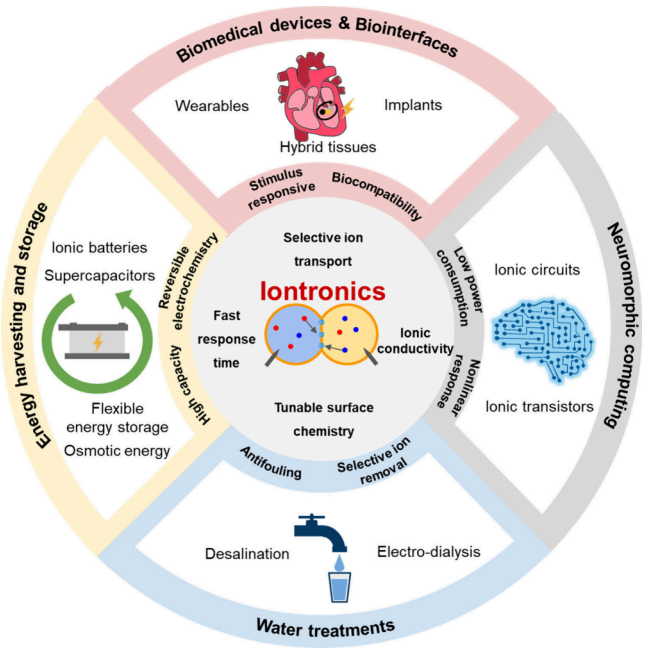

Figure 8. Emerging application fields of iontronics. Iontronics offers transformative potential in biomedical applications, enabling devices that can seamlessly interface with biological tissues. Bioiontronics exhibit low-voltage operation and biocompatibility to ensure safety, and mechanical compliance to match the softness of tissues. By mimicking the ionic signaling of neurons, iontronics offers great potential for neuromorphic computing, featuring hysteretic resistance states, low-power operation, and memory responses that mimic synaptic functions. In the development of energy systems, iontronics is playing an increasingly significant role, with applications including iontronic thermoelectric generators, supercapacitors, osmotic energy harvesters, and batteries. Iontronics can also leverage the controlled movement of ions to achieve selective ion removal and antifouling capabilities, thereby enhancing the efficiency and sustainability of water treatment processes such as desalination and electrodialysis.

response and improve biocompatibility. Recently, a molecularly tailored liquid/liquid (L/L) interfacial ultramicro iontronics (L/L-UIs) supported by an ultramicropipette was presented. The iontronic probe was filled with an organic gel containing lipophilic bis-thioureas ionophores, thereby exhibiting exceptional ion selectivity and sensitivity (Figure 9a).[344] The device demonstrated the potential for *in situ* sensing of other essential but electrochemically silent ions or biomolecules in the brain, thereby advancing both fundamental neuroscience and clinical diagnostics.

Extending beyond implantation, on-skin iontronic devices have emerged as a powerful platform for noninvasive physiological sensing.[345−347] These systems often contain iontronic hydrogels and are structured with microfluidic channels, which can collect sweat or interstitial fluids.[89] Ion transport in these devices occurs through hydrated polymer networks or capillary-driven flow, often modulated by electric fields or concentration gradients. This enables the real-time detection of biochemical markers, such as pH, electrolytes, lactate, glucose, and strains. By mimicking the permeability and softness of human skin, iontronic sensors achieve intimate, stable contact over prolonged periods, enabling continuous and unobtrusive health monitoring in daily life or clinical settings. To enhance pressure-sensing performance in such devices, a recent strategy used crown ethers (CE) as ion-selective mobility amplifiers combined within a poly(vinyl alcohol) (PVA) hydrogel (Figure 9b).[276] The resulting modified hydrogel (PVA-CE) achieved a 30-fold improvement in piezoionic response, enhancing the sensitivity of unmodified PVA from 49 nV Pa^{-1} to 1490 nV Pa^{-1} under pressure below 1 kPa. It featured an ultralow detection limit of 0.2 Pa and a rapid response time of 18.1 ms. The iontronic hydrogel enabled the construction of high-resolution piezoionic skins capable of mapping pressure distributions analogous to the human somatosensory system.

Wearable iontronic devices combine mechanical durability and flexibility, and ion sensitivity to support long-term, mobile healthcare. Integrated into textiles, patches, or soft substrates, these systems can incorporate components such as ion-selective nanopores, electrolyte-gated transistors, and soft sensors.[31] The devices are often self-contained and are designed to function under motion, bending, and other environmental fluctuations. One example was the development of air-operable electrochromic artificial muscles (EAMs) based on vanadium pentoxide nanowires and carbon nanotube yarn (Figure 9c).[348] The EAMs exhibited dual functions of mechanical actuation and color change, achieving a contractile stroke of ∼12% in ambient air under ±4 V, which was accompanied by a visible color transition from yellow to gray. With a reflectance contrast of up to 51%, they provided intuitive visual feedback. A toroidal configuration further enhanced mechanical resilience and response speed, positioning EAMs as promising candidates for bioinspired wearable prosthetics. Another advancement was a textile-based iontronic touch panel, which was fabricated through an in situ growth strategy to ensure skin compatibility and high-resolution tactile sensing.[349] The iontronic interface offered superior mechanical strength of ∼114 MPa and long-term wearability (>7 days). The panel showed a broad pressure-sensing range, from ultralight touches (<3 mg) to heavy loads (>10 kg), enabling practical applications such as wearable keyboards and other forms of human−machine interfaces. Beyond these examples, iontronic sensors that regulate ion dynamics through external physical or chemical fields also represent an emerging direction. Light-driven iontronic devices have been reported for biomimetic visual sensing and color recognition, highlighting their potential in artificial sensory systems.[350,351] Triboelectric-driven iontronics enables self-powered operation, supporting applications such as underwater remote sensing and threshold-triggered sensors, thereby broadening the scope of iontronics in extreme environments. In addition, pressure-sensitive iontronic hydrogels provide versatile platforms for tactile sensing, in which hydrogel deformation modulates ionic conduction, enabling flexible, robust pressure sensors for wearable and biomedical applications.[352]

5.2. Neuromorphic Computing

The field of neuromorphic computing aims to emulate the adaptive, parallel, and energy-efficient processing capabilities of the human brain. Conventional computing architectures, constrained by the separation of memory and logic in von Neumann systems, are becoming increasingly inadequate for tasks that require real-time learning, pattern recognition, and context-aware responses. Iontronics presents a promising alternative by drawing inspiration directly from how biological systems process information, where ionic fluxes facilitate communication and memory at synapses. By controlling ion transport, iontronic devices can replicate the time-dependent

https://doi.org/10.1021/acs.chemrev.5c00579
Chem. Rev. 2025, 125, 11840−11877

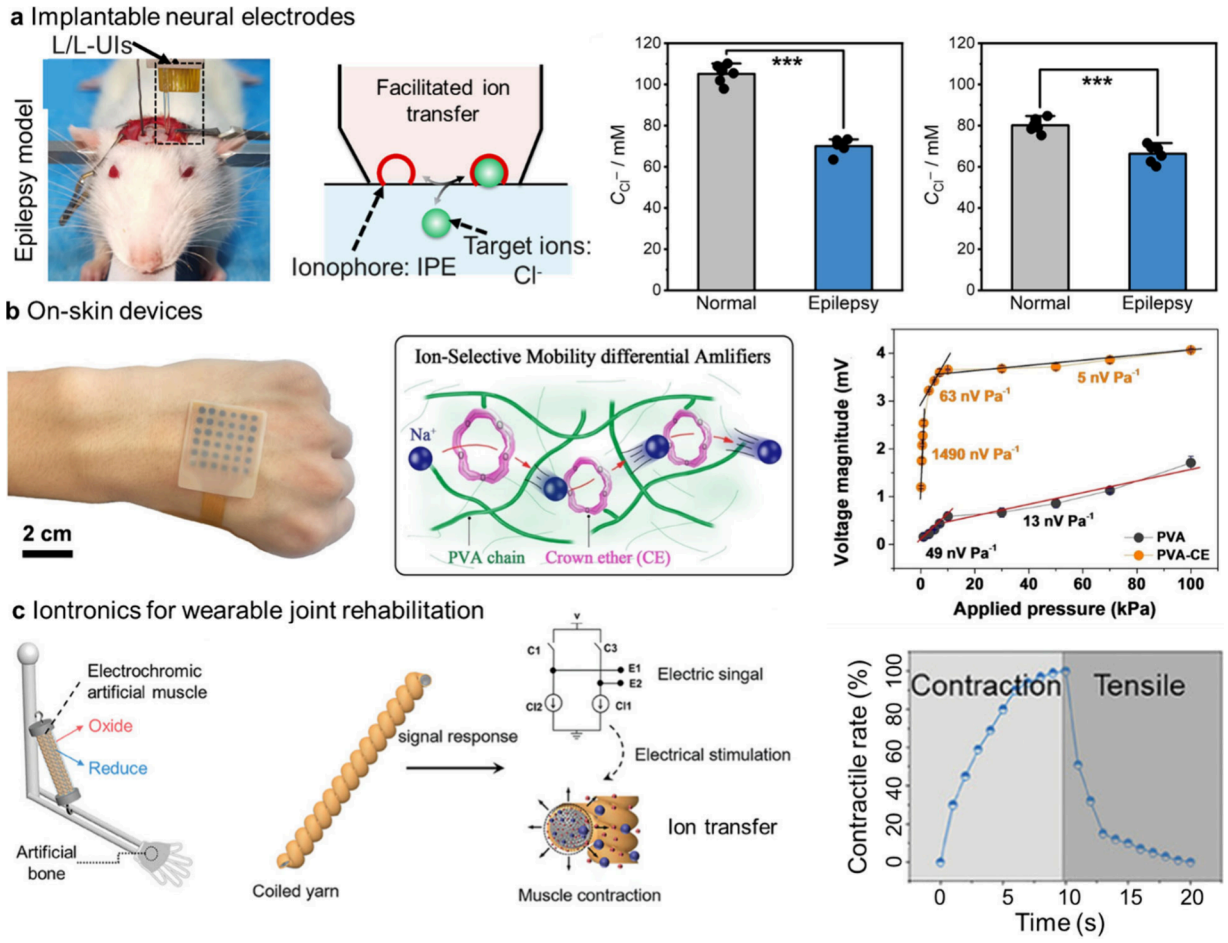

Figure 9. Bioiontronics. (a) Left, *in vivo* determination of Cl^- in the neurodegenerative disease model by the implantable neural electrodes. Middle, dynamic tracking of neuronal chloride regulation mediated by implantable iontronic neural probes *in vivo*. Right, the Cl^- levels obtained by the implantable neural electrodes in the epilepsy rat model's hippocampus and striatum.[344] Reproduced with permission from ref 344. Copyright 2024 American Association for the Advancement of Science. (b) Left, schematic illustration of on-skin ion-selective mobility differential amplifier. Middle, the crown ether is used as an ion-selective mobility differential amplifier for enhancing the pressure-induced voltage response. Right, the PVA-CE hydrogel demonstrates a 30-fold increase in piezoelectric coefficient, reaching a value of 1490 nV Pa^{-1} within a pressure range of 0−1 kPa, which is significantly higher than the unmodified PVA's 49 nV Pa^{-1}.[276] Reproduced with permission from ref 276. Copyright 2024 Wiley. (c) Left, reversible actuation of a wearable iontronic muscle positioned between an artificial human joint. Middle, the actuation mechanism of the iontronic muscle through ion insertion and extraction. Right, the corresponding variation in contractile rate of the iontronic muscle.[348] Reproduced with permission from ref 348. Copyright 2024 Wiley.

and history-sensitive behaviors that drive neural computation, paving a way to artificial intelligence hardware.

One of the foundational elements of iontronic neuromorphic systems is the iontronic transistor.[190] Unlike conventional transistors that modulate current via electrons or holes, iontronic transistors use ions in the gating medium to control electronic conductivity in the channel. These devices often employ electrolyte gating, in which an electric field induces ion movement toward or away from the channel interface, thereby altering ionic conductivity through electrostatic or electrochemical mechanisms. This time-dependent ionic modulation enables iontronic transistors to emulate synaptic behaviors, including short-term plasticity and long-term memory, which are essential for dynamic signal processing. Recent advances have extended these principles to soft-matter platforms through innovative fabrication strategies for iontronics. A recent study demonstrated that chemically cross-linking the semiconducting polymer poly(3-hexylthiophene-2,5-diyl) (P3HT) with di*tert*-butyl peroxide resulted in a stable active layer with enhanced ion mobility and improved ion-trapping ability. In parallel, a dual-ion gel configuration, combining a conventional ion gel 1-Butyl-3-methylimidazolium bis(trifluoromethylsulfonyl)imide (BMIM:TFSI) with a chitosan-based layer, was developed to improve ion transport (Figure 10a).[353] The synergy of cross-linked semiconductors and ion-enhancing gels resulted in an iontronic electrochemical transistor with high transconductance of 25 F cm^{-1} V^{-1} s^{-1} and long-term synaptic plasticity, demonstrating potential in emulating the behavior of biological synapses.

Iontronic memristor represents another important type of neuromorphic device. Iontronic memristors exhibit resistive switching behavior due to the movement and redistribution of ions within the device structure. Typical mechanisms include filament formation via cation migration, such as silver or copper ions, or modulation of a conductive polymer's redox state through ion intercalation. These ionic processes lead to nonvolatile changes in conductance, enabling synaptic weight storage that reflects learning rules such as long-term potentiation or depression. Iontronic memristors are inherently analog and can enable continuous conductance tuning, a significant

https://doi.org/10.1021/acs.chemrev.5c00579
Chem. Rev. 2025, 125, 11840−11877

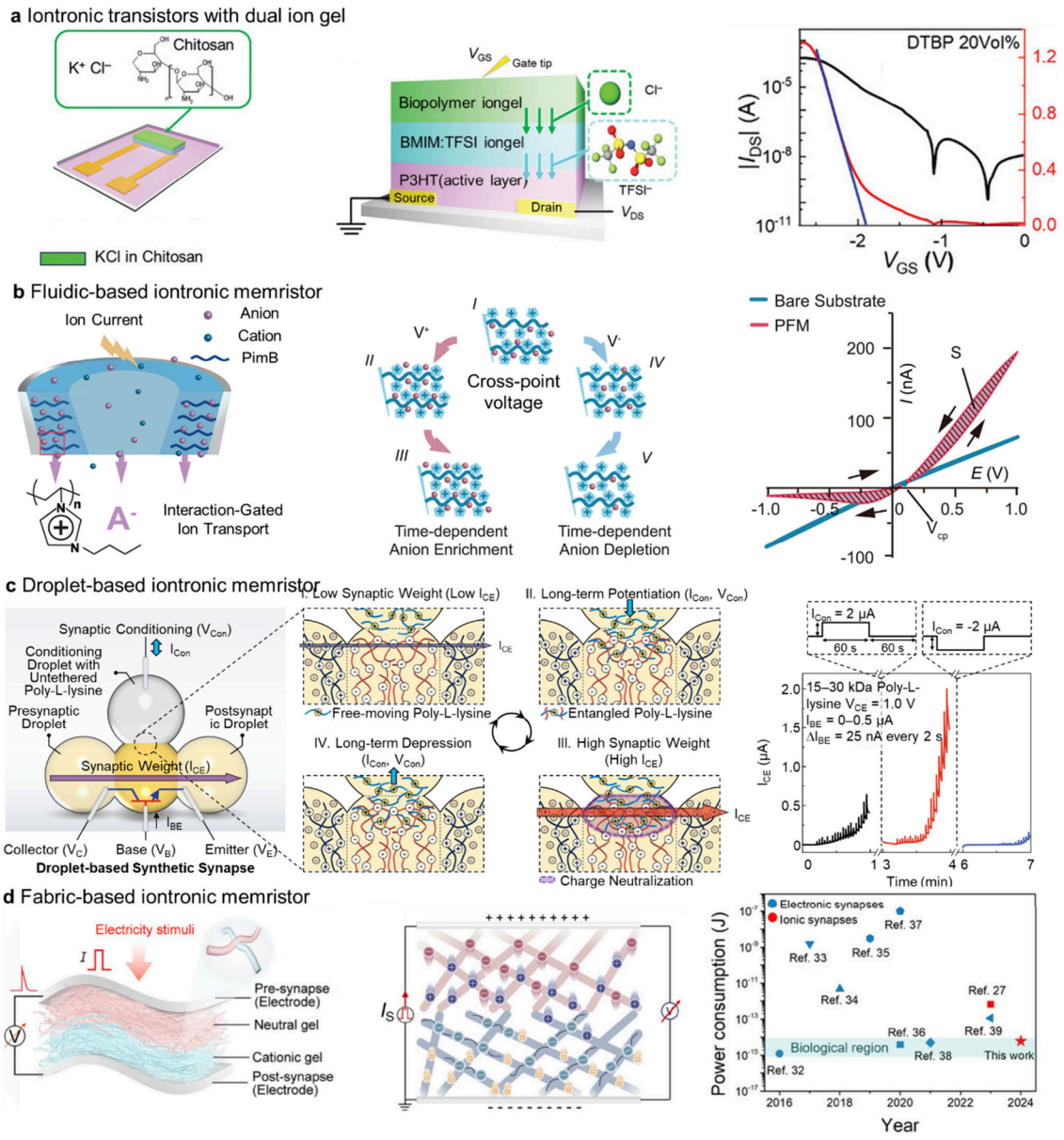

Figure 10. Iontronics for neuromorphic computing. (a) Left, an iontronic transistor with dual ion gel and biopolymer. Middle, the structure of a P3HT iontronic transistor with BMIM:TFSI ion gel and biopolymer-based ion gel. The V_{GS} was applied to the biopolymer-based ion gel via direct contact of the gate tip. Right, transfer characteristic of the iontronic transistor.[353] Reproduced with permission from ref 353. Copyright 2024 Wiley. (b) Left, schematic of the chemical-electric transduction of a polyelectrolyte-confined fluidic-based iontronic memristor. Middle, time-dependent ion redistribution processes in PFMs at potentials higher than the cross-point voltage (from I to III) and lower than the cross-point voltage (from I to V). Right, I−V characteristics of PFM and a bare micropipette. The hysteresis loop area is shaded in purple.[354] Reproduced with permission from ref 354. Copyright 2023 American Association for the Advancement of Science. (c) Left, Schematic of the synthetic synapse composed of an npn-type droplet-based iontronic transistor and a conditioning droplet connected to the base droplet. The collector, base, and emitter droplets emulate the presynaptic neuron, synaptic cleft, and postsynaptic neuron, respectively. Middle, the conditioning droplet modulates synaptic weight by delivering poly-L-lysine into the base droplet (transition from I to III) or retracting it (transition from III to IV, then back to I). Arrows indicate current directions: anions serve as charge carriers for the output current (I_{CE}), while cationic poly-L-lysine carries the conditioning current (I_{Con}). Right, Output characteristics of the synthetic synapse following the application of potentiating and depressing I_{Con}, demonstrating synaptic plasticity through modulation of I_{CE}.[79] Reproduced with permission from ref 79. Copyright 2024 American Association for the Advancement of Science. (d) Left, Schematic illustration of the fabric-based iontronic memristor, featuring a bilayer architecture that emulates the structure of a biological synaptic junction. Middle, representation of ion distribution within the device under current pulse stimulation; free anions and cations migrate toward the electrodes, forming electric double layers at the interfaces between the ion-gel and electrodes. Right, the device's energy consumption per synaptic event is comparable to that of biological synapses.[191] Reproduced with permission from ref 191. Copyright 2025 Wiley.

advantage over digital switching elements for brain-like computation. Recent developments include polyelectrolyte-confined fluidic memristors (PFMs), which were shown to replicate neuromorphic functions through ion-polymer interactions that yielded robust ion memory and hysteresis (Figure 10b).[354] PFMs emulated diverse electric pulse patterns at low energy cost, and their fluidic nature allowed for chemical-electrical signal transduction within a single unit. Structurally analogous to biological ion channels, PFMs provided a chemically versatile platform for integrating with living systems,

https://doi.org/10.1021/acs.chemrev.5c00579
Chem. Rev. 2025, 125, 11840−11877

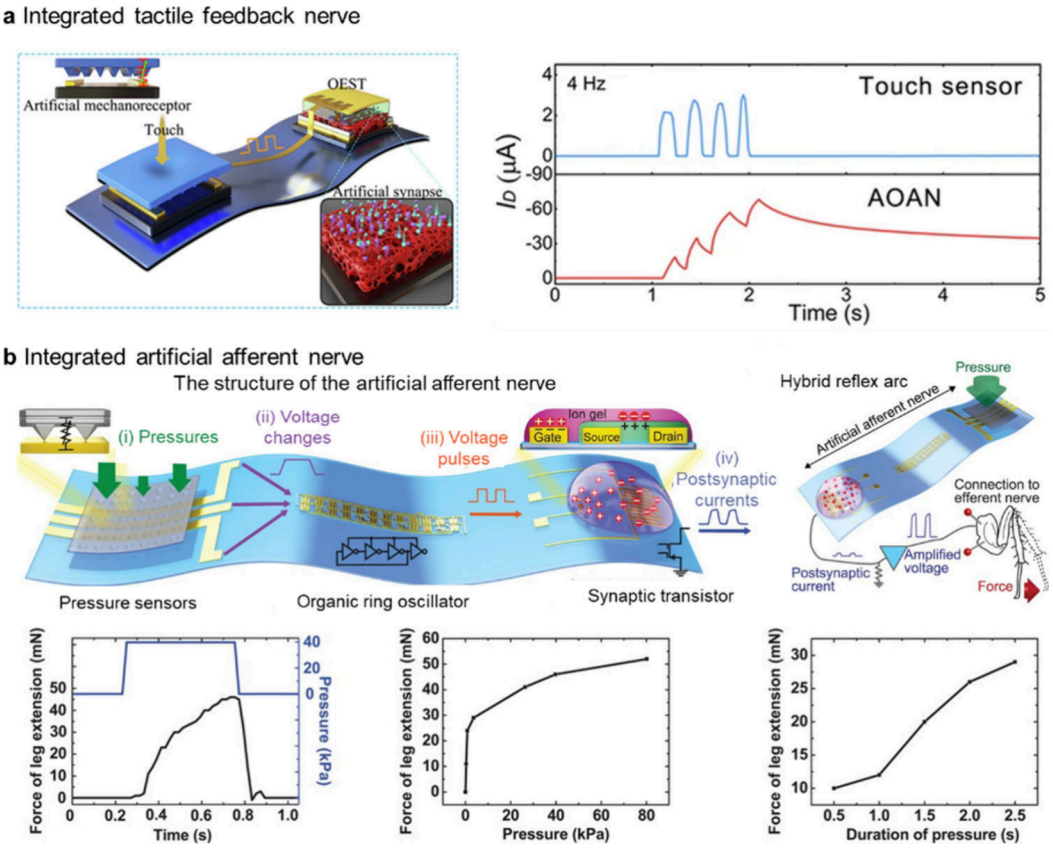

Figure 11. The integrated neuromorphic hardware. (a) Left, the operation of organic electrochemical synaptic transistors (OESTs) mimics the tactile feedback of mechanoreceptors. Right, postsynaptic current triggered by sliding objects on the Integrated neuromorphic hardware, which are collected by the touch sensor and AOAN, respectively.[361] Reproduced with permission from ref 361. Copyright 2024 Springer Nature. (b) Top left, the integrated neuromorphic hardware consists of an artificial afferent nerve, which is composed of pressure sensors, an organic ring oscillator, and a synaptic transistor. The illustration depicts a simplified ring oscillator connected to a synaptic transistor. Top right, the hybrid reflex arc comprises an artificial afferent nerve and a biological efferent nerve. Bottom left, the figure shows the isometric contraction force of the tibial extensor muscle in response to pressure on the artificial afferent nerve, as depicted in (b). The pressure intensity and duration were measured at 39.8 kPa and 0.5 s, respectively. Bottom middle, a summary of the maximum isometric contraction force of the tibial extensor muscle, which depends on the intensity of the pressure. The stimulus application duration was 0.5 s for all measurements. Bottom right, the effects of the duration of the pressure stimulus on the maximum isometric contraction force of the tibial extensor muscle. The amplitude of pressure was fixed at 360 Pa.[362] Reproduced with permission from ref 362. Copyright 2018 American Association for the Advancement of Science.

advancing the design of adaptive, multifunctional neuromorphic interfaces. Moreover, the production of droplet-based iontronic memristors was achieved through the assembly of microscale hydrogel droplets. (Figure 10c) The pulses of current were applied to the conditioning droplet to drive the positively charged poly-L-lysine into or remove it from the base droplet, which contained negatively charged hydrogel. The poly-L-lysine, in turn, modulated the charge selectivity of the base droplet. The movement of the poly-L-lysine was reflected in the output characteristics (I_{CE}) of the memristor, which displayed ion potentiation (i.e., an I_{CE} increase) and depression (i.e., an I_{CE} decrease).[79] In addition, by introducing ion-gel nanofiber networks that mimicked biological synapses, ultralow-power artificial synapses were developed (Figure 10d).[191] These flexible devices transmitted signals via ion-induced capacitive coupling, achieving ephaptic-like communication with an ultralow energy consumption of ∼6 femtojoules. Hysteretic ion transport in these systems gave rise to synaptic memory effects, which enhanced the performance of reservoir computing. Moreover, arrays of such devices exhibited collective oscillatory behavior, enabling working memory functions and emulating the dynamics of a neuronal network.

Building on these device-level components, researchers have begun constructing integrated neuromorphic hardware systems composed of arrays of iontronic devices.[355] Early demonstrations include crossbar arrays of iontronic memristors for pattern classification, iontronic synaptic matrices interfaced with conventional neurons for hybrid systems, and even fully iontronic platforms that perform reservoir computing and spatiotemporal signal processing.[356] For instance, protonic graphene oxide devices were integrated with iontronic gates to realize artificial neural networks.[357] Hybrid circuits combining OECTs and memristive elements also demonstrated in-sensor computing functions.[358,359] These integrated systems leveraged the low-power, soft-material advantages of iontronics and exhibited the feasibility of building large-scale, analog neuromorphic architectures.[360]

In the context of bioinspired somatosensory integration, flexible iontronics have been used to construct an artificial organic afferent nerve (AOAN) that mimics the distributed processing of biological skin (Figure 11a).[361] These systems integrated pressure sensors with ring oscillators to convert pressure inputs (1−80 kPa) into spike trains (0−100 Hz), which were then processed by synaptic iontronic transistors to

https://doi.org/10.1021/acs.chemrev.5c00579
Chem. Rev. 2025, 125, 11840−11877

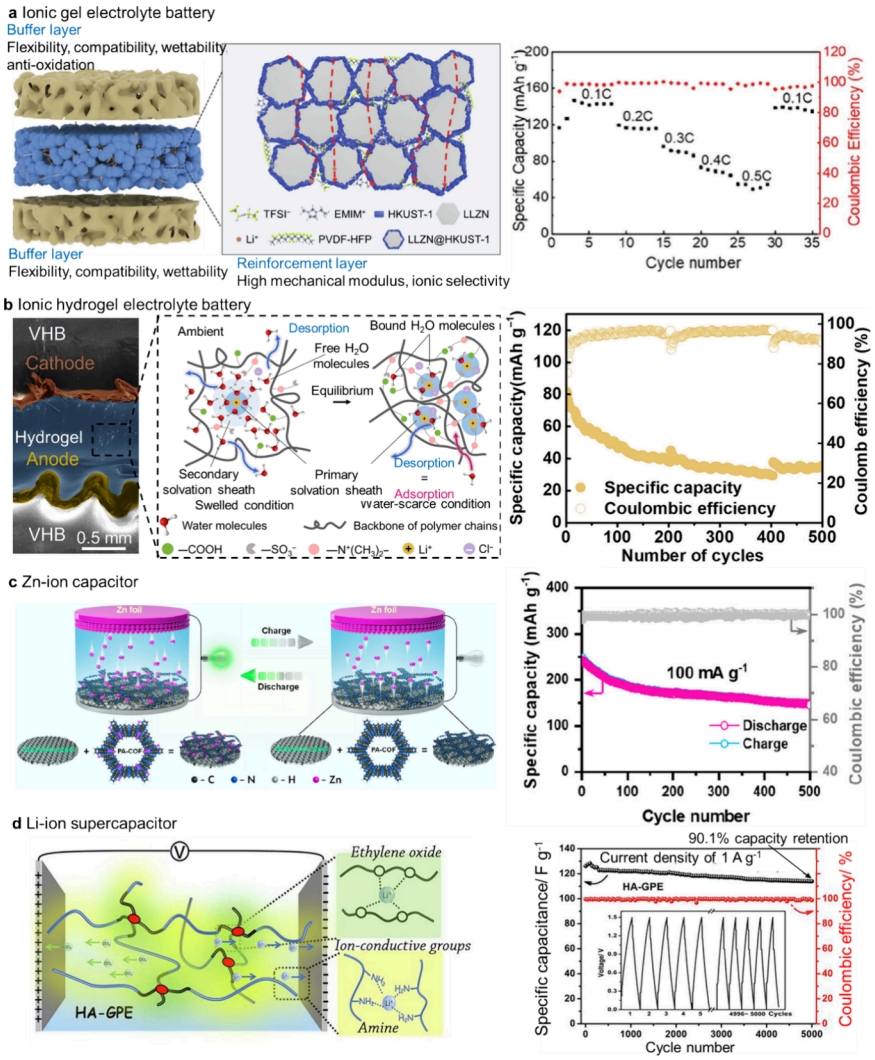

Figure 12. Iontronics for energy harvesting and storage. (a) Left, an iontronic device features a reinforcement layer sandwiched between two buffer layers for high-performance LIBs. Middle, lithium-ion-conducting paths along the iontronic parts in the reinforcement layer. Right, battery stability performance at different rates.[367] Reproduced with permission from ref 367. Copyright 2023 Elsevier. (b) Left, the structure of an iontronic hydrogel electrolyte battery. Middle, the lithium solvation shells in the zwitterionic hydrogel under swollen and water-scarce conditions. Right, specific capacity and coulomb efficiency of the iontronic hydrogel electrolyte battery over cycles at 1 C.[368] Reproduced with permission from ref 368. Copyright 2025 American Association for the Advancement of Science. (c) Left, configuration of a zinc-ion capacitor, in which zinc ions serve a dual role as energy carriers and charge transport media. Right, galvanostatic cycling performance at a current density of 0.1 A g^{-1}.[369] Reproduced from ref 369. Copyright 2020 American Chemical Society. (d) Left, the structure of a lithium-ion supercapacitor, in which lithium ions function as the charge carriers for balancing charge between the electrodes during operation. The ion-conductive groups in the hydrophobic association hydrogel electrolyte (HA-GPE) improve fast lithium-ion transport of lithium-ion supercapacitors. Right, cycling performance of the lithium-ion supercapacitor collected for the current density of 1 A g^{-1}.[371] Reproduced with permission from ref 371. Copyright 2019 Elsevier.

recognize complex tactile patterns. Hierarchical structures enabled the detection of object motion, the fusion of multipoint pressure stimuli, and even Braille recognition. Coupling such artificial nerves with motor pathways enabled hybrid ionic-electronic reflex arcs capable of muscle actuation, highlighting their potential in neurorobotics and neuroprosthetics. In another approach, low-bias artificial afferent nerves based on pressure-sensitive iontronic transistors and mechanoreceptors were developed to enable intelligent robotic touch (Figure 11b).[362] These integrated devices mimicked dendritic integration for directional sensing, while their distributed architecture reduced processing overhead. Integrated into a closed-loop robotic system, they enabled rapid detection and prevention of object slippage by using spike-encoded tactile signal programming. These advancements signify the role of iontronics in low-power, biomimetic tactile systems that integrate sensing, computing, and actuation into a unified platform.

5.3. Energy Harvesting and Storage

Conventional electrochemical systems often rely on rigid, metallic, and resource-intensive materials that are inadequate for emerging demands, such as biointegrated devices and environmentally friendly platforms. Iontronics presents a new approach that uses soft materials with capabilities of fast ion transport and ionic-electronic interactions to achieve energy storage and harvesting. These systems harness ion transport through electrolytes, polymers, and hybrid materials. Iontronics has emerged as a promising interdisciplinary platform for advancing energy storage systems, such as lithium-ion,[363] zinc-ion,[364] and sodium-ion batteries.[275,365]

https://doi.org/10.1021/acs.chemrev.5c00579
Chem. Rev. 2025, 125, 11840−11877

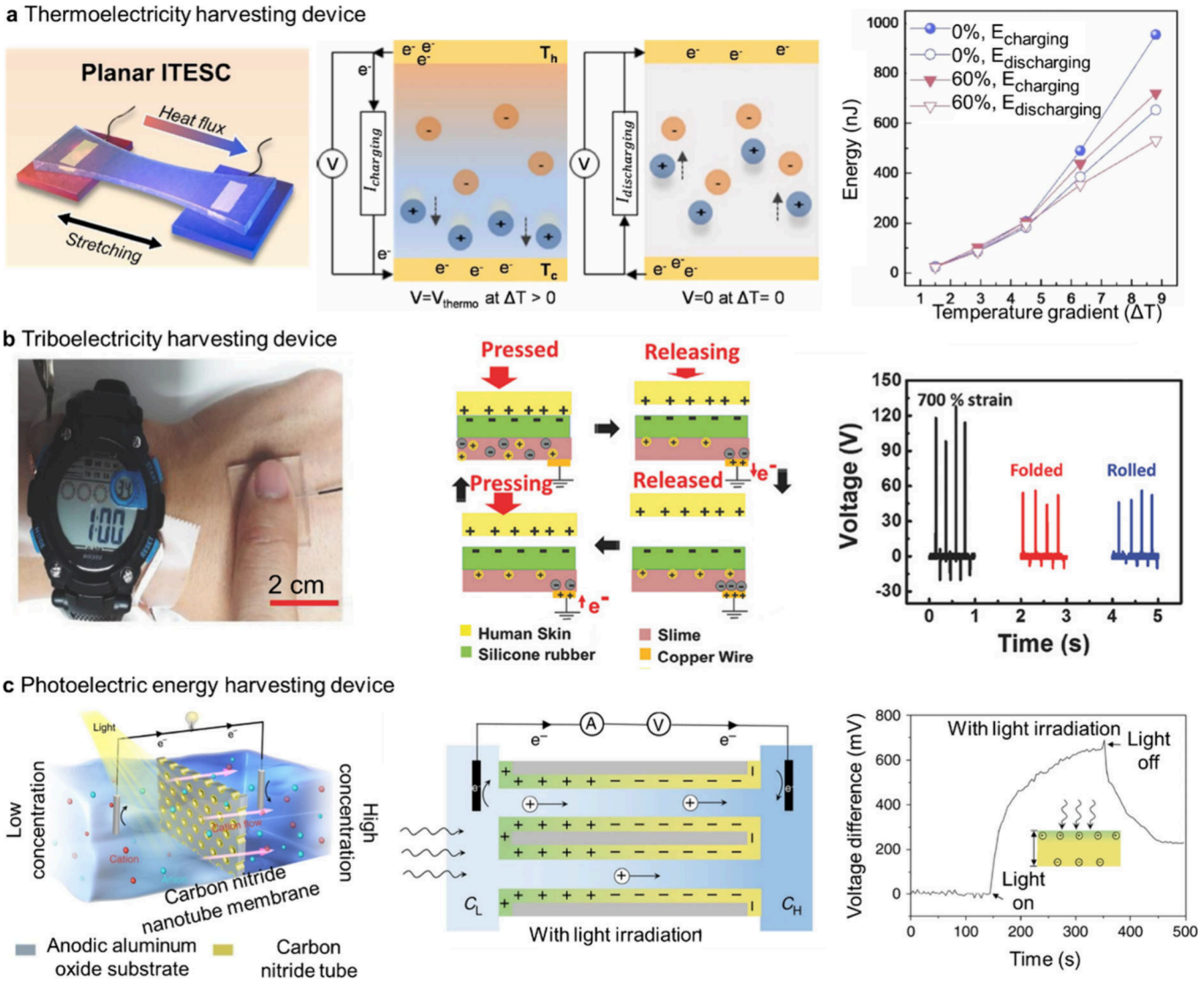

Figure 13. Iontronics for energy harvesting devices. (a) Left, the configuration of the stretchable thermoelectricity harvesting device for generating electricity. Middle, ion movement with and without a temperature difference on both sides. Right, iontronic thermoelectric performance was maintained under various tensile strains.[377] Reproduced with permission from ref 377. Copyright 2023 Elsevier. (b) Left, a transparent and stretchable triboelectric nanogenerator for energy harvesting. Middle: triboelectric energy-harvesting mechanism based on the contact-separation process. Right, the device can withstand a uniaxial strain of up to 700% while maintaining its triboelectric performance.[380] Reproduced with permission from ref 380. Copyright 2017 Wiley. (c) Left, the light-induced ion pump, which can facilitate the transportation of ions in opposition to a concentration gradient. Middle, the surface charge distribution on the nanotube after illumination results in a heterogeneous charge distribution due to the separation of electrons and holes. Right, the voltage difference between illuminated and nonilluminated sides.[381] Reproduced from ref 381. Available under a CC-BY 4.0 license. Copyright 2019 Springer Nature.

For instance, in lithium-ion batteries (LIBs), iontronic elements can be used in both electrode and electrolyte designs, enhancing the performance, safety, and stability of LIBs. For anodes, one approach involved using iontronic elements as carbon precursors to form conductive coatings on active materials, such as $Li_4Ti_5O_{12}$ (LTO).[366] Different from conventional solid carbon sources, iontronic elements penetrate the porous structure of electrode particles due to their fluid nature. Upon thermal treatment, they decompose to form graphitized, nitrogen-doped carbon coatings, resulting in a 3D mixed-conducting network that enhances both electron and ion transport. Moreover, ionic framework-based iontronics is emerging as a structurally integrated component in cathodes. These materials provide well-defined pathways for ion conduction within a crystalline, porous matrix, making them potential scaffolds for hosting redox-active sites or facilitating direct lithium-ion diffusion through the electrode structure. In the electrolyte, iontronic elements are integral to the development of composite solid electrolytes, in which they function synergistically with ceramic fillers and polymer matrix. As shown in Figure 12a, the ionic liquid was integrated into the polymer matrix as a buffer layer to enhance the interface contact and wettability with the electrodes. In the reinforcement layer, the ionic conducting nanocomposite material was used to provide lithium-ion conduction pathways in ceramics ($Li_{6.75}La_3Zr_{1.75}Nb_{0.25}O_{12}$), and was introduced as an efficient matrix for ion selectivity.[367] Moreover, traditional liquid electrolytes based on organic solvents often suffer from flammability, volatility, limited electrochemical stability, and performance degradation due to moisture penetration. In

https://doi.org/10.1021/acs.chemrev.5c00579
Chem. Rev. 2025, 125, 11840−11877

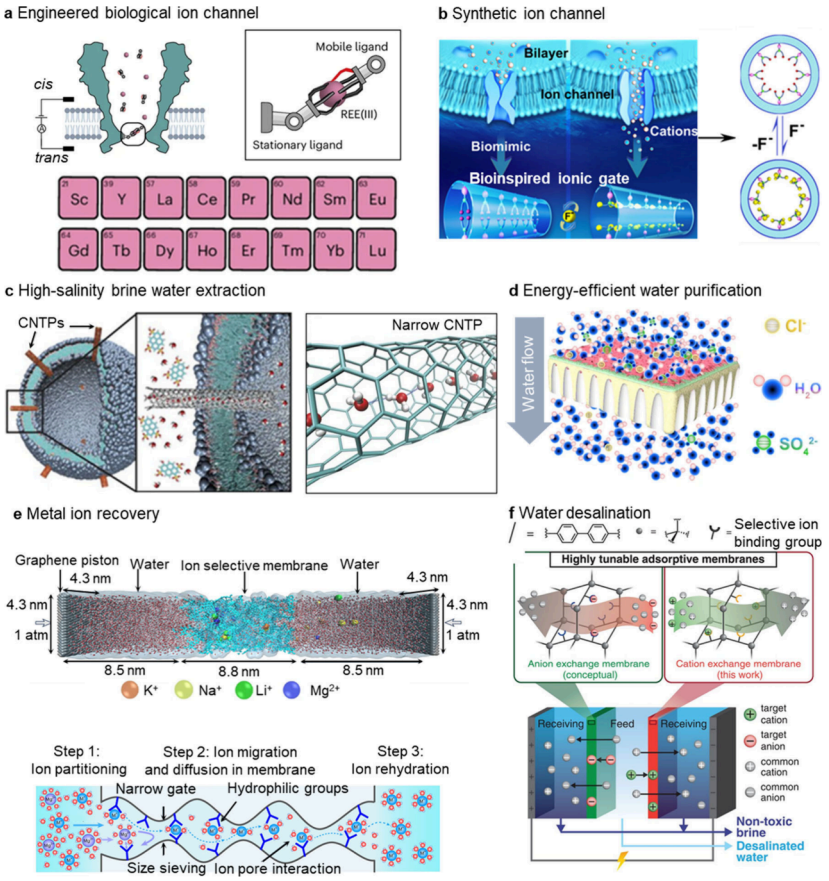

Figure 14. Iontronics for water treatments. (a) An engineered biological ion channel to detect REEs.[387] Bottom, a summary of the detectable REEs. Reproduced with permission from ref 387. Copyright 2025 Springer Nature. (b) A synthetic ion channel closes at the resting state and opens for cation transport upon binding of the fluoride ion (displayed in yellow) to the lumen receptor (gating).[389] Reproduced from ref 389. Copyright 2014 American Chemical Society. (c) Narrow CNTPs enable fast water extraction from high-salinity brine.[392] Left, a vesicle embedded CNTP letting the water molecules pass through. Right, close-ups showing the arrangement of water molecules passing through the CNTPs. Reproduced with permission from ref 392. Copyright 2017 American Association for the Advancement of Science. (d) Schematics of a polyamide membrane composed of nanochannels for fast water permeation and ion selection.[394] Reproduced from ref 394. Available under a CC-BY 4.0 license. Copyright 2023 Springer Nature. (e) Metal ion recovery through an ion separation membrane.[397] Top: The setup for ion separation by two water channels separated by an ion-selective membrane. Bottom: ion separation is derived by an electric field across the membrane. Reproduced from ref 397. Available under a CC-BY 4.0 license. Copyright 2025 Springer Nature. (f) A highly tunable composite membrane for the electrodialysis-based process, which embeds porous aromatic frameworks with selective ion-binding sites into cation-exchange polymer matrices.[398] Reproduced with permission from ref 398. Copyright 2021 American Association for the Advancement of Science.

contrast, iontronic elements bring some advantageous properties. They are nonflammable, nonvolatile, and remain stable over wide electrochemical windows (often exceeding 3 V). For instance, as shown in Figure 12b, the water-scarce hydrogel electrolyte with fluorine-free lithium salt was designed with an encircling stretchable elastomer (VHB) to achieve wide electrochemical stability window up to 3 V in ambient air without packaging, while balancing high stretchability of 1400%, ion conductivity of 41 mS cm^{-1}, and self-healing capabilities for mechanically and chemically safe stretchable LIBs.[368] The iontronic element enhanced the performance of aqueous lithium batteries by reducing lithium−water coordination through strong binding of lithium ions. Under low water content, competitive binding frees lithium ions, improving ion mobility. Moreover, by combining 1-Ethyl-3-methylimidazolium dicyanamide ionic liquid with a flexible polymer, a thermally stable iontronic electrolyte with high ionic conductivity and mechanical robustness was obtained, which could be used in flexible and wearable LIBs.

Iontronic capacitors leverage EDL formation or pseudocapacitive behavior to store energy at the interface between ion-conducting electrolytes and high-surface-area electrodes. For example, Zinc-ion capacitors have garnered increasing attention due to their favorable combination of high-power density, environmental benignity, and intrinsic safety (Figure 12c).[369,370] However, similar to aqueous electrochemical systems, iontronic capacitors face challenges related to charge transport dynamics, interfacial instability, and limited control over ion migration pathways. Iontronics could address these limitations by introducing electrically reconfigurable interfaces and smart ion modulation techniques. Iontronic components, such as electrolytes with unique 3D ionic transport channels, were designed for iontronic capacitors, which facilitated uniform ion distribution and fast ion conduction during charge−discharge cycles.[371,372] Iontronics reduced the risk of localized overconcentration, dendritic growth, and hydrogen evolution. Additionally, such control enhanced the reversibility and rate performance of iontronic capacitors, enabling them to operate efficiently at high current densities. As shown in Figure 12d, the ion-conductive

https://doi.org/10.1021/acs.chemrev.5c00579
Chem. Rev. 2025, 125, 11840−11877

groups have been demonstrated to enhance the lithium-ion transport of the electrolyte employed in lithium-ion supercapacitors.[371] This enhancement has been demonstrated to yield improvements in energy storage capacity, power output, and cycle life.

Iontronics can also be used in osmotic energy harvesting, a process that converts osmotic energy from salinity gradients into electrical output. Recent advances in 2D nanofluidic membranes, such as graphene oxide and MXenes, have enabled the development of flexible and printable devices with significantly improved selectivity, current density, and stability.[212,373,374] Coupling ion transport with interfacial redox reactions can further enhance power densities while overcoming the limited power output of electronics, thereby enabling solid-state, high-performance osmotic converters.[375] Fully printed eel-inspired systems have demonstrated the feasibility of scalable, low-cost fabrication of iontronic power sources.[376]

Besides, in iontronic thermoelectric systems, ion-based elastomeric conductors have been developed to convert thermal gradients into electrical energy with high flexibility and environmental robustness. A recent example demonstrated a fully stretchable iontronic thermoelectric capacitor composed of a stable, high-performance iontronic thermoelectric elastomer and gold nanowire electrodes (Figure 13a).[377] This device had a high thermopower output of ∼39 mV K^{-1} and an ionic conductivity of 0.4 mS cm^{-1} under 250% tensile strain, and showed excellent in-air stability exceeding 60 days. The integration of iontronic thermoelectric devices and stretchable substrates enables energy harvesting even during dynamic deformation, making it suitable for wearable thermal sensors and on-skin generators. Iontronics has also been used in the development of deformable, self-healing, and transparent triboelectric energy harvesters.[378,379] As shown in Figure 13b, a notable advancement was the use of slime-based ionic conductors as current collectors in triboelectric nanogenerators (TENGs).[380] These iontronic-skin TENGs demonstrated remarkable properties, including 92% optical transparency, stretchability up to 700% strain, and an energy generation efficiency 12 times that of conventional silver-based collectors. Most notably, the system exhibited autonomous self-healing, recovering full performance even after 300 cycles of complete breakage. For photoelectric systems, iontronics enables active, directional ion transport driven by light. For instance, an artificial light-driven ion pump based on a carbon nitride nanotube membrane achieved uphill ion transport against a concentration gradient of up to 5000-fold (Figure 13c).[381] Upon illumination, the separation of photoexcited charge carriers across the membrane generated a transmembrane potential, which drove the ion flow. This system demonstrated a stable open-circuit voltage of 550 mV and a current density of 2.4 μA cm^{-2}, with scalability through membrane arrays. Importantly, it showed a novel pathway for converting light into ionic current using simple, cost-effective polymeric materials, suggesting new directions in iontronic solar energy conversion.

5.4. Water Treatments and Environmental Sustainability

Ion channels and iontronic systems are emerging as versatile tools in water technologies, enabling applications ranging from ion detection and separation to water purification. One major driver for nanopore-based ion detection is the monitoring of toxic metal ions, such as arsenic, lead, and mercury, which are crucial for assessing water safety in contaminated areas.[382,383] For instance, Braha et al. engineered a hetero-oligomeric αHL nanopore,[384] composed of 6 wild-type subunits and one mutant with histidine residues, capable of selectively detecting cobalt, zinc, and cadmium ions. Similarly, another study demonstrated the use of a mutant αHL in combination with a chelating peptide to detect toxic thorium ions in water, without cross-reactivity to other metal ions, such as lead, nickel, and mercury.[385]

Beyond toxicity screening, ion nanopores are being explored for the detection and recovery of valuable metals, including rare-earth elements (REEs), which are widely used in electronics, manufacturing, and medical science.[386] Given their environmental and economic costs, efficient REE sensing is essential. To this end, Sun et al. developed a highly selective platform based on the MspA nanopore, functionalized with a nitrilotriacetic aptamer and a secondary ligand, achieving a nanomolar sensitivity limit across all 16 natural REEs.[387] As shown in Figure 14a, REE can be captured by the modified ligands at the pore constriction, enabling gating events for measurements.

Ion-specific detection has also been extended to biologically relevant ions, such as fluoride ion, which is essential for normal body function but can cause disease at high doses.[388] Liu et al., for example, created a fluoride-sensitive iontronic gate using polyimide nanochannels functionalized with 4-aminophenylboronic acid.[389] In fluoride's absence, the nanochannel remained closed, while in its presence, reversible binding induced a conformational shift, opening the channel to ions and modulating ionic current (Figure 14b). The sensor exhibited high selectivity for fluoride ions, with a 2.3-fold increase in current upon fluoride addition. In contrast, other halogenated anions, such as chloride and bromide ions, produced minimal changes in current. The system can maintain performance over at least six reversible on−off cycles.

In addition to detection, ion nanopores enable advanced water purification and ion separation strategies. A key challenge in membrane design for desalination and purification is overcoming the permeability-selectivity trade-off.[390,391] Narrow carbon nanotube porins (CNTPs), with diameters of ∼0.8 nm, have been embedded in lipid bilayers to facilitate ultrafast water transport while maintaining high ion selectivity.[392] As shown in Figure 14c, water molecules aligned within the confined channel, resulting in flow rates surpassing those of biological aquaporins and larger diameter CNTPs, with 2.3×10^{10} water molecules per second for narrow CNTPs, 1.9×10^{9} for wide CNTPs, and 3.9×10^{9} for aquaporin.[393] These nanopores sustained performance even at an elevated salinity of 1 M KCl, exceeding seawater levels of around 0.6 M KCl, making them promising for desalination. To enhance scalability and robustness, several efforts have replaced lipid bilayers with polymeric scaffolds.[394,395] Zhao et al., for instance, developed a polyamide membrane with nanoscale ordered structures by incorporating a carbon nitride ($g\text{-}C_3N_4$) sheet during the interfacial polymerization process.[394] As shown in Figure 14d, this structural modification yielded both high water permeance of 105 L m^2 h^{-1} bar^{-1} and an anion selectivity for chloride ion over sulfate ion with a ratio of ∼130, enabling low-pressure operation and improved energy efficiency. Ion separation is another crucial function of nanopores, particularly in resource recovery during wastewater treatment.[396] Yang et al. designed an ion-selective porous membrane (Figure 14e) that enabled the separation of lithium, sodium, and potassium ions from larger ions, such as magnesium ions, for resource recovery.[397] This mechanism involved the partitioning, dehydration within the micropores, translocation, and subsequent rehydration under an applied electric field. Adsorptive membranes offer a complementary approach to water

https://doi.org/10.1021/acs.chemrev.5c00579
Chem. Rev. 2025, 125, 11840−11877

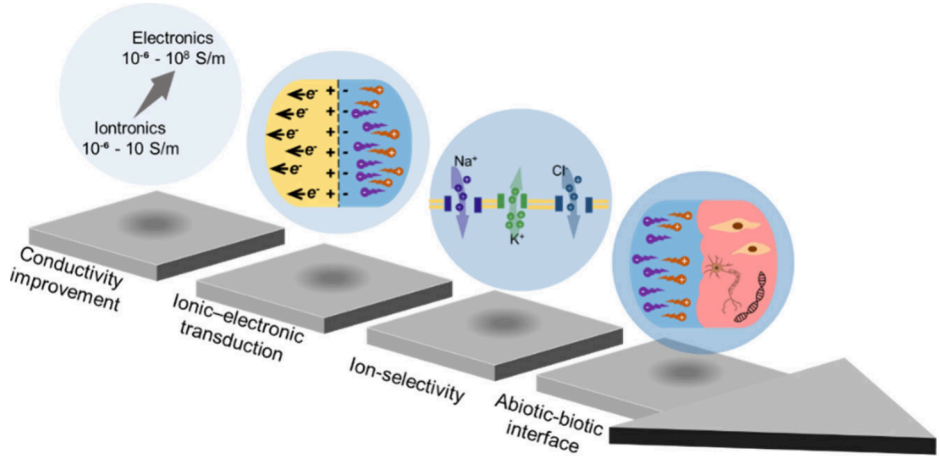

Figure 15. Key challenges for future iontronics research. Addressing challenges in ionic conductivity, ion selectivity, signal conversion between iontronics and electronics, and iontronic-biotic interfaces will enable the development of next-generation intelligent iontronic systems and bioiontronics.

purification and desalination by combining separation and removal processes.[398,399] Uliana et al., embedded porous aromatic frameworks within sulfonated polysulfone cation exchange membranes, enabling both ion transport for water desalination and the capture of target ions for the removal of toxic waste (Figure 14f).[398] This system achieved greater than 97% desalination efficiency, while selectively adsorbing toxic ions, such as lead and mercury, from various water sources, including groundwater, brackish water, and industrial wastewater. Lastly, ion-blocking strategies have been used to develop water-purification membranes.[400−403] Han et al. made graphene oxide membranes with quasi-vertical, asymmetric channels supported on mixed cellulose ester substrates.[403] These membranes exhibited ultrahigh water permeances of ∼4200 L m^{-2} h^{-1} bar^{-1} and >99% rejection rates for heavy metals. Other studies have explored multidimensional architectures for performance optimization.[404] For example, a mixed-dimensional polyamide membrane composed of 1D nanotubes on 2D nanofilm surfaceachieved 30 L m^{-2} h^{-1} bar^{-1} water permeation and >80% rejection rates.[404] Together, these technologies highlight the potential of iontronics as efficient approaches for water desalination and purification.

6. SUMMARY AND OUTLOOK

Iontronics has emerged as a promising paradigm that complements and extends beyond certain capabilities of conventional electronics. Iontronic devices offer unique advantages by leveraging ion transport rather than electron transport, mimicking biological processes and enabling the use of biological soft materials. Both biological components, such as peptide nanopore Alm and protein nanopore αHL, and artificial materials, including CNTs, polymer membranes, and hydrogels, can be used to produce artificial iontronic devices. The versatility of iontronic systems is reflected in their scalability and diversity of forms, spanning from microscale architectures, such as microscale dropletronic networks with nanopore connections, to macroscale implementations, such as wearable sensors. These devices have demonstrated utility across a wide array of applications, including biointerfaces and biosensors, neuromorphic computing, energy conversion and storage, water treatment, and environmental sustainability.

Despite the progress, several critical challenges hinder further application and integration of the artificial iontronic systems (Figure 15). One of the main challenges is to improve ion conductivity while maintaining device stability and functionality. Unlike electrons in conventional electronic devices, which exhibit conductivity of up to 10^8 S m^{-1}, ions typically experience higher resistance and slower mobility due to the reduced fluidity of liquid or electrolytes in iontronic devices, which have a conductivity of less than 10 S m^{-1}. This limitation significantly affects the response speed and energy efficiency of iontronic devices. Developing new high-conductivity iontronic materials and optimizing ion transport pathways within iontronic devices are essential for achieving faster, more efficient ionic conduction. Innovations such as nanostructured ion channels or hybrid organic−inorganic electrolytes could potentially address this issue by enhancing ion mobility without compromising stability.

The signal transduction between iontronic devices and conventional electronic systems remains a challenge due to the fundamental differences between ionic and electronic charge carriers. Addressing this challenge requires an understanding of the mechanisms governing charge transfer at the ionic−electronic interface. Both Faradaic processes, which involve interfacial redox reactions, and non-Faradaic processes, which involve capacitive ionic−electronic pairing, fundamentally influence the efficiency with which iontronic devices convert ionic signals into electronic signals and vice versa.[29,405] The interfacial impedance ($Z_{interface}$) is commonly modeled as a parallel circuit consisting of a charge-transfer resistor (R_e) and an EDL capacitor (C_e), mathematically expressed as $Z_{interface}=(1/R_e+sC_e)^{-1}$, where s represents the signal frequency. Here, R_e reflects the kinetic barrier of interfacial charge transfer determined by Faradaic reactions, while C_e relates to the capacitive coupling of ionic−electronic pairs. Their interplay governs pseudocapacitive interfacial processes, in which interfacial redox reactions and ionic−electronic couplings co-occur. The optimization of this balance can be achieved by enhancing interfacial reaction activity and increasing the accessible surface area.[68,406] Beyond the well-studied differences between ionic and electronic carriers, a key frontier lies in developing new coupling mechanisms, such as ionic−electronic Coulomb drag, which could enable novel routes for signal conversion and amplification.[149] In parallel, reducing R_e remains a central design goal. Promising strategies include the use of 3D porous electrodes that maximize electrochemically active surface area, shorten ion diffusion paths, and enhance ionic−electronic

https://doi.org/10.1021/acs.chemrev.5c00579
Chem. Rev. 2025, 125, 11840−11877

interfacial coupling, as well as the design of mixed-conductive polymers that integrate ionic and electronic conductivity within a single framework to facilitate more efficient interfacial charge transfer.[407−410] Looking ahead, future research should not only balance Faradaic and non-Faradaic contributions to minimize $Z_{interface}$ but also engineer conformal and adaptive interfaces capable of maintaining high C_e and low R_e under varying mechanical and electrical conditions. Such approaches will be essential to achieving seamless integration between iontronic and electronic systems, thereby unlocking their potential in practical applications.

In biological systems, membrane channels exhibit remarkably high selectivity for specific ions, which is essential for precise physiological functions, including neural signaling, muscle contraction, and ion homeostasis. Most biological nanopores are highly specialized for the transport of a single ion species or a narrow group of similar ions rather than accommodating multiple ions simultaneously. This specificity arises from precise pore sizes, electrostatic interactions, dynamic conformational changes, and stimulus-responsive gating mechanisms. As a result, biological nanopores strike a balance between high selectivity and conductivity for single ion species, which have been optimized through evolution for their specific physiological roles. In contrast, iontronic devices cannot easily distinguish among various ions. Nevertheless, precise ion selectivity is essential for maintaining signal fidelity when interfacing with biological tissues. Similarly, in neuromorphic systems, iontronic devices cannot replicate the dynamic ion exchanges that occur during neural signaling, which demands the ability to regulate multiple ionic species simultaneously. To address these challenges, future research can focus on bioinspired design approaches that mimic the selective gating mechanisms of natural nanopores, integrate dynamic control mechanisms that respond to external stimuli, and develop hybrid structures that combine biomimetic features with synthetic robustness. Additionally, adaptive interfaces capable of real-time modulation of ion selectivity can also be explored to achieve a balance between high conductivity and dynamic selectivity.

The last critical challenge is the formation of a stable and efficient interface between iontronics and biological tissues. To ensure adequate performance and long-term durability, iontronic devices must address several key factors, including interface conformity with biological systems, mechanical compatibility, motion artifact control, and long-term stability. The interface conformity to biology and mechanical compatibility require iontronic materials that are soft, flexible, and biocompatible to maintain intimate contact without irritation or detachment.[343] Motion-artifact control demands that iontronic devices incorporate damping materials that can reduce artifacts brought by deformation and strain. Additionally, integrating motion-compensation algorithms into the signal-processing pipeline can further enhance signal fidelity under dynamic conditions.[343] Iontronics must also maintain stable performance over extended periods, especially in wearable or implantable applications. Factors such as mechanical fatigue, material degradation, biofouling, and ionic leakage can compromise the system's longevity. Developing durable, resilient materials is crucial for reliable, long-term operation. Incorporating suitable encapsulations may enhance device performance under physiological conditions, ensuring consistent data quality during prolonged use.

Looking ahead, iontronics is expected to emerge as a crucial technique for biohybrid systems, organoids, and organic electronics. However, compared with mature electronic devices, iontronic devices remain constrained by three pressing challenges. First, device performance is still limited. Many iontronic devices suffer from limited operational stability, wide signal deviation, and slower switching response than their electronic counterparts. Second, scalable manufacturing remains underdeveloped. Many present manufacturing approaches often rely on manual assembly, which hinders reproducibility and integration for scale-up. Third, the development of integrated iontronic circuits or systems is still in its early stages, with only rudimentary demonstrations of iontronic logic gates and simple networks, far from the complexity and density required for massive information processing. Overcoming these barriers will be decisive for transforming iontronic devices from promising laboratory prototypes into practical technologies with real-world impact. The combination of biological tissues with synthetic components can integrate the adaptive and signal-processing capabilities of living systems, along with the stability, scalability, and modularity of artificial systems. From bioactuators powered by muscle tissues to synthetic tissues integrating neurons,[411,412] biohybrid systems offer significant promise for applications ranging from robotics to regenerative medicine and intelligent implants. Iontronics, which could be termed bioiontronics in this context, will play a vital role in integrated biohybrid systems. The system will combine an electronic interface for communicating with external hardware, an iontronic transduction layer that converts electronic signals into biologically relevant cues, and a biological actuation layer, in which engineered cells can communicate with the targeted tissue through native signaling pathways. This stratified design could enhance signal specificity and enable multimodal output while maintaining biocompatibility. Emerging techniques in 3D bioprinting and soft microfluidics have the potential to enable this transition. Beyond this, bioiontronics offers the opportunity to facilitate bidirectional ionic communication between artificial systems and excitable biological tissues, such as the brain and nerves, opening new perspectives in neuromodulation and biological intelligence.[413]

AUTHOR INFORMATION

Corresponding Author

Yujia Zhang − *Laboratory for Bio-Iontronics (BION), Institute of Electrical and Micro Engineering, École Polytechnique Fédérale de Lausanne (EPFL), Lausanne 1015, Switzerland;* orcid.org/0000-0003-3703-8048; Email: yujia.zhang@epfl.ch

Authors

Jiabei Luo − *Laboratory for Bio-Iontronics (BION), Institute of Electrical and Micro Engineering, École Polytechnique Fédérale de Lausanne (EPFL), Lausanne 1015, Switzerland*

Antoine Remy − *Laboratory for Bio-Iontronics (BION), Institute of Electrical and Micro Engineering, École Polytechnique Fédérale de Lausanne (EPFL), Lausanne 1015, Switzerland*

Complete contact information is available at: https://pubs.acs.org/10.1021/acs.chemrev.5c00579

Author Contributions

‡J.L. and A.R. contributed equally. J.L., A.R., and Y.Z. conceived the idea and wrote the paper. All authors read and revised the manuscript. CRediT: **Jiabei Luo** conceptualization, writing -

https://doi.org/10.1021/acs.chemrev.5c00579
Chem. Rev. 2025, 125, 11840−11877

original draft, writing - review & editing; **Antoine Théo Remy** conceptualization, writing - original draft, writing - review & editing; **Yujia Zhang** conceptualization, funding acquisition, project administration, supervision, writing - original draft, writing - review & editing.

Notes

The authors declare no competing financial interest.

Biographies

Jiabei Luo received his B.Sc. in Composite Materials and Engineering and his Ph.D. in Materials Science from Donghua University (China), where he focused on the development of hydrogel bioelectronic interfaces. In 2025, he joined the Laboratory for Bio-Iontronics as a Postdoctoral Researcher and is currently working on multifunctional microdroplet systems and hydrogel wearables.

Antoine Remy received his B.Sc. and M.Sc. degrees in Bioengineering from the École Polytechnique Fédérale de Lausanne (Switzerland), where he specialized in neuroengineering and the development of compliant neural probes. In 2025, he joined the Laboratory for Bio-Iontronics to work on next-generation iontronic systems.

Yujia Zhang is a Tenure Track Assistant Professor of Electrical and Micro Engineering at the School of Engineering, École Polytechnique Fédérale de Lausanne (Switzerland). He is the principal investigator of the Laboratory for Bio-Iontronics (BION). A major interest of his laboratory is the development of iontronic biointerfaces for medicine and hybrid intelligent systems. Recently, his group pioneered dropletronics, in which networks of microscale soft droplets serve as versatile bioiontronic and bioelectronic devices.

ACKNOWLEDGMENTS

This work was supported by a grant from the École Polytechnique Fédérale de Lausanne (EPFL, Y.Z.).

REFERENCES

(1) Zidan, M. A.; Strachan, J. P.; Lu, W. D. The Future of Electronics Based on Memristive Systems. *Nature electronics* **2018**, *1* (1), 22.
(2) van De Burgt, Y.; Melianas, A.; Keene, S. T.; Malliaras, G.; Salleo, A. Organic Electronics for Neuromorphic Computing. *Nature electronics* **2018**, *1* (7), 386.
(3) Zhang, W.; Gao, B.; Tang, J.; Yao, P.; Yu, S.; Chang, M.-F.; Yoo, H.-J.; Qian, H.; Wu, H. Neuro-Inspired Computing Chips. *Nature electronics* **2020**, *3* (7), 371.
(4) Yasuda, H.; Buskohl, P. R.; Gillman, A.; Murphey, T. D.; Stepney, S.; Vaia, R. A.; Raney, J. R. Mechanical Computing. *Nature* **2021**, *598* (7879), 39.
(5) Rogers, J. A.; Someya, T.; Huang, Y. Materials and Mechanics for Stretchable Electronics. *science* **2010**, *327* (5973), 1603.
(6) Shin, J.; Song, J. W.; Flavin, M. T.; Cho, S.; Li, S.; Tan, A.; Pyun, K. R.; Huang, A. G.; Wang, H.; Jeong, S.; et al. A Non-Contact Wearable Device for Monitoring Epidermal Molecular Flux. *Nature* **2025**, *640* (8058), 375.
(7) Clausen, D.; Farley, M.; Little, A.; Kasper, K.; Moreno, J.; Limesand, L.; Gutruf, P. Wearable Continuous Diffusion-Based Skin Gas Analysis. *Nat. Commun.* **2025**, *16*, 4343.
(8) Mahmood, M.; Mzurikwao, D.; Kim, Y.-S.; Lee, Y.; Mishra, S.; Herbert, R.; Duarte, A.; Ang, C. S.; Yeo, W.-H. Fully Portable and Wireless Universal Brain−Machine Interfaces Enabled by Flexible Scalp Electronics and Deep Learning Algorithm. *Nature Machine Intelligence* **2019**, *1* (9), 412.
(9) Yang, W.; Lin, S.; Gong, W.; Lin, R.; Jiang, C.; Yang, X.; Hu, Y.; Wang, J.; Xiao, X.; Li, K.; et al. Single Body-Coupled Fiber Enables Chipless Textile Electronics. *Science* **2024**, *384* (6691), 74.
(10) Ha, K.-H.; Yoo, J.; Li, S.; Mao, Y.; Xu, S.; Qi, H.; Wu, H.; Fan, C.; Yuan, H.; Kim, J.-T.; et al. Full Freedom-of-Motion Actuators as Advanced Haptic Interfaces. *Science* **2025**, *387* (6741), 1383.
(11) Kim, J.; Campbell, A. S.; de Ávila, B. E.-F.; Wang, J. Wearable Biosensors for Healthcare Monitoring. *Nature biotechnology* **2019**, *37* (4), 389.
(12) Zhang, Y.; Rytkin, E.; Zeng, L.; Kim, J. U.; Tang, L.; Zhang, H.; Mikhailov, A.; Zhao, K.; Wang, Y.; Ding, L.; et al. Millimetre-Scale Bioresorbable Optoelectronic Systems for Electrotherapy. *Nature* **2025**, *640* (8057), 77.
(13) Kasper, K. A.; Romero, G. F.; Perez, D. L.; Miller, A. M.; Gonzales, D. A.; Siqueiros, J.; Margolis, D. S.; Gutruf, P. Continuous Operation of Battery-Free Implants Enables Advanced Fracture Recovery Monitoring. *Science Advances* **2025**, *11* (19), No. eadt7488.
(14) Steinmetz, N. A.; Aydin, C.; Lebedeva, A.; Okun, M.; Pachitariu, M.; Bauza, M.; Beau, M.; Bhagat, J.; Böhm, C.; Broux, M.; et al. Neuropixels 2.0: A Miniaturized High-Density Probe for Stable, Long-Term Brain Recordings. *Science* **2021**, *372* (6539), No. eabf4588.
(15) Paulk, A. C.; Kfir, Y.; Khanna, A. R.; Mustroph, M. L.; Trautmann, E. M.; Soper, D. J.; Stavisky, S. D.; Welkenhuysen, M.; Dutta, B.; Shenoy, K. V.; et al. Large-Scale Neural Recordings with Single Neuron Resolution Using Neuropixels Probes in Human Cortex. *Nature neuroscience* **2022**, *25* (2), 252.
(16) Cooper, C. B.; Root, S. E.; Michalek, L.; Wu, S.; Lai, J.-C.; Khatib, M.; Oyakhire, S. T.; Zhao, R.; Qin, J.; Bao, Z. Autonomous Alignment and Healing in Multilayer Soft Electronics Using Immiscible Dynamic Polymers. *Science* **2023**, *380* (6648), 935.
(17) Durand, S.; Heller, G. R.; Ramirez, T. K.; Luviano, J. A.; Williford, A.; Sullivan, D. T.; Cahoon, A. J.; Farrell, C.; Groblewski, P. A.; Bennett, C.; et al. Acute Head-Fixed Recordings in Awake Mice with Multiple Neuropixels Probes. *Nat. Protoc.* **2023**, *18* (2), 424.
(18) Zhong, D.; Wu, C.; Jiang, Y.; Yuan, Y.; Kim, M.-g.; Nishio, Y.; Shih, C.-C.; Wang, W.; Lai, J.-C.; Ji, X.; et al. High-Speed and Large-Scale Intrinsically Stretchable Integrated Circuits. *Nature* **2024**, *627* (8003), 313.
(19) Yuk, H.; Wu, J.; Zhao, X. Hydrogel Interfaces for Merging Humans and Machines. *Nature Reviews Materials* **2022**, *7* (12), 935.
(20) Choi, Y. S.; Jeong, H.; Yin, R. T.; Avila, R.; Pfenniger, A.; Yoo, J.; Lee, J. Y.; Tzavelis, A.; Lee, Y. J.; Chen, S. W.; Knight, H. S.; Kim, S.; Ahn, H. Y.; Wickerson, G.; Vazquez-Guardado, A.; Higbee-Dempsey, E.; Russo, B. A.; Napolitano, M. A.; Holleran, T. J.; Razzak, L. A.; Miniovich, A. N.; Lee, G.; Geist, B.; Kim, B.; Han, S. L.; Brennan, J. A.; Aras, K.; Kwak, S. S.; Kim, J.; Waters, E. A.; Yang, X. X.; Burrell, A.; Chun, K. S.; Liu, C.; Wu, C. S.; Rwei, A. Y.; Spann, A. N.; Banks, A.; Johnson, D.; Zhang, Z. J.; Haney, C. R.; Jin, S. H.; Sahakian, A. V.; Huang, Y. G.; Trachiotis, G. D.; Knight, B. P.; Arora, R. K.; Efimov, I. R.; Rogers, J. A. A Transient, Closed-Loop Network of Wireless, Body-Integrated Devices for Autonomous Electrotherapy. *Science* **2022**, *376* (6596), 1006.
(21) Wu, S. J.; Zhao, X. Bioadhesive Technology Platforms. *Chem. Rev.* **2023**, *123* (24), 14084.
(22) Wu, J.; Deng, J.; Theocharidis, G.; Sarrafian, T. L.; Griffiths, L. G.; Bronson, R. T.; Veves, A.; Chen, J.; Yuk, H.; Zhao, X. Adhesive Anti-Fibrotic Interfaces on Diverse Organs. *Nature* **2024**, *630* (8016), 360.
(23) Bisri, S. Z.; Shimizu, S.; Nakano, M.; Iwasa, Y. Endeavor of Iontronics: From Fundamentals to Applications of Ion-Controlled Electronics. *Adv. Mater.* **2017**, *29* (25), 1607054.
(24) Chang, Y.; Wang, L.; Li, R.; Zhang, Z.; Wang, Q.; Yang, J.; Guo, C. F.; Pan, T. First Decade of Interfacial Iontronic Sensing: From Droplet Sensors to Artificial Skins. *Adv. Mater.* **2021**, *33* (7), 2003464.
(25) Dai, S.; Liu, X.; Liu, Y.; Xu, Y.; Zhang, J.; Wu, Y.; Cheng, P.; Xiong, L.; Huang, J. Emerging Iontronic Neural Devices for Neuromorphic Sensory Computing. *Adv. Mater.* **2023**, *35* (39), 2300329.
(26) Zhang, H.; Wang, S.; Wang, L.; Li, S.; Liu, H.; Zhu, X.; Chen, Y.; Xu, G.; Zhang, M.; Liu, Q.; et al. Bio-Inspired Retina by Regulating Ion-Confined Transport in Hydrogels. *Adv. Mater.* **2025**, *37* (18), 2500809.

https://doi.org/10.1021/acs.chemrev.5c00579
Chem. Rev. 2025, 125, 11840−11877

(27) Zhang, M.; Xu, G.; Zhang, H.; Xiao, K. Nanofluidic Volatile Threshold Switching Ionic Memristor: A Perspective. *ACS Nano* **2025**, *19* (11), 10589.
(28) Yang, C.; Suo, Z. Hydrogel Ionotronics. *Nature Reviews Materials* **2018**, *3* (6), 125.
(29) Yuk, H.; Lu, B.; Zhao, X. Hydrogel Bioelectronics. *Chem. Soc. Rev.* **2019**, *48* (6), 1642.
(30) Li, S.; Cong, Y.; Fu, J. Tissue Adhesive Hydrogel Bioelectronics. *J. Mater. Chem. B* **2021**, *9* (22), 4423.
(31) Luo, J.; Zhang, H.; Sun, C.; Jing, Y.; Li, K.; Li, Y.; Zhang, Q.; Wang, H.; Luo, Y.; Hou, C. Topological Mxene Network Enabled Mixed Ion−Electron Conductive Hydrogel Bioelectronics. *ACS Nano* **2024**, *18* (5), 4008.
(32) Liu, N.; Ma, H.; Li, M.; Qin, R.; Li, P. Electroconductive Hydrogels for Bioelectronics: Challenges and Opportunities. *FlexMat* **2024**, *1*, 269.
(33) Liu, M.; Tao, T. H.; Zhang, Y. Silk Materials Light up the Green Society. *Advanced Energy and Sustainability Research* **2021**, *2* (6), 2100035.
(34) Liu, M.; Zhang, Y.; Tao, T. H. Recent Progress in Bio-Integrated Intelligent Sensing System. *Advanced Intelligent Systems* **2022**, *4* (6), 2100280.
(35) Liu, M.; Zhang, Y.; Wang, J.; Qin, N.; Yang, H.; Sun, K.; Hao, J.; Shu, L.; Liu, J.; Chen, Q.; Zhang, P.; Tao, T. H. A Star-Nose-Like Tactile-Olfactory Bionic Sensing Array for Robust Object Recognition in Non-Visual Environments. *Nat. Commun.* **2022**, *13* (1), 79.
(36) Li, J.; Liu, Y.; Yuan, L.; Zhang, B.; Bishop, E. S.; Wang, K.; Tang, J.; Zheng, Y.-Q.; Xu, W.; Niu, S.; et al. A Tissue-Like Neurotransmitter Sensor for the Brain and Gut. *Nature* **2022**, *606* (7912), 94.
(37) Tehrani, F.; Teymourian, H.; Wuerstle, B.; Kavner, J.; Patel, R.; Furmidge, A.; Aghavali, R.; Hosseini-Toudeshki, H.; Brown, C.; Zhang, F.; et al. An Integrated Wearable Microneedle Array for the Continuous Monitoring of Multiple Biomarkers in Interstitial Fluid. *Nature Biomedical Engineering* **2022**, *6* (11), 1214.
(38) Zhang, A.; Zhao, S.; Tyson, J.; Deisseroth, K.; Bao, Z. Applications of Synthetic Polymers Directed toward Living Cells. *Nature Synthesis* **2024**, *3* (8), 943.
(39) Zhao, C.; Park, J.; Root, S. E.; Bao, Z. Skin-Inspired Soft Bioelectronic Materials, Devices and Systems. *Nature Reviews Bioengineering* **2024**, *2* (8), 671.
(40) Gouaux, E.; MacKinnon, R. Principles of Selective Ion Transport in Channels and Pumps. *Science* **2005**, *310* (5753), 1461.
(41) Maier, J. Nanoionics: Ion Transport and Electrochemical Storage in Confined Systems. *Nature materials* **2005**, *4* (11), 805.
(42) Zhang, M.; Zhao, P.; Li, P.; Ji, Y.; Liu, G.; Jin, W. Designing Biomimic Two-Dimensional Ionic Transport Channels for Efficient Ion Sieving. *ACS Nano* **2021**, *15* (3), 5209.
(43) Xue, Y.; Xia, Y.; Yang, S.; Alsaid, Y.; Fong, K. Y.; Wang, Y.; Zhang, X. Atomic-Scale Ion Transistor with Ultrahigh Diffusivity. *Science* **2021**, *372* (6541), 501.
(44) Zuo, P.; Ye, C.; Jiao, Z.; Luo, J.; Fang, J.; Schubert, U. S.; McKeown, N. B.; Liu, T. L.; Yang, Z.; Xu, T. Near-Frictionless Ion Transport within Triazine Framework Membranes. *Nature* **2023**, *617* (7960), 299.
(45) Allen, W. E.; Chen, M. Z.; Pichamoorthy, N.; Tien, R. H.; Pachitariu, M.; Luo, L.; Deisseroth, K. Thirst Regulates Motivated Behavior through Modulation of Brainwide Neural Population Dynamics. *Science* **2019**, *364* (6437), No. eaav3932.
(46) Marques, J. C.; Li, M.; Schaak, D.; Robson, D. N.; Li, J. M. Internal State Dynamics Shape Brainwide Activity and Foraging Behaviour. *Nature* **2020**, *577* (7789), 239.
(47) Madore, K. P.; Khazenzon, A. M.; Backes, C. W.; Jiang, J.; Uncapher, M. R.; Norcia, A. M.; Wagner, A. D. Memory Failure Predicted by Attention Lapsing and Media Multitasking. *Nature* **2020**, *587* (7832), 87.
(48) Hallschmid, M.; Born, J. A Brain Signal That Coordinates Thought with Metabolism. *Nature* **2021**, *597*, 39.
(49) Welsch, L.; Kieffer, B. L. Opioid Peptide Signal in the Brain Makes Mice Hungrier for Reward. *Nature* **2021**, *598*, 568.
(50) Tong, X.; Ao, Y.; Faas, G. C.; Nwaobi, S. E.; Xu, J.; Haustein, M. D.; Anderson, M. A.; Mody, I.; Olsen, M. L.; Sofroniew, M. V.; et al. Astrocyte Kir4. 1 Ion Channel Deficits Contribute to Neuronal Dysfunction in Huntington's Disease Model Mice. *Nature Neuroscience* **2014**, *17* (5), 694.
(51) Jung, Y.; Kennedy, A.; Chiu, H.; Mohammad, F.; Claridge-Chang, A.; Anderson, D. J. Neurons That Function within an Integrator to Promote a Persistent Behavioral State in Drosophila. *Neuron* **2020**, *105* (2), 322.
(52) Anderson, M. A.; Squair, J. W.; Gautier, M.; Hutson, T. H.; Kathe, C.; Barraud, Q.; Bloch, J.; Courtine, G. Natural and Targeted Circuit Reorganization after Spinal Cord Injury. *Nature Neuroscience* **2022**, *25* (12), 1584.
(53) He, Z.; Dony, L.; Fleck, J. S.; Szałata, A.; Li, K. X.; Slišković, I.; Lin, H.-C.; Santel, M.; Atamian, A.; Quadrato, G.; et al. An Integrated Transcriptomic Cell Atlas of Human Neural Organoids. *Nature* **2024**, *635* (8039), 690.
(54) Watanabe, M.; Thomas, M. L.; Zhang, S.; Ueno, K.; Yasuda, T.; Dokko, K. Application of Ionic Liquids to Energy Storage and Conversion Materials and Devices. *Chem. Rev.* **2017**, *117* (10), 7190.
(55) Lee, H. R.; Kim, C. C.; Sun, J. Y. Stretchable Ionics−a Promising Candidate for Upcoming Wearable Devices. *Adv. Mater.* **2018**, *30* (42), 1704403.
(56) Jo, Y. J.; Ok, J.; Kim, S. Y.; Kim, T. i. Stretchable and Soft Organic−Ionic Devices for Body-Integrated Electronic Systems. *Advanced Materials Technologies* **2022**, *7* (2), 2001273.
(57) Sun, S.; Li, M.; Shi, X. L.; Chen, Z. G. Advances in Ionic Thermoelectrics: From Materials to Devices. *Adv. Energy Mater.* **2023**, *13* (9), 2203692.
(58) Ye, Y.; Yu, L.; Lizundia, E.; Zhu, Y.; Chen, C.; Jiang, F. Cellulose-Based Ionic Conductor: An Emerging Material toward Sustainable Devices. *Chem. Rev.* **2023**, *123* (15), 9204.
(59) Wen, J.; Zhou, L.; Ye, T. Polymer Ionogels and Their Application in Flexible Ionic Devices. *SmartMat* **2024**, *5* (2), No. e1253.
(60) Arbring Sjöström, T.; Berggren, M.; Gabrielsson, E. O.; Janson, P.; Poxson, D. J.; Seitanidou, M.; Simon, D. T. A Decade of Iontronic Delivery Devices. *Advanced Materials Technologies* **2018**, *3* (5), 1700360.
(61) Wang, H. L.; Guo, Z. H.; Pu, X.; Wang, Z. L. Ultralight Iontronic Triboelectric Mechanoreceptor with High Specific Outputs for Epidermal Electronics. *Nano-Micro Letters* **2022**, *14* (1), 86.
(62) Peng, P.; Yang, F.; Wang, Z.; Wei, D. Integratable Paper-Based Iontronic Power Source for All-in-One Disposable Electronics. *Adv. Energy Mater.* **2023**, *13* (42), 2302360.
(63) Kumar, R.; Srivastava, P.; Kumar, T.; Beniwal, S.; Mansoorie, F. N.; Bag, M. Iontronics in Hybrid Halide Perovskites for Smart Portable Electronic Devices and Their Challenges. *ACS Applied Electronic Materials* **2024**, *6* (9), 6325.
(64) Li, Y.; Bai, N.; Chang, Y.; Liu, Z.; Liu, J.; Li, X.; Yang, W.; Niu, H.; Wang, W.; Wang, L.; et al. Flexible Iontronic Sensing. *Chem. Soc. Rev.* **2025**, *54* (10), 4651.
(65) Liu, Y.; Peng, P.; Qian, H.; Wang, Z. L.; Wei, D. Nanoconfined Iontronics and Its Electronic Applications. *Nano Research Energy* **2025**, *4* (2), No. e9120156.
(66) Liu, W.; Mei, T.; Cao, Z.; Li, C.; Wu, Y.; Wang, L.; Xu, G.; Chen, Y.; Zhou, Y.; Wang, S.; et al. Bioinspired Carbon Nanotube−Based Nanofluidic Ionic Transistor with Ultrahigh Switching Capabilities for Logic Circuits. *Science Advances* **2024**, *10* (11), No. eadj7867.
(67) Peng, P.; Yang, F.; Li, X.; Li, S.; Wang, Z.; Wei, D. High-Power Iontronics Enabled by Nanoconfined Ion Dynamics. *Cell Reports Physical Science* **2024**, *5* (2), 101824.
(68) Peng, P.; Qian, H.; Liu, J.; Wang, Z.; Wei, D. Bioinspired Ionic Control for Energy and Information Flow. *International Journal of Smart and Nano Materials* **2024**, *15* (1), 198.
(69) Maglia, G.; Heron, A. J.; Hwang, W. L.; Holden, M. A.; Mikhailova, E.; Li, Q.; Cheley, S.; Bayley, H. Droplet Networks with Incorporated Protein Diodes Show Collective Properties. *Nat. Nanotechnol.* **2009**, *4* (7), 437.

(70) He, X.; Zhang, K.; Li, T.; Jiang, Y.; Yu, P.; Mao, L. Micrometer-Scale Ion Current Rectification at Polyelectrolyte Brush-Modified Micropipets. *J. Am. Chem. Soc.* **2017**, *139* (4), 1396.
(71) Esfandiar, A.; Radha, B.; Wang, F.; Yang, Q.; Hu, S.; Garaj, S.; Nair, R. R.; Geim, A.; Gopinadhan, K. Size Effect in Ion Transport through Angstrom-Scale Slits. *Science* **2017**, *358* (6362), 511.
(72) Li, Z.; Misra, R. P.; Li, Y.; Yao, Y.-C.; Zhao, S.; Zhang, Y.; Chen, Y.; Blankschtein, D.; Noy, A. Breakdown of the Nernst−Einstein Relation in Carbon Nanotube Porins. *Nat. Nanotechnol.* **2023**, *18* (2), 177.
(73) Chen, W.; Zhai, L.; Zhang, S.; Zhao, Z.; Hu, Y.; Xiang, Y.; Liu, H.; Xu, Z.; Jiang, L.; Wen, L. Cascade-Heterogated Biphasic Gel Iontronics for Electronic-to-Multi-Ionic Signal Transmission. *Science* **2023**, *382* (6670), 559.
(74) Tybrandt, K.; Larsson, K. C.; Richter-Dahlfors, A.; Berggren, M. Ion Bipolar Junction Transistors. *Proc. Natl. Acad. Sci. U. S. A.* **2010**, *107* (22), 9929.
(75) Villar, G.; Graham, A. D.; Bayley, H. A Tissue-Like Printed Material. *Science* **2013**, *340* (6128), 48.
(76) Han, C.-G.; Qian, X.; Li, Q.; Deng, B.; Zhu, Y.; Han, Z.; Zhang, W.; Wang, W.; Feng, S.-P.; Chen, G.; et al. Giant Thermopower of Ionic Gelatin near Room Temperature. *Science* **2020**, *368* (6495), 1091.
(77) Zhao, H.; Wang, S.; Li, T.; Liu, Y.; Tang, Y.; Zhang, Z.; Li, H.; Li, Y.; Li, X.; Li, G.; et al. Stretchable Multi-Channel Ionotronic Electrodes for in Situ Dual-Modal Monitoring of Muscle−Vascular Activity. *Adv. Funct. Mater.* **2024**, *34*, 2308686.
(78) Dobashi, Y.; Yao, D.; Petel, Y.; Nguyen, T. N.; Sarwar, M. S.; Thabet, Y.; Ng, C. L.; Scabeni Glitz, E.; Nguyen, G. T. M.; Plesse, C.; et al. Piezoionic Mechanoreceptors: Force-Induced Current Generation in Hydrogels. *Science* **2022**, *376* (6592), 502.
(79) Zhang, Y.; Tan, C. M.; Toepfer, C. N.; Lu, X.; Bayley, H. Microscale Droplet Assembly Enables Biocompatible Multifunctional Modular Iontronics. *Science* **2024**, *386* (6725), 1024.
(80) Sun, T.; Qing, G.; Su, B.; Jiang, L. Functional Biointerface Materials Inspired from Nature. *Chem. Soc. Rev.* **2011**, *40* (5), 2909.
(81) Hou, Y.; Zhou, Y.; Yang, L.; Li, Q.; Zhang, Y.; Zhu, L.; Hickner, M. A.; Zhang, Q.; Wang, Q. Flexible Ionic Diodes for Low-Frequency Mechanical Energy Harvesting. *Adv. Energy Mater.* **2017**, *7* (5), 1601983.
(82) Gomes, B. S.; Simões, B.; Mendes, P. M. The Increasing Dynamic, Functional Complexity of Bio-Interface Materials. *Nature Reviews Chemistry* **2018**, *2* (3), 0120.
(83) Fuller, E. J.; Keene, S. T.; Melianas, A.; Wang, Z.; Agarwal, S.; Li, Y.; Tuchman, Y.; James, C. D.; Marinella, M. J.; Yang, J. J.; et al. Parallel Programming of an Ionic Floating-Gate Memory Array for Scalable Neuromorphic Computing. *Science* **2019**, *364* (6440), 570.
(84) Xiao, K.; Jiang, L.; Antonietti, M. Ion Transport in Nanofluidic Devices for Energy Harvesting. *Joule* **2019**, *3* (10), 2364.
(85) Lv, D.; Zheng, S.; Cao, C.; Li, K.; Ai, L.; Li, X.; Yang, Z.; Xu, Z.; Yao, X. Defect-Enhanced Selective Ion Transport in an Ionic Nanocomposite for Efficient Energy Harvesting from Moisture. *Energy Environ. Sci.* **2022**, *15* (6), 2601.
(86) Zhao, C.; Wang, Y.; Tang, G.; Ru, J.; Zhu, Z.; Li, B.; Guo, C. F.; Li, L.; Zhu, D. Ionic Flexible Sensors: Mechanisms, Materials, Structures, and Applications. *Adv. Funct. Mater.* **2022**, *32* (17), 2110417.
(87) Chen, K.; Ho, D. Piezoionics: Mechanical-to-Ionic Transduction for Sensing, Biointerface, and Energy Harvesting. *Aggregate* **2024**, *5* (1), No. e425.
(88) Xie, Z.; Xiang, Z.; Fu, X.; Lin, Z.; Jiao, C.; Zheng, K.; Yang, M.; Qin, X.; Ye, D. Decoupled Ionic and Electronic Pathways for Enhanced Osmotic Energy Harvesting. *ACS Energy Letters* **2024**, *9* (5), 2092.
(89) Cui, X.; Xi, Y.; Tu, S.; Zhu, Y. An Overview of Flexible Sensors from Ionic Liquid-Based Gels. *TrAC Trends in Analytical Chemistry* **2024**, *174*, 117662.
(90) Jentsch, T. J.; Hübner, C. A.; Fuhrmann, J. C. Ion Channels: Function Unravelled by Dysfunction. *Nature cell biology* **2004**, *6* (11), 1039.
(91) Kunzelmann, K. Ion Channels and Cancer. *J. Membr. Biol.* **2005**, *205* (3), 159.
(92) Smith, R. S.; Walsh, C. A. Ion Channel Functions in Early Brain Development. *Trends in Neurosciences* **2020**, *43* (2), 103.
(93) Cochet-Bissuel, M.; Lory, P.; Monteil, A. The Sodium Leak Channel, NALCN, in Health and Disease. *Frontiers in cellular neuroscience* **2014**, *8*, 132.
(94) Zhao, Q.; Zhou, H.; Chi, S.; Wang, Y.; Wang, J.; Geng, J.; Wu, K.; Liu, W.; Zhang, T.; Dong, M.-Q.; et al. Structure and Mechanogating Mechanism of the Piezo1 Channel. *Nature* **2018**, *554* (7693), 487.
(95) Nilius, B.; Watanabe, H.; Vriens, J. The Trpv4 Channel: Structure-Function Relationship and Promiscuous Gating Behaviour. *Pflügers Archiv* **2003**, *446*, 298.
(96) Yellen, G. The Voltage-Gated Potassium Channels and Their Relatives. *nature* **2002**, *419* (6902), 35.
(97) Karlin, A. Emerging Structure of the Nicotinic Acetylcholine Receptors. *Nat. Rev. Neurosci.* **2002**, *3* (2), 102.
(98) Dani, J. A. Neuronal Nicotinic Acetylcholine Receptor Structure and Function and Response to Nicotine. *International Review of Neurobiology* **2015**, *124*, 3.
(99) Doyle, D. A.; Cabral, J. M.; Pfuetzner, R. A.; Kuo, A.; Gulbis, J. M.; Cohen, S. L.; Chait, B. T.; MacKinnon, R. The Structure of the Potassium Channel: Molecular Basis of K^+ Conduction and Selectivity. *science* **1998**, *280* (5360), 69.
(100) Noskov, S. Y.; Roux, B. Ion Selectivity in Potassium Channels. *Biophys. Chem.* **2006**, *124* (3), 279.
(101) Shi, W.; Friedman, A. K.; Baker, L. A. Nanopore Sensing. *Analytical chemistry* **2017**, *89* (1), 157.
(102) Wei, C.; Pohorille, A. Multi-Oligomeric States of Alamethicin Ion Channel: Assemblies and Conductance. *Biophys. J.* **2023**, *122* (12), 2531.
(103) Ying, Y.-L.; Hu, Z.-L.; Zhang, S.; Qing, Y.; Fragasso, A.; Maglia, G.; Meller, A.; Bayley, H.; Dekker, C.; Long, Y.-T. Nanopore-Based Technologies Beyond DNA Sequencing. *Nat. Nanotechnol.* **2022**, *17* (11), 1136.
(104) Dorey, A.; Howorka, S. Nanopore DNA Sequencing Technologies and Their Applications Towards Single-Molecule Proteomics. *Nat. Chem.* **2024**, *16* (3), 314.
(105) Harriss, L. M.; Cronin, B.; Thompson, J. R.; Wallace, M. I. Imaging Multiple Conductance States in an Alamethicin Pore. *J. Am. Chem. Soc.* **2011**, *133* (37), 14507.
(106) Song, L.; Hobaugh, M. R.; Shustak, C.; Cheley, S.; Bayley, H.; Gouaux, J. E. Structure of Staphylococcal α-Hemolysin, a Heptameric Transmembrane Pore. *Science* **1996**, *274* (5294), 1859.
(107) Stefureac, R.; Long, Y.-t.; Kraatz, H.-B.; Howard, P.; Lee, J. S. Transport of α-Helical Peptides through A-Hemolysin and Aerolysin Pores. *Biochemistry* **2006**, *45* (30), 9172.
(108) Peraro, M. D.; Van Der Goot, F. G. Pore-Forming Toxins: Ancient, but Never Really out of Fashion. *Nature reviews microbiology* **2016**, *14* (2), 77.
(109) Zhou, W.; Qiu, H.; Guo, Y.; Guo, W. Molecular Insights into Distinct Detection Properties of α-Hemolysin, Mspa, Csgg, and Aerolysin Nanopore Sensors. *J. Phys. Chem. B* **2020**, *124* (9), 1611.
(110) Crnković, A.; Srnko, M.; Anderluh, G. Biological Nanopores: Engineering on Demand. *Life* **2021**, *11* (1), 27.
(111) Goyal, P.; Van Gerven, N.; Jonckheere, W.; Remaut, H. Crystallization and Preliminary X-Ray Crystallographic Analysis of the Curli Transporter Csgg. *Structural Biology and Crystallization Communications* **2013**, *69* (12), 1349.
(112) Goyal, P.; Krasteva, P. V.; Van Gerven, N.; Gubellini, F.; Van den Broeck, I.; Troupiotis-Tsaïlaki, A.; Jonckheere, W.; Péhau-Arnaudet, G.; Pinkner, J. S.; Chapman, M. R.; et al. Structural and Mechanistic Insights into the Bacterial Amyloid Secretion Channel Csgg. *Nature* **2014**, *516* (7530), 250.
(113) Butler, T. Z.; Pavlenok, M.; Derrington, I. M.; Niederweis, M.; Gundlach, J. H. Single-Molecule DNA Detection with an Engineered Mspa Protein Nanopore. *Proc. Natl. Acad. Sci. U. S. A.* **2008**, *105* (52), 20647.

https://doi.org/10.1021/acs.chemrev.5c00579
Chem. Rev. 2025, 125, 11840−11877

(114) Laszlo, A. H.; Derrington, I. M.; Gundlach, J. H. Mspa Nanopore as a Single-Molecule Tool: From Sequencing to Sprnt. *Methods* **2016**, *105*, 75.
(115) Kelkar, D. A.; Chattopadhyay, A. The Gramicidin Ion Channel: A Model Membrane Protein. *Biochimica et Biophysica Acta (BBA)-Biomembranes* **2007**, *1768* (9), 2011.
(116) Ryu, H.; Lee, H.; Iwata, S.; Choi, S.; Ki Kim, M.; Kim, Y.-R.; Maruta, S.; Min Kim, S.; Jeon, T.-J. Investigation of Ion Channel Activities of Gramicidin a in the Presence of Ionic Liquids Using Model Cell Membranes. *Sci. Rep.* **2015**, *5* (1), 11935.
(117) Xue, Y.-W.; Itoh, H.; Dan, S.; Inoue, M. Gramicidin a Accumulates in Mitochondria, Reduces Atp Levels, Induces Mitophagy, and Inhibits Cancer Cell Growth. *Chemical Science* **2022**, *13* (25), 7482.
(118) Brewer, D.; Mason, F.; Taylor, A. The Production of Alamethicins by Trichoderma Spp. *Canadian journal of microbiology* **1987**, *33* (7), 619.
(119) Leitgeb, B.; Szekeres, A.; Manczinger, L.; Vagvolgyi, C.; Kredics, L. The History of Alamethicin: A Review of the Most Extensively Studied Peptaibol. *Chemistry & Biodiversity* **2007**, *4*, 1027.
(120) Pieta, P.; Mirza, J.; Lipkowski, J. Direct Visualization of the Alamethicin Pore Formed in a Planar Phospholipid Matrix. *Proc. Natl. Acad. Sci. U. S. A.* **2012**, *109* (52), 21223.
(121) Howorka, S. Building Membrane Nanopores. *Nature Nanotechnol.* **2017**, *12* (7), 619.
(122) Terwilliger, T. C.; Weissman, L.; Eisenberg, D. The Structure of Melittin in the Form I Crystals and Its Implication for Melittin's Lytic and Surface Activities. *Biophysical journal* **1982**, *37* (1), 353.
(123) Raghuraman, H.; Chattopadhyay, A. Melittin: A Membrane-Active Peptide with Diverse Functions. *Bioscience reports* **2007**, *27* (4−5), 189.
(124) Fennouri, A.; Mayer, S. F.; Schroeder, T. B.; Mayer, M. Single Channel Planar Lipid Bilayer Recordings of the Melittin Variant Melp5. *Biochimica et Biophysica Acta (BBA)-Biomembranes* **2017**, *1859* (10), 2051.
(125) Sun, L.; Hristova, K.; Bondar, A.-N.; Wimley, W. C. Structural Determinants of Peptide Nanopore Formation. *ACS Nano* **2024**, *18* (24), 15831.
(126) Zan, B.; Ulmschneider, M. B.; Ulmschneider, J. P. The Difference between Melp5 and Melittin Membrane Poration. *Sci. Rep.* **2025**, *15* (1), 7442.
(127) Akasaki, K.; Karasawa, K.; Watanabe, M.; Yonehara, H.; Umezawa, H. Monazomycin, a New Antibiotic Produced by a Streptomyces. *Journal of Antibiotics, Series A* **1963**, *16* (3), 127.
(128) Becucci, L.; Guidelli, R. Kinetics of Channel Formation in Bilayer Lipid Membranes (Blms) and Tethered Blms: Monazomycin and Melittin. *Langmuir* **2007**, *23* (10), 5601.
(129) Haro-Reyes, T.; Díaz-Peralta, L.; Galván-Hernández, A.; Rodríguez-López, A.; Rodríguez-Fragoso, L.; Ortega-Blake, I. Polyene Antibiotics Physical Chemistry and Their Effect on Lipid Membranes; Impacting Biological Processes and Medical Applications. *Membranes* **2022**, *12* (7), 681.
(130) Tosteson, M.; Tosteson, D. The Sting. Melittin Forms Channels in Lipid Bilayers. *Biophysical journal* **1981**, *36* (1), 109.
(131) Sansom, M. Alamethicin and Related Peptaibols—Model Ion Channels. *Eur. Biophys. J.* **1993**, *22*, 105.
(132) Maraj, J. J.; Haughn, K. P.; Inman, D. J.; Sarles, S. A. Sensory Adaptation in Biomolecular Memristors Improves Reservoir Computing Performance. *Advanced Intelligent Systems* **2023**, *5* (8), 2300049.
(133) Maraj, J. J.; Najem, J. S.; Ringley, J. D.; Weiss, R. J.; Rose, G. S.; Sarles, S. A. Short-Term Facilitation-Then-Depression Enables Adaptive Processing of Sensory Inputs by Ion Channels in Biomolecular Synapses. *ACS Applied Electronic Materials* **2021**, *3* (10), 4448.
(134) Heyer, R.; Muller, R. U.; Finkelstein, A. Inactivation of Monazomycin-Induced Voltage-Dependent Conductance in Thin Lipid Membranes. Ii. Inactivation Produced by Monazomycin Transport through the Membrane. *J. Gen. Physiol.* **1976**, *67* (6), 731.
(135) Chua, L. Resistance Switching Memories Are Memristors. In *Handbook of Memristor Networks*; Springer, 2019; pp 197−230.
(136) Najem, J. S.; Taylor, G. J.; Weiss, R. J.; Hasan, M. S.; Rose, G.; Schuman, C. D.; Belianinov, A.; Collier, C. P.; Sarles, S. A. Memristive Ion Channel-Doped Biomembranes as Synaptic Mimics. *ACS Nano* **2018**, *12* (5), 4702.
(137) Yang, J. J.; Strukov, D. B.; Stewart, D. R. Memristive Devices for Computing. *Nat. Nanotechnol.* **2013**, *8* (1), 13.
(138) Jiang, Q.; Liu, M. Recent Progress in Artificial Neurons for Neuromodulation. *Journal of Functional Biomaterials* **2024**, *15* (8), 214.
(139) Schroeder, T. B.; Guha, A.; Lamoureux, A.; VanRenterghem, G.; Sept, D.; Shtein, M.; Yang, J.; Mayer, M. An Electric-Eel-Inspired Soft Power Source from Stacked Hydrogels. *Nature* **2017**, *552* (7684), 214.
(140) Guha, A.; Kalkus, T. J.; Schroeder, T. B.; Willis, O. G.; Rader, C.; Ianiro, A.; Mayer, M. Powering Electronic Devices from Salt Gradients in Aa-Battery-Sized Stacks of Hydrogel-Infused Paper. *Adv. Mater.* **2021**, *33* (31), 2101757.
(141) Liu, J.; Qing, Y.; Zhou, L.; Chen, S.; Li, X.; Zhang, Y.; Bayley, H. Enzyme-Enabled Droplet Biobattery for Powering Synthetic Tissues. *Angew. Chem., Int. Ed.* **2024**, *63* (44), No. e202408665.
(142) Zhang, Y.; Sun, T.; Yang, X.; Zhou, L.; Tan, C. M.; Lei, M.; Bayley, H. A Microscale Soft Lithium-Ion Battery for Tissue Stimulation. *Nature Chemical Engineering* **2024**, *1* (11), 691.
(143) Siwy, Z.; Heins, E.; Harrell, C. C.; Kohli, P.; Martin, C. R. Conical-Nanotube Ion-Current Rectifiers: The Role of Surface Charge. *J. Am. Chem. Soc.* **2004**, *126* (35), 10850.
(144) Wu, K.; Xiao, K.; Chen, L.; Zhou, R.; Niu, B.; Zhang, Y.; Wen, L. Biomimetic Voltage-Gated Ultrasensitive Potassium-Activated Nanofluidic Based on a Solid-State Nanochannel. *Langmuir* **2017**, *33* (34), 8463.
(145) Qian, H.; Wei, D.; Wang, Z. Bionic Iontronics Based on Nano-Confined Structures. *Nano Research* **2023**, *16* (9), 11718.
(146) Xiong, T.; Li, W.; Yu, P.; Mao, L. Fluidic Memristor: Bringing Chemistry to Neuromorphic Devices. *Innovation* **2023**, *4* (3), 100435.
(147) Zhang, S.; Jiang, J.; Deng, H. Nanoconfined ion and water transport through nanoporous atomically thin membranes: Fabrication and mechanism. *Cell Reports Physical Science* **2025**, *6* (3), 102465.
(148) Ye, T.; Hou, G.; Li, W.; Wang, C.; Yi, K.; Liu, N.; Liu, J.; Huang, S.; Gao, J. Artificial Sodium-Selective Ionic Device Based on Crown-Ether Crystals with Subnanometer Pores. *Nat. Commun.* **2021**, *12* (1), 5231.
(149) Jiang, Y.; Liu, W.; Wang, T.; Wu, Y.; Mei, T.; Wang, L.; Xu, G.; Wang, Y.; Liu, N.; Xiao, K. A Nanofluidic Chemoelectrical Generator with Enhanced Energy Harvesting by Ion-Electron Coulomb Drag. *Nat. Commun.* **2024**, *15* (1), 8582.
(150) Hong, S.; Al Marzooqi, F.; El-Demellawi, J. K.; Al Marzooqi, N.; Arafat, H. A.; Alshareef, H. N. Ion-Selective Separation Using Mxene-Based Membranes: A Review. *ACS Materials Letters* **2023**, *5* (2), 341.
(151) Zhang, Z.; Wen, L.; Jiang, L. Nanofluidics for Osmotic Energy Conversion. *Nature Reviews Materials* **2021**, *6* (7), 622.
(152) Yang, L.; Cao, L. N.; Li, S.; Peng, P.; Qian, H.; Amaratunga, G.; Yang, F.; Wang, Z. L.; Wei, D. MOFs/MXene Nano-Hierarchical Porous Structures for Efficient Ion Dynamics. *Nano Energy* **2024**, *129*, 110076.
(153) Voyer, N.; Robitaille, M. Novel Functional Artificial Ion Channel. *J. Am. Chem. Soc.* **1995**, *117* (24), 6599.
(154) Goto, C.; Yamamura, M.; Satake, A.; Kobuke, Y. Artificial Ion Channels Showing Rectified Current Behavior. *J. Am. Chem. Soc.* **2001**, *123* (49), 12152.
(155) Zhang, Z.; Huang, X.; Qian, Y.; Chen, W.; Wen, L.; Jiang, L. Engineering Smart Nanofluidic Systems for Artificial Ion Channels and Ion Pumps: From Single-Pore to Multichannel Membranes. *Adv. Mater.* **2020**, *32* (4), 1904351.
(156) Zheng, S. p.; Huang, L. b.; Sun, Z.; Barboiu, M. Self-Assembled Artificial Ion-Channels toward Natural Selection of Functions. *Angew. Chem., Int. Ed.* **2021**, *60* (2), 566.

https://doi.org/10.1021/acs.chemrev.5c00579
Chem. Rev. 2025, 125, 11840−11877

(157) Gamper, N.; Shapiro, M. S. Regulation of Ion Transport Proteins by Membrane Phosphoinositides. *Nat. Rev. Neurosci.* **2007**, *8* (12), 921.
(158) Downs, C. A.; Helms, M. N. Regulation of Ion Transport by Oxidants. *American Journal of Physiology-Lung Cellular and Molecular Physiology* **2013**, *305* (9), L595.
(159) Hilgemann, D. W. Regulation of Ion Transport from within Ion Transit Pathways. *J. Gen. Physiol.* **2020**, *152* (1), No. e201912455.
(160) Ali, M.; Yameen, B.; Cervera, J.; Ramirez, P.; Neumann, R.; Ensinger, W.; Knoll, W.; Azzaroni, O. Layer-by-Layer Assembly of Polyelectrolytes into Ionic Current Rectifying Solid-State Nanopores: Insights from Theory and Experiment. *J. Am. Chem. Soc.* **2010**, *132* (24), 8338.
(161) Karnik, R.; Fan, R.; Yue, M.; Li, D.; Yang, P.; Majumdar, A. Electrostatic Control of Ions and Molecules in Nanofluidic Transistors. *Nano Lett.* **2005**, *5* (5), 943.
(162) Cheng, L.-J.; Guo, L. J. Ionic Current Rectification, Breakdown, and Switching in Heterogeneous Oxide Nanofluidic Devices. *ACS Nano* **2009**, *3* (3), 575.
(163) Bu, Y.; Ahmed, Z.; Yobas, L. A Nanofluidic Memristor Based on Ion Concentration Polarization. *Analyst* **2019**, *144* (24), 7168.
(164) Mei, T.; Liu, W.; Sun, F.; Chen, Y.; Xu, G.; Huang, Z.; Jiang, Y.; Wang, S.; Chen, L.; Liu, J.; et al. Bio-Inspired Two-Dimensional Nanofluidic Ionic Transistor for Neuromorphic Signal Processing. *Angew. Chem., Int. Ed.* **2024**, *63* (17), No. e202401477.
(165) Daiguji, H. Ion Transport in Nanofluidic Channels. *Chem. Soc. Rev.* **2010**, *39* (3), 901.
(166) Zhang, Y.; Chen, D.; He, W.; Tan, J.; Yang, Y.; Yuan, Q. Bioinspired Solid-State Ion Nanochannels: Insight from Channel Fabrication and Ion Transport. *Advanced Materials Technologies* **2023**, *8* (12), 2202014.
(167) Liu, P.; Kong, X.-Y.; Jiang, L.; Wen, L. Ion Transport in Nanofluidics under External Fields. *Chem. Soc. Rev.* **2024**, *53* (6), 2972.
(168) Zhou, K.; Perry, J. M.; Jacobson, S. C. Transport and Sensing in Nanofluidic Devices. *Annual Review of Analytical Chemistry* **2011**, *4* (1), 321.
(169) Roman, J.; Français, O.; Jarroux, N.; Patriarche, G.; Pelta, J.; Bacri, L.; Le Pioufle, B. Solid-State Nanopore Easy Chip Integration in a Cheap and Reusable Microfluidic Device for Ion Transport and Polymer Conformation Sensing. *ACS Sensors* **2018**, *3* (10), 2129.
(170) Kim, S.-R.; Zhan, Y.; Davis, N.; Bellamkonda, S.; Gillan, L.; Hakola, E.; Hiltunen, J.; Javey, A. Electrodermal Activity as a Proxy for Sweat Rate Monitoring During Physical and Mental Activities. *Nature Electronics* **2025**, *8*, 353.
(171) Yang, Q.; Ye, Z.; Wu, R.; Lv, H.; Li, C.; Xu, K.; Yang, G. A Highly Sensitive Iontronic Bimodal Sensor with Pressure-Temperature Discriminability for Robot Skin. *Advanced Materials Technologies* **2023**, *8* (21), 2300561.
(172) Li, J.; Zhang, F.; Xia, X.; Zhang, K.; Wu, J.; Liu, Y.; Zhang, C.; Cai, X.; Lu, J.; Xu, L. An Ultrasensitive Multimodal Intracranial Pressure Biotelemetric System Enabled by Exceptional Point and Iontronics. *Nat. Commun.* **2024**, *15* (1), 9557.
(173) Zhang, M.; Yu, R.; Tao, X.; He, Y.; Li, X.; Tian, F.; Chen, X.; Huang, W. Mechanically Robust and Highly Conductive Ionogels for Soft Ionotronics. *Adv. Funct. Mater.* **2023**, *33* (10), 2208083.
(174) Yang, Z.; Duan, Q.; Zang, J.; Zhao, Y.; Zheng, W.; Xiao, R.; Zhang, Z.; Hu, L.; Wu, G.; Nan, X.; et al. Boron Nitride-Enabled Printing of a Highly Sensitive and Flexible Iontronic Pressure Sensing System for Spatial Mapping. *Microsystems & Nanoengineering* **2023**, *9* (1), 68.
(175) Zhang, Y.; Tao, T. H. Skin-Friendly Electronics for Acquiring Human Physiological Signatures. *Adv. Mater.* **2019**, *31* (49), 1905767.
(176) Liu, M.; Zhang, Y.; Zhang, Y.; Zhou, Z.; Qin, N.; Tao, T. H. Robotic Manipulation under Harsh Conditions Using Self-Healing Silk-Based Iontronics. *Advanced Science* **2022**, *9* (2), 2102596.
(177) Lei, Z.; Dai, C.; Hallett, J.; Shiflett, M. Introduction: Ionic Liquids for Diverse Applications. *Chem. Rev.* **2024**, *124* (12), 7533−7535.
(178) Zhang, Y.; Tao, T. H. A Bioinspired Wireless Epidermal Photoreceptor for Artificial Skin Vision. *Adv. Funct. Mater.* **2020**, *30* (22), 2000381.
(179) Sun, H.; Xue, X.; Robilotto, G. L.; Zhang, X.; Son, C.; Chen, X.; Cao, Y.; Nan, K.; Yang, Y.; Fennell, G.; Jung, J.; Song, Y.; Li, H.; Lu, S.-H.; Liu, Y.; Li, Y.; Zhang, W.; He, J.; Wang, X.; Li, Y.; Mickle, A. D.; Zhang, Y. Liquid-Based Encapsulation for Implantable Bioelectronics across Broad Ph Environments. *Nat. Commun.* **2025**, *16* (1), 1019.
(180) Zhu, S.; Chen, S.; Jiang, F.; Fu, C.; Fu, T.; Lin, D.; Meng, Z.; Lin, Y.; Lee, P. S. Biopolymeric Ionotronics Based on Biodegradable Wool Keratin. *Adv. Mater.* **2025**, *37* (22), 2414191.
(181) Wang, J.; Wang, T.; Liu, H.; Wang, K.; Moses, K.; Feng, Z.; Li, P.; Huang, W. Flexible Electrodes for Brain−Computer Interface System. *Adv. Mater.* **2023**, *35* (47), 2211012.
(182) Zhao, Z.; Cao, Z.; Wu, Z.; Du, W.; Meng, X.; Chen, H.; Wu, Y.; Jiang, L.; Liu, M. Bicontinuous Vitrimer Heterogels with Wide-Span Switchable Stiffness-Gated Iontronic Coordination. *Science Advances* **2024**, *10* (10), No. eadl2737.
(183) Zhang, H.; Wang, S.; Wang, L.; Li, S.; Liu, H.; Zhu, X.; Chen, Y.; Xu, G.; Zhang, M.; Liu, Q.; et al. Bio-Inspired Retina by Regulating Ion-Confined Transport in Hydrogels. *Adv. Mater.* **2025**, *37*, 2500809.
(184) Ye, G.; Song, D.; Song, J.; Zhao, Y.; Liu, N. A Fully Biodegradable and Biocompatible Ionotronic Skin for Transient Electronics. *Adv. Funct. Mater.* **2023**, *33* (50), 2303990.
(185) Li, C.; Cheng, J.; He, Y.; He, X.; Xu, Z.; Ge, Q.; Yang, C. Polyelectrolyte Elastomer-Based Ionotronic Sensors with Multi-Mode Sensing Capabilities Via Multi-Material 3d Printing. *Nat. Commun.* **2023**, *14* (1), 4853.
(186) Li, X.; Li, R.; Li, S.; Wang, Z. L.; Wei, D. Triboiontronics with Temporal Control of Electrical Double Layer Formation. *Nat. Commun.* **2024**, *15* (1), 6182.
(187) Jiang, F.; Poh, W. C.; Chen, J.; Gao, D.; Jiang, F.; Guo, X.; Chen, J.; Lee, P. S. Ion Rectification Based on Gel Polymer Electrolyte Ionic Diode. *Nat. Commun.* **2022**, *13* (1), 6669.
(188) Wu, X.; Xu, P.; Zhang, Z.; Yang, Q.; Huang, X.; Pan, P.; Liu, X. Ultrasoft Iontronics: Stretchable Diodes Enabled by Ionically Conductive Bottlebrush Elastomers. *Adv. Funct. Mater.* **2025**, *35*, 2503859.
(189) Shi, Z.; Liu, P.; Zhu, G.; Qu, X.; Cui, Y.; Wang, W.; Zhang, Y.; Dong, X. Ionic Diodes: Pioneering the Future of Ionotronics in Electronics and Beyond. *ACS Appl. Mater. Interfaces* **2025**, *17*, 34892.
(190) Mei, T.; Liu, W.; Xu, G.; Chen, Y.; Wu, M.; Wang, L.; Xiao, K. Ionic Transistors. *ACS Nano* **2024**, *18* (6), 4624.
(191) Chen, Y.; Xia, J.; Qu, Y.; Zhang, H.; Mei, T.; Zhu, X.; Xu, G.; Li, D.; Wang, L.; Liu, Q.; Xiao, K. Ephaptic Coupling in Ultralow-Power Ion-Gel Nanofiber Artificial Synapses for Enhanced Working Memory. *Adv. Mater.* **2025**, *37* (16), 2419013.
(192) Huang, M.; Schwacke, M.; Onen, M.; Del Alamo, J.; Li, J.; Yildiz, B. Electrochemical Ionic Synapses: Progress and Perspectives. *Adv. Mater.* **2023**, *35* (37), 2205169.
(193) Schwacke, M.; Zguns, P.; del Alamo, J.; Li, J.; Yildiz, B. Electrochemical Ionic Synapses with Mg2+ as the Working Ion. *Advanced Electronic Materials* **2024**, *10* (5), 2300577.
(194) He, Y.; Cheng, Y.; Yang, C.; Guo, C. F. Creep-Free Polyelectrolyte Elastomer for Drift-Free Iontronic Sensing. *Nat. Mater.* **2024**, *23* (8), 1107.
(195) Li, S.; Zhang, Z.; Yang, F.; Li, X.; Peng, P.; Du, Y.; Zeng, Q.; Willatzen, M.; Wang, Z. L.; Wei, D. Transistor-Like Triboiontronics with Record-High Charge Density for Self-Powered Sensors and Neurologic Analogs. *Device* **2024**, *2* (6), 100332.
(196) Li, X.; Wei, Y.; Gao, X.; Zhang, Z.; Wang, Z. L.; Wei, D. Harnessing Triboiontronic Maxwell's Demon by Triboelectric-Induced Polarization for Efficient Energy-Information Flow. *Joule* **2025**, *9* (5), 101888.
(197) Isaksson, J.; Kjäll, P.; Nilsson, D.; Robinson, N.; Berggren, M.; Richter-Dahlfors, A. Electronic Control of Ca2+ Signalling in Neuronal Cells Using an Organic Electronic Ion Pump. *Nat. Mater.* **2007**, *6* (9), 673.

https://doi.org/10.1021/acs.chemrev.5c00579
Chem. Rev. 2025, 125, 11840−11877

(198) Chung, T. D.; Han, S. H.; Jeon, J.; Kim, S. I.; Oh, M.-A.; Cho, W.; Yoon, S.-h.; Kim, J. Y.; Shin, C. I. In *Electrochemical Neural Interface and Iontronics, Electrochemical Society Meeting Abstracts prime2020*; The Electrochemical Society, Inc.: 2020; pp 2792. DOI: 10.1149/MA2020-02442792mtgabs.
(199) Arbring Sjöström, T.; Ivanov, A. I.; Kiani, N.; Bernacka-Wojcik, I.; Samuelsson, J.; Saarela Unemo, H.; Xydias, D.; Vagiaki, L. E.; Psilodimitrakopoulos, S.; Konidakis, I.; et al. Miniaturized Iontronic Micropipettes for Precise and Dynamic Ionic Modulation of Neuronal and Astrocytic Activity. *Small* **2025**, *21* (16), 2410906.
(200) Bringer, M. R.; Gerdts, C. J.; Song, H.; Tice, J. D.; Ismagilov, R. F. Microfluidic Systems for Chemical Kinetics That Rely on Chaotic Mixing in Droplets. *Philosophical Transactions of the Royal Society of London. Series A: Mathematical, Physical and Engineering Sciences* **2004**, *362* (1818), 1087.
(201) Booth, M. J.; Restrepo Schild, V.; Downs, F. G.; Bayley, H. Functional Aqueous Droplet Networks. *Molecular BioSystems* **2017**, *13* (9), 1658.
(202) Stephenson, E. B.; Korner, J. L.; Elvira, K. S. Challenges and Opportunities in Achieving the Full Potential of Droplet Interface Bilayers. *Nat. Chem.* **2022**, *14* (8), 862.
(203) Zhao, H.; Wang, S.; Li, T.; Liu, Y.; Tang, Y.; Zhang, Z.; Li, H.; Li, Y.; Li, X.; Li, G.; et al. Stretchable Multi-Channel Ionotronic Electrodes for in Situ Dual-Modal Monitoring of Muscle−Vascular Activity. *Adv. Funct. Mater.* **2024**, *34* (2), 2308686.
(204) Zhang, Y.; Zhou, Z.; Fan, Z.; Zhang, S.; Zheng, F.; Liu, K.; Zhang, Y.; Shi, Z.; Chen, L.; Li, X.; et al. Self-Powered Multifunctional Transient Bioelectronics. *Small* **2018**, *14* (35), 1802050.
(205) Liu, M.; Zhang, Y.; Liu, K.; Zhang, G.; Mao, Y.; Chen, L.; Peng, Y.; Tao, T. H. Biomimicking Antibacterial Opto-Electro Sensing Sutures Made of Regenerated Silk Proteins. *Adv. Mater.* **2021**, *33* (1), 2004733.
(206) Chang, B.; Luo, J.; Liu, J.; Zhang, B.; Zhu, M.; Li, k.; Li, Y.; Zhang, Q.; Shi, G.; Hou, C. A High-Performance Composite Fiber with an Organohydrogel Sheath for Electrocardiogram Monitoring. *Journal of Materials Chemistry C* **2024**, *12* (32), 12413.
(207) Chang, B.; Luo, J.; Xia, J.; Sun, C.; Li, K.; Li, Y.; Zhang, Q.; Wang, H.; Hou, C. Conductive Elastic Composite Electrode and Its Application in Electrocardiogram Monitoring Clothing. *ACS Applied Electronic Materials* **2023**, *5* (4), 2026.
(208) Xu, M.; Lin, Z.; Tong, X.; Yang, D.; Shao, Y. Biomaterial-Based Fibrous Implantable Probes for Tissue-Electronics Interface. *Adv. Mater.* **2025**, *37*, 2504372.
(209) Cao, X.; Ye, C.; Cao, L.; Shan, Y.; Ren, J.; Ling, S. Biomimetic Spun Silk Ionotronic Fibers for Intelligent Discrimination of Motions and Tactile Stimuli. *Adv. Mater.* **2023**, *35* (36), 2300447.
(210) O'Neill, S. J.; Huang, Z.; Chen, X.; Sala, R. L.; McCune, J. A.; Malliaras, G. G.; Scherman, O. A. Highly Stretchable Dynamic Hydrogels for Soft Multilayer Electronics. *Science Advances* **2024**, *10* (29), No. eadn5142.
(211) Tropp, J.; Collins, C. P.; Xie, X.; Daso, R. E.; Mehta, A. S.; Patel, S. P.; Reddy, M. M.; Levin, S. E.; Sun, C.; Rivnay, J. Conducting Polymer Nanoparticles with Intrinsic Aqueous Dispersibility for Conductive Hydrogels. *Adv. Mater.* **2024**, *36* (1), 2306691.
(212) Peng, P.; Qian, H.; Yang, F.; Wei, D. Scalable, Light Rechargeable Energy Storage Based on Osmotic Effects and Photochemical Reactions in a Hair-Thin Filament. *Adv. Energy Mater.* **2025**, *15* (25), 2405547.
(213) Kovtyukhova, N.; Martin, B.; Mbindyo, J.; Mallouk, T.; Cabassi, M.; Mayer, T. Layer-by-Layer Self-Assembly Strategy for Template Synthesis of Nanoscale Devices. *Materials Science and Engineering: C* **2002**, *19* (1−2), 255.
(214) De Villiers, M. M.; Otto, D. P.; Strydom, S. J.; Lvov, Y. M. Introduction to Nanocoatings Produced by Layer-by-Layer (Lbl) Self-Assembly. *Adv. Drug Delivery Rev.* **2011**, *63* (9), 701.
(215) Tian, W.; VahidMohammadi, A.; Wang, Z.; Ouyang, L.; Beidaghi, M.; Hamedi, M. M. Layer-by-Layer Self-Assembly of Pillared Two-Dimensional Multilayers. *Nat. Commun.* **2019**, *10* (1), 2558.
(216) Zhu, Y.; Guo, Y.; Cao, K.; Zeng, S.; Jiang, G.; Liu, Y.; Cheng, W.; Bai, W.; Weng, X.; Chen, W.; et al. A General Strategy for Synthesizing Biomacromolecular Ionogel Membranes via Solvent-Induced Self-Assembly. *Nature Synthesis* **2023**, *2* (9), 864.
(217) Liu, M.; Zhang, L.; Rostami, J.; Zhang, T.; Matthews, K.; Chen, S.; Fan, W.; Zhu, Y.; Chen, J.; Huang, M.; et al. Tough Mxene-Cellulose Nanofibril Ionotronic Dual-Network Hydrogel Films for Stable Zinc Anodes. *ACS Nano* **2025**, *19* (13), 13399.
(218) Amoli, V.; Kim, J. S.; Jee, E.; Chung, Y. S.; Kim, S. Y.; Koo, J.; Choi, H.; Kim, Y.; Kim, D. H. A Bioinspired Hydrogen Bond-Triggered Ultrasensitive Ionic Mechanoreceptor Skin. *Nat. Commun.* **2019**, *10* (1), 4019.
(219) Abgrall, P.; Nguyen, N. T. Nanofluidic Devices and Their Applications. *Analytical chemistry* **2008**, *80* (7), 2326.
(220) Xiao, K.; Wen, L.; Jiang, L. Biomimetic Solid-State Nanochannels: From Fundamental Research to Practical Applications. *Small* **2016**, *12* (21), 2810.
(221) Huang, Y.; Zhang, W.; Xia, F.; Jiang, L. Solid-State Nanochannel-Based Sensing Systems: Development, Challenges, and Opportunities. *Langmuir* **2022**, *38* (8), 2415.
(222) Li, Y.; Wang, P.; Meng, C.; Chen, W.; Zhang, L.; Guo, S. A Brief Review of Miniature Flexible and Soft Tactile Sensors for Interventional Catheter Applications. *Soft Science* **2022**, *2*, 6.
(223) Chen, R.; Zhang, Z.; Deng, K.; Wang, D.; Ke, H.; Cai, L.; Chang, C.-w.; Pan, T. Blink-Sensing Glasses: A Flexible Iontronic Sensing Wearable for Continuous Blink Monitoring. *IScience* **2021**, *24* (5), 102399.
(224) Zhou, Y.; Morais-Cabral, J. H.; Kaufman, A.; MacKinnon, R. Chemistry of Ion Coordination and Hydration Revealed by a K^+ Channel−Fab Complex at 2.0 Å Resolution. *Nature* **2001**, *414* (6859), 43.
(225) Berneche, S.; Roux, B. Energetics of Ion Conduction through the K^+ Channel. *Nature* **2001**, *414* (6859), 73.
(226) Mironenko, A.; Zachariae, U.; de Groot, B. L.; Kopec, W. The Persistent Question of Potassium Channel Permeation Mechanisms. *J. Mol. Biol.* **2021**, *433* (17), 167002.
(227) Wang, Y.; Hu, Y.; Guo, J.-P.; Gao, J.; Song, B.; Jiang, L. A Physical Derivation of High-Flux Ion Transport in Biological Channel Via Quantum Ion Coherence. *Nat. Commun.* **2024**, *15* (1), 7189.
(228) Fragasso, A.; Schmid, S.; Dekker, C. Comparing Current Noise in Biological and Solid-State Nanopores. *ACS Nano* **2020**, *14* (2), 1338.
(229) Liang, S.; Xiang, F.; Tang, Z.; Nouri, R.; He, X.; Dong, M.; Guan, W. Noise in Nanopore Sensors: Sources, Models, Reduction, and Benchmarking. *Nanotechnology and Precision Engineering* **2020**, *3* (1), 9.
(230) Kellenberger, S.; Gautschi, I.; Schild, L. A Single Point Mutation in the Pore Region of the Epithelial Na^+ Channel Changes Ion Selectivity by Modifying Molecular Sieving. *Proc. Natl. Acad. Sci. U. S. A.* **1999**, *96* (7), 4170.
(231) Zhao, S.; Restrepo-Pérez, L.; Soskine, M.; Maglia, G.; Joo, C.; Dekker, C.; Aksimentiev, A. Electro-Mechanical Conductance Modulation of a Nanopore Using a Removable Gate. *ACS Nano* **2019**, *13* (2), 2398.
(232) Xiong, Y.; Han, J.; Wang, Y.; Wang, Z. L.; Sun, Q., Emerging Iontronic Sensing: Materials, Mechanisms, and Applications. Research *Research***2022**, *2022*, 9867378.
(233) Anderson, B. N.; Assad, O. N.; Gilboa, T.; Squires, A. H.; Bar, D.; Meller, A. Probing Solid-State Nanopores with Light for the Detection of Unlabeled Analytes. *ACS Nano* **2014**, *8* (11), 11836.
(234) Lee, K.; Park, K. B.; Kim, H. J.; Yu, J. S.; Chae, H.; Kim, H. M.; Kim, K. B. Recent Progress in Solid-State Nanopores. *Adv. Mater.* **2018**, *30* (42), 1704680.
(235) Yan, H.; Chen, T.; Hu, G.; Ma, J.; Wu, L.; Tu, J. A Long-Term Stable Solid-State Nanopore for the Dynamic Monitoring of DNA Synthesis. *Anal. Chim. Acta* **2025**, *1344*, 343710.
(236) Li, S.; Pan, N.; Zhu, Z.; Li, R.; Li, B.; Chu, J.; Li, G.; Chang, Y.; Pan, T. All-in-One Iontronic Sensing Paper. *Adv. Funct. Mater.* **2019**, *29* (11), 1807343.

(237) Sha, J.; Shi, H.; Zhang, Y.; Chen, C.; Liu, L.; Chen, Y. Salt Gradient Improving Signal-to-Noise Ratio in Solid-State Nanopore. *ACS Sensors* **2017**, *2* (4), 506.
(238) Lei, X.; Zhang, J.; Hong, H.; Yuan, Z.; Liu, Z. Controllable Shrinking Fabrication of Solid-State Nanopores. *Micromachines* **2022**, *13* (6), 923.
(239) Wanunu, M.; Meller, A. Chemically Modified Solid-State Nanopores. *Nano Lett.* **2007**, *7* (6), 1580.
(240) Wei, R.; Tampé, R.; Rant, U. Stochastic Sensing of Proteins with Receptor-Modified Solid-State Nanopores. *Biophys. J.* **2012**, *102* (3), 429a.
(241) Hu, R.; Tong, X.; Zhao, Q. Four Aspects About Solid-State Nanopores for Protein Sensing: Fabrication, Sensitivity, Selectivity, and Durability. *Adv. Healthcare Mater.* **2020**, *9* (17), 2000933.
(242) Abu Jalboush, S.; Wadsworth, I. D.; Sethi, K.; Rogers, L. C.; Hollis, T.; Hall, A. R. Improving the Performance of Selective Solid-State Nanopore Sensing Using a Polyhistidine-Tagged Monovalent Streptavidin. *ACS Sensors* **2024**, *9* (3), 1602.
(243) Adiga, S. P.; Jin, C.; Curtiss, L. A.; Monteiro-Riviere, N. A.; Narayan, R. J. Nanoporous Membranes for Medical and Biological Applications. *Wiley Interdisciplinary Reviews: Nanomedicine and Nanobiotechnology* **2009**, *1* (5), 568.
(244) Tang, Z.; Lu, B.; Zhao, Q.; Wang, J.; Luo, K.; Yu, D. Surface Modification of Solid-State Nanopores for Sticky-Free Translocation of Single-Stranded DNA. *Small* **2014**, *10* (21), 4332.
(245) Yang, L.; Hu, J.; Li, M. C.; Xu, M.; Gu, Z. Y. Solid-State Nanopores: Chemical Modifications, Interactions, and Functionalities. *Chemistry—An Asian Journal* **2022**, *17* (22), No. e202200775.
(246) Andersen, D. C.; Krummen, L. Recombinant Protein Expression for Therapeutic Applications. *Curr. Opin. Biotechnol.* **2002**, *13* (2), 117.
(247) Wurm, F. M. Production of Recombinant Protein Therapeutics in Cultivated Mammalian Cells. *Nature biotechnology* **2004**, *22* (11), 1393.
(248) Assenberg, R.; Wan, P. T.; Geisse, S.; Mayr, L. M. Advances in Recombinant Protein Expression for Use in Pharmaceutical Research. *Curr. Opin. Struct. Biol.* **2013**, *23* (3), 393.
(249) Gopal, G. J.; Kumar, A. Strategies for the Production of Recombinant Protein in Escherichia Coli. *protein journal* **2013**, *32*, 419.
(250) Rosano, G. L.; Ceccarelli, E. A. Recombinant Protein Expression in Escherichia Coli: Advances and Challenges. *Frontiers in microbiology* **2014**, *5*, 172.
(251) Ahmadi, A. G.; Nair, S. Geometry of Nanopore Devices Fabricated by Electron Beam Lithography: Simulations and Experimental Comparisons. *Microelectronic engineering* **2013**, *112*, 149.
(252) Zheng, H.; Liu, Y.; Cao, F.; Wu, S.; Jia, S.; Cao, A.; Zhao, D.; Wang, J. Electron Beam-Assisted Healing of Nanopores in Magnesium Alloys. *Sci. Rep.* **2013**, *3* (1), 1920.
(253) Kim, H.-M.; Park, K.-B.; Kim, H.-J.; Chae, H.; Yu, J.-S.; Lee, K.; Kim, K.-B. The Dynamics of Electron Beam Scattering on Metal Membranes: Nanopore Formation in Metal Membranes Using Transmission Electron Microscopy. *Nano Convergence* **2018**, *5*, 32.
(254) Kwok, H.; Briggs, K.; Tabard-Cossa, V. Nanopore Fabrication by Controlled Dielectric Breakdown. *PloS one* **2014**, *9* (3), No. e92880.
(255) Pud, S.; Verschueren, D.; Vukovic, N.; Plesa, C.; Jonsson, M. P.; Dekker, C. Self-Aligned Plasmonic Nanopores by Optically Controlled Dielectric Breakdown. *Nano Lett.* **2015**, *15* (10), 7112.
(256) Briggs, K.; Charron, M.; Kwok, H.; Le, T.; Chahal, S.; Bustamante, J.; Waugh, M.; Tabard-Cossa, V. Kinetics of Nanopore Fabrication During Controlled Breakdown of Dielectric Membranes in Solution. *Nanotechnology* **2015**, *26* (8), 084004.
(257) Schmidt, T.; Zhang, M.; Yu, S.; Linnros, J. Fabrication of Ultra-High Aspect Ratio Silicon Nanopores by Electrochemical Etching. *Appl. Phys. Lett.* **2014**, *105*, 123111.
(258) Chen, Q.; Wang, Y.; Deng, T.; Liu, Z. Fabrication of Nanopores and Nanoslits with Feature Sizes Down to 5 Nm by Wet Etching Method. *Nanotechnology* **2018**, *29* (8), 085301.
(259) Chen, Q.; Liu, Z. Fabrication and Applications of Solid-State Nanopores. *Sensors* **2019**, *19* (8), 1886.
(260) Abou Chaaya, A.; Le Poitevin, M.; Cabello-Aguilar, S.; Balme, S.; Bechelany, M.; Kraszewski, S.; Picaud, F.; Cambedouzou, J.; Balanzat, E.; Janot, J.-M.; et al. Enhanced Ionic Transport Mechanism by Gramicidin a Confined inside Nanopores Tuned by Atomic Layer Deposition. *J. Phys. Chem. C* **2013**, *117* (29), 15306.
(261) Cuevas, A. L.; Dominguez, A.; Zamudio-García, J.; Vega, V.; González, A. S.; Marrero-López, D.; Prida, V. M.; Benavente, J. Optical and Electrochemical Properties of a Nanostructured Zno Thin Layer Deposited on a Nanoporous Alumina Structure Via Atomic Layer Deposition. *Materials* **2024**, *17* (6), 1412.
(262) Bang, J.; Kim, S. H.; Drockenmuller, E.; Misner, M. J.; Russell, T. P.; Hawker, C. J. Defect-Free Nanoporous Thin Films from Abc Triblock Copolymers. *J. Am. Chem. Soc.* **2006**, *128* (23), 7622.
(263) Gong, B.; Shao, Z. Self-Assembling Organic Nanotubes with Precisely Defined, Sub-Nanometer Pores: Formation and Mass Transport Characteristics. *Acc. Chem. Res.* **2013**, *46* (12), 2856.
(264) Li, L.; Tian, W.; VahidMohammadi, A.; Rostami, J.; Chen, B.; Matthews, K.; Ram, F.; Pettersson, T.; Wågberg, L.; Benselfelt, T.; et al. Ultrastrong Ionotronic Films Showing Electrochemical Osmotic Actuation. *Adv. Mater.* **2023**, *35* (45), 2301163.
(265) Feng, Z.; He, Q.; Wang, X.; Qiu, J.; Wu, H.; Lin, Y.; Wu, Y.; Yang, J. Waterproof Iontronic Yarn for Highly Sensitive Biomechanical Strain Monitoring in Wearable Electronics. *Advanced Fiber Materials* **2024**, *6* (3), 925.
(266) Lu, H.; Zhang, Y.; Zhu, M.; Li, S.; Liang, H.; Bi, P.; Wang, S.; Wang, H.; Gan, L.; Wu, X.-E.; et al. Intelligent Perceptual Textiles Based on Ionic-Conductive and Strong Silk Fibers. *Nat. Commun.* **2024**, *15* (1), 3289.
(267) Chen, J.; Zhu, G.; Wang, J.; Chang, X.; Zhu, Y. Multifunctional Iontronic Sensor Based on Liquid Metal-Filled Ho Llow Ionogel Fibers in Detecting Pressure, Temperature, and Proximity. *ACS Appl. Mater. Interfaces* **2023**, *15* (5), 7485.
(268) Fang, L.; Zhou, Y.; Huang, Q. Ionic Conductive Textiles for Wearable Technology. *Adv. Mater.* **2025**, 2502140.
(269) Li, R.; Si, Y.; Zhu, Z.; Guo, Y.; Zhang, Y.; Pan, N.; Sun, G.; Pan, T. Supercapacitive Iontronic Nanofabric Sensing. *Adv. Mater.* **2017**, *29* (36), 1700253.
(270) Liu, Y.; Zhao, C.; Xiong, Y.; Yang, J.; Jiao, H.; Zhang, Q.; Cao, R.; Wang, Z. L.; Sun, Q. Versatile Ion-Gel Fibrous Membrane for Energy-Harvesting Iontronic Skin. *Adv. Funct. Mater.* **2023**, *33* (37), 2303723.
(271) Wang, S.; Yan, X.; Zhang, T.; Li, L.; Li, R.; Ramakrishna, S.; Long, Y. Z.; Han, W. All-Nanofiber Iontronic Sensor with Multiple Sensory Capabilities for Wearable Electronics. *Advanced Materials Technologies* **2024**, *9* (9), 2301791.
(272) Chhetry, A.; Kim, J.; Yoon, H.; Park, J. Y. Ultrasensitive Interfacial Capacitive Pressure Sensor Based on a Randomly Distributed Microstructured Iontronic Film for Wearable Applications. *ACS Appl. Mater. Interfaces* **2019**, *11* (3), 3438.
(273) Wu, R.; Hao, J.; Cui, Y.; Zhou, J.; Zhao, D.; Zhang, S.; Wang, J.; Zhou, Y.; Jiang, L. Multi-Control of Ion Transport in a Field-Effect Iontronic Device Based on Sandwich-Structured Nanochannels. *Adv. Funct. Mater.* **2023**, *33* (4), 2208095.
(274) Yuan, H.; Zhang, Q.; Cheng, Y.; Xu, R.; Li, H.; Tian, M.; Ma, J.; Jiao, T. Double-Sided Microstructured Flexible Iontronic Pressure Sensor with Wide Linear Sensing Range. *J. Colloid Interface Sci.* **2024**, *670*, 41.
(275) Zhang, F.; He, B.; Xin, Y.; Zhu, T.; Zhang, Y.; Wang, S.; Li, W.; Yang, Y.; Tian, H. Emerging Chemistry for Wide-Temperature Sodium-Ion Batteries. *Chem. Rev.* **2024**, *124* (8), 4778.
(276) Yang, K.; Li, B.; Ma, Z.; Xu, J.; Wang, D.; Zeng, Z.; Ho, D. Ion-Selective Mobility Differential Amplifier: Enhancing Pressure-Induced Voltage Response in Hydrogels. *Angew. Chem., Int. Ed.* **2025**, *64* (2), No. e202415000.
(277) Yin, A.; Chen, R.; Ning, J.; Luo, J.; Ren, Z.; Liu, H.; Meng, Y.; Wang, P.; Fan, S.; Qi, X.; et al. In-Situ Formed Quasi-Homogeneous Iontronic Sensors with Ultrawide Sensing Range for Human-Machine Interaction. *Chemical Engineering Journal* **2025**, *505*, 159139.

(278) Fried, J. P.; Swett, J. L.; Nadappuram, B. P.; Mol, J. A.; Edel, J. B.; Ivanov, A. P.; Yates, J. R. In Situ Solid-State Nanopore Fabrication. *Chem. Soc. Rev.* **2021**, *50* (8), 4974.
(279) Storm, A.; Chen, J.; Ling, X.; Zandbergen, H.; Dekker, C. Fabrication of Solid-State Nanopores with Single-Nanometre Precision. *Nature materials* **2003**, *2* (8), 537.
(280) Kox, R.; Chen, C.; Maes, G.; Lagae, L.; Borghs, G. Shrinking Solid-State Nanopores Using Electron-Beam-Induced Deposition. *Nanotechnology* **2009**, *20* (11), 115302.
(281) Kim, H.-M.; Lee, M.-H.; Kim, K.-B. Theoretical and Experimental Study of Nanopore Drilling by a Focused Electron Beam Intransmission Electron Microscopy. *Nanotechnology* **2011**, *22* (27), 275303.
(282) Goto, Y.; Yanagi, I.; Matsui, K.; Yokoi, T.; Takeda, K.-i. Integrated Solid-State Nanopore Platform for Nanopore Fabrication Via Dielectric Breakdown, DNA-Speed Deceleration and Noise Reduction. *Sci. Rep.* **2016**, *6* (1), 31324.
(283) Fang, S.; Yin, B.; Xie, W.; Zhou, D.; Tang, P.; He, S.; Yuan, J.; Wang, D. A Novel Dielectric Breakdown Apparatus for Solid-State Nanopore Fabrication with Transient High Electric Field. *Rev. Sci. Instrum.* **2020**, *91*, 093203.
(284) Waugh, M.; Briggs, K.; Gunn, D.; Gibeault, M.; King, S.; Ingram, Q.; Jimenez, A. M.; Berryman, S.; Lomovtsev, D.; Andrzejewski, L.; et al. Solid-State Nanopore Fabrication by Automated Controlled Breakdown. *Nat. Protoc.* **2020**, *15* (1), 122.
(285) Khan, M. S.; Williams, J. D. Fabrication of Solid State Nanopore in Thin Silicon Membrane Using Low Cost Multistep Chemical Etching. *Materials* **2015**, *8* (11), 7389.
(286) Yuan, Z.; Wang, C.; Yi, X.; Ni, Z.; Chen, Y.; Li, T. Solid-State Nanopore. *Nanoscale Res. Lett.* **2018**, *13*, 56.
(287) Wang, C.-M.; Kong, D.-L.; Chen, Q.; Xue, J.-M. Surface Engineering of Synthetic Nanopores by Atomic Layer Deposition and Their Applications. *Frontiers of Materials Science* **2013**, *7*, 335.
(288) Park, K.-B.; Kim, H.-J.; Kang, Y.-H.; Yu, J.-S.; Chae, H.; Lee, K.; Kim, H.-M.; Kim, K.-B. Highly Reliable and Low-Noise Solid-State Nanopores with an Atomic Layer Deposited Zno Membrane on a Quartz Substrate. *Nanoscale* **2017**, *9* (47), 18772.
(289) Liu, H.; Zhou, Q.; Wang, W.; Fang, F.; Zhang, J. Solid-State Nanopore Array: Manufacturing and Applications. *Small* **2023**, *19* (6), 2205680.
(290) Gualandi, C.; Zucchelli, A.; Fernández Osorio, M.; Belcari, J.; Focarete, M. L. Nanovascularization of Polymer Matrix: Generation of Nanochannels and Nanotubes by Sacrificial Electrospun Fibers. *Nano Lett.* **2013**, *13* (11), 5385.
(291) Nishimura, K.; Morimoto, Y.; Mori, N.; Takeuchi, S. Formation of Branched and Chained Alginate Microfibers Using Theta-Glass Capillaries. *Micromachines* **2018**, *9* (6), 303.
(292) Squires, A. H.; Hersey, J. S.; Grinstaff, M. W.; Meller, A. A Nanopore−Nanofiber Mesh Biosensor to Control DNA Translocation. *J. Am. Chem. Soc.* **2013**, *135* (44), 16304.
(293) Zhou, Q.; Xie, J.; Bao, M.; Yuan, H.; Ye, Z.; Lou, X.; Zhang, Y. Engineering Aligned Electrospun Plla Microfibers with Nano-Porous Surface Nanotopography for Modulating the Responses of Vascular Smooth Muscle Cells. *J. Mater. Chem. B* **2015**, *3* (21), 4439.
(294) Feng, T.; Liu, Y.; Lv, Y.; Shao, Y.; Niu, L.; Mi, D. Nanopore Structure of Pla@ Sf Aligned Composite Electrospun Fiber Membrane Enhances Growth Behavior of Peripheral Nerve Cells. *Frontiers in Materials* **2025**, *12*, 1570738.
(295) Cho, Y.; Beak, J. W.; Sagong, M.; Ahn, S.; Nam, J. S.; Kim, I. D. Electrospinning and Nanofiber Technology: Fundamentals, Innovations, and Applications. *Adv. Mater.* **2025**, *37*, 2500162.
(296) Joo, W.; Park, M. S.; Kim, J. K. Block Copolymer Film with Sponge-Like Nanoporous Strucutre for Antireflection Coating. *Langmuir* **2006**, *22* (19), 7960.
(297) Sun, M.; Han, K.; Hu, R.; Liu, D.; Fu, W.; Liu, W. Advances in Micro/Nanoporous Membranes for Biomedical Engineering. *Adv. Healthcare Mater.* **2021**, *10* (7), 2001545.
(298) Khattab, T. A.; Dacrory, S.; Abou-Yousef, H.; Kamel, S. Development of Microporous Cellulose-Based Smart Xerogel Reversible Sensor Via Freeze Drying for Naked-Eye Detection of Ammonia Gas. *Carbohydr. Polym.* **2019**, *210*, 196.
(299) Dang, W.; Wang, B.; Xu, Z.; Zhang, X.; Li, F.; Zhao, K.; Hu, X.; Tang, Y. Pore Structure, Thermal Insulation and Compressive Property of Zro2 Nanofiber Aerogels with Carbon Junction Fabricated by Freeze Drying. *J. Non-Cryst. Solids* **2023**, *600*, 122031.
(300) Jani, A. M. M.; Losic, D.; Voelcker, N. H. Nanoporous Anodic Aluminium Oxide: Advances in Surface Engineering and Emerging Applications. *Prog. Mater. Sci.* **2013**, *58* (5), 636.
(301) Lee, W.; Park, S.-J. Porous Anodic Aluminum Oxide: Anodization and Templated Synthesis of Functional Nanostructures. *Chem. Rev.* **2014**, *114* (15), 7487.
(302) Liu, S.; Tian, J.; Zhang, W. Fabrication and Application of Nanoporous Anodic Aluminum Oxide: A Review. *Nanotechnology* **2021**, *32* (22), 222001.
(303) Zhang, S.; Wang, J.; Yaroshchuk, A.; Du, Q.; Xin, P.; Bruening, M. L.; Xia, F. Addressing Challenges in Ion-Selectivity Characterization in Nanopores. *J. Am. Chem. Soc.* **2024**, *146* (16), 11036.
(304) Li, Q.; Zhao, Q.; Lu, B.; Zhang, H.; Liu, S.; Tang, Z.; Qu, L.; Zhu, R.; Zhang, J.; You, L.; et al. Size Evolution and Surface Characterization of Solid-State Nanopores in Different Aqueous Solutions. *Nanoscale* **2012**, *4* (5), 1572.
(305) Zhan, W.; Zhang, J.; Zhang, Q.; Ye, Z.; Li, B.; Zhang, C.; Yang, Z.; Xue, L.; Zhang, Z.; Ma, F.; et al. Flexible Iontronics with Super Stretchability, Toughness and Enhanced Conductivity Based on Collaborative Design of High-Entropy Topology and Multivalent Ion−Dipole Interactions. *Materials Horizons* **2024**, *11* (17), 4159.
(306) Xu, G.; Cui, H.; Wang, L.; Zhang, M.; Liu, W.; Mei, T.; Wu, B.; Wan, C.; Xiao, K. ÅngströM-Scale-Channel Iontronic Memristors for Neuromorphic Computing. *ACS Appl. Mater. Interfaces* **2025**, *17* (23), 34659−34668.
(307) Prete, D.; Colosimo, A.; Demontis, V.; Medda, L.; Zannier, V.; Bellucci, L.; Tozzini, V.; Sorba, L.; Beltram, F.; Pisignano, D.; et al. Heat-Driven Iontronic Nanotransistors. *Advanced Science* **2023**, *10* (7), 2204120.
(308) Wang, P.; Zhang, K.; Liao, J.; Wang, X.; Simon, G. P.; Liu, J. Z.; Li, D. Mesoscale Dynamics of Electrosorbed Ions in Fast-Charging Carbon-Based Nanoporous Electrodes. *Nat. Nanotechnol.* **2025**, *20*, 1228.
(309) Liao, J.; Wang, P.; Jiang, W. J.; Du, X.; Liu, J. Z.; Li, D. Unraveling the Impact of Electrosorbed Ions on the Scaling Behavior of Fast-Charging Dynamics of Nanoporous Electrodes toward Digital Design of Iontronic Devices. *Adv. Mater.* **2025**, *37*, 2506177.
(310) Sabbagh, B.; Fraiman, N. E.; Fish, A.; Yossifon, G. Designing with Iontronic Logic Gates− from a Single Polyelectrolyte Diode to an Integrated Ionic Circuit. *ACS Appl. Mater. Interfaces* **2023**, *15* (19), 23361.
(311) Li, J.; Fologea, D.; Rollings, R.; Ledden, B. Characterization of Protein Unfolding with Solid-State Nanopores. *Protein and Peptide Letters* **2014**, *21* (3), 256.
(312) Pang, Y.; Hu, X.; Wang, S.; Chen, S.; Soliman, M. Y.; Deng, H. Characterization of Adsorption Isotherm and Density Profile in Cylindrical Nanopores: Modeling and Measurement. *Chemical Engineering Journal* **2020**, *396*, 125212.
(313) Thommes, M.; Schlumberger, C. Characterization of Nanoporous Materials. *Annu. Rev. Chem. Biomol. Eng.* **2021**, *12* (1), 137.
(314) Hartel, A. J.; Shekar, S.; Ong, P.; Schroeder, I.; Thiel, G.; Shepard, K. L. High Bandwidth Approaches in Nanopore and Ion Channel Recordings-a Tutorial Review. *Anal. Chim. Acta* **2019**, *1061*, 13.
(315) Govorunova, E. G.; Sineshchekov, O. A.; Brown, L. S.; Spudich, J. L. Biophysical Characterization of Light-Gated Ion Channels Using Planar Automated Patch Clamp. *Frontiers in Molecular Neuroscience* **2022**, *15*, 976910.
(316) Obergrussberger, A.; Rinke-Weiß, I.; Goetze, T. A.; Rapedius, M.; Brinkwirth, N.; Becker, N.; Rotordam, M. G.; Hutchison, L.; Madau, P.; Pau, D.; et al. The Suitability of High Throughput Automated Patch Clamp for Physiological Applications. *Journal of Physiology* **2022**, *600* (2), 277.

https://doi.org/10.1021/acs.chemrev.5c00579
Chem. Rev. 2025, 125, 11840−11877

(317) Zhou, L.; Zhou, Y.; Baker, L. A. Measuring Ions with Scanning Ion Conductance Microscopy. *Electrochemical Society Interface* **2014**, *23* (2), 47.
(318) Page, A.; Perry, D.; Unwin, P. R. Multifunctional Scanning Ion Conductance Microscopy. *Proceedings of the Royal Society A: Mathematical, Physical and Engineering Sciences* **2017**, *473* (2200), 20160889.
(319) Takahashi, Y.; Ida, H.; Matsumae, Y.; Komaki, H.; Zhou, Y.; Kumatani, A.; Kanzaki, M.; Shiku, H.; Matsue, T. 3d Electrochemical and Ion Current Imaging Using Scanning Electrochemical−Scanning Ion Conductance Microscopy. *Phys. Chem. Chem. Phys.* **2017**, *19* (39), 26728.
(320) Zhu, C.; Huang, K.; Siepser, N. P.; Baker, L. A. Scanning Ion Conductance Microscopy. *Chem. Rev.* **2021**, *121* (19), 11726.
(321) Happel, P.; Thatenhorst, D.; Dietzel, I. D. Scanning Ion Conductance Microscopy for Studying Biological Samples. *Sensors* **2012**, *12* (11), 14983.
(322) Lab, M. J.; Bhargava, A.; Wright, P. T.; Gorelik, J. The Scanning Ion Conductance Microscope for Cellular Physiology. *American Journal of Physiology-Heart and Circulatory Physiology* **2013**, *304*, H1.
(323) Holzinger, A.; Neusser, G.; Austen, B. J.; Gamero-Quijano, A.; Herzog, G.; Arrigan, D. W.; Ziegler, A.; Walther, P.; Kranz, C. Investigation of Modified Nanopore Arrays Using FIB/SEM Tomography. *Faraday Discuss.* **2018**, *210*, 113.
(324) Chang, H.; Iqbal, S. M.; Stach, E. A.; King, A. H.; Zaluzec, N. J.; Bashir, R. Fabrication and Characterization of Solid-State Nanopores Using a Field Emission Scanning Electron Microscope. *Appl. Phys. Lett.* **2006**, *88*, 103109.
(325) Sajeer P, M.; Simran; Nukala, P.; Varma, M. M. Tem Based Applications in Solid State Nanopores: From Fabrication to Liquid in-Situ Bio-Imaging. *Micron* **2022**, *162*, 103347.
(326) Deng, D.; Yan, C.; Pan, X.; Mahfouz, M.; Wang, J.; Zhu, J.-K.; Shi, Y.; Yan, N. Structural Basis for Sequence-Specific Recognition of DNA by Tal Effectors. *Science* **2012**, *335* (6069), 720.
(327) Kurtjak, M.; Kereïche, S.; Klepac, D.; Križan, H.; Perčić, M.; Krušić Alić, V.; Lavrin, T.; Lenassi, M.; Wechtersbach, K.; Kojc, N.; et al. Unveiling the Native Morphology of Extracellular Vesicles from Human Cerebrospinal Fluid by Atomic Force and Cryogenic Electron Microscopy. *Biomedicines* **2022**, *10* (6), 1251.
(328) Wu, J.; Yan, Z.; Li, Z.; Qian, X.; Lu, S.; Dong, M.; Zhou, Q.; Yan, N. Structure of the Voltage-Gated Calcium Channel Cav1. 1 at 3.6 Å Resolution. *Nature* **2016**, *537* (7619), 191.
(329) Zhang, X.; Ren, W.; DeCaen, P.; Yan, C.; Tao, X.; Tang, L.; Wang, J.; Hasegawa, K.; Kumasaka, T.; He, J.; et al. Crystal Structure of an Orthologue of the Nachbac Voltage-Gated Sodium Channel. *Nature* **2012**, *486*, 130.
(330) Shen, H.; Zhou, Q.; Pan, X.; Li, Z.; Wu, J.; Yan, N. Structure of a Eukaryotic Voltage-Gated Sodium Channel at near-Atomic Resolution. *Science* **2017**, *355* (6328), No. eaal4326.
(331) Li, L.; Xu, S.; Li, X.; Gao, H.; Yang, L.; Jiang, C. Design of Microfluidic Fluorescent Sensor Arrays for Real-Time and Synchronously Visualized Detection of Multi-Component Heavy Metal Ions. *Chemical Engineering Journal* **2024**, *493*, 152636.
(332) Mei, X.; Zhou, L.; Zhu, L.; Wang, B. Composite Nanofiber Membrane-Based Microfluidic Fluorescence Sensors for Sweat Analysis. *Anal. Chem.* **2025**, *97* (1), 492.
(333) Meeseepong, M.; Ghosh, G.; Shrivastava, S.; Lee, N.-E. Fluorescence-Enhanced Microfluidic Biosensor Platform Based on Magnetic Beads with Highly Stable Zno Nanorods for Biomarker Detection. *ACS Appl. Mater. Interfaces* **2023**, *15* (18), 21754.
(334) Lu, S.-Y.; Tseng, C.-C.; Yu, C.-X.; Chen, T.-L.; Huang, K.-H.; Fu, L.-M.; Wu, P.-H. Rapid Microfluidic Fluorescence Detection Platform for Determination of Whole Blood Sodium. *Sens. Actuators, B* **2024**, *400*, 134839.
(335) Liu, X.; Song, D.; He, X.; Wang, Z.; Zeng, M.; Deng, K. Nanopore Structure of Deep-Burial Coals Explored by AFM. *Fuel* **2019**, *246*, 9.
(336) Si, W.; Yang, H.; Li, K.; Wu, G.; Zhang, Y.; Kan, Y.; Xie, X.; Sha, J.; Liu, L.; Chen, Y. Investigation on the Interaction Length and Access Resistance of a Nanopore with an Atomic Force Microscopy. *Science China Technological Sciences* **2017**, *60*, 552.
(337) Zhang, Y.; Chen, X.; Chen, D.; Yao, Z.; Xu, S.; McArdle, P.; Qazilbash, M. M.; Liu, M. Partially Metal-Coated Tips for near-Field Nanospectroscopy. *Physical Review Applied* **2021**, *15* (1), 014048.
(338) Meyer, R. L.; Zhou, X.; Tang, L.; Arpanaei, A.; Kingshott, P.; Besenbacher, F. Immobilisation of Living Bacteria for Afm Imaging under Physiological Conditions. *Ultramicroscopy* **2010**, *110* (11), 1349.
(339) Trewby, W.; Voïtchovsky, K. Nanoscale Probing of Local Dielectric Changes at the Interface between Solids and Aqueous Saline Solutions. *Faraday Discuss.* **2023**, *246*, 387.
(340) Siretanu, I.; van Lin, S. R.; Mugele, F. Ion Adsorption and Hydration Forces: A Comparison of Crystalline Mica Vs. Amorphous Silica Surfaces. *Faraday Discuss.* **2023**, *246*, 274.
(341) Luo, J.; Sun, C.; Chang, B.; Jing, Y.; Li, K.; Li, Y.; Zhang, Q.; Wang, H.; Hou, C. Mxene-Enabled Self-Adaptive Hydrogel Interface for Active Electroencephalogram Interactions. *ACS Nano* **2022**, *16* (11), 19373.
(342) Boahen, E. K.; Kim, J. H.; Choi, H.; Kong, Z.; Kim, D. H. Interfacial Iontronics in Bioelectronics: From Skin-Attachable to Implantable Devices. *Korean Journal of Chemical Engineering* **2025**, *42*, 1993.
(343) Luo, J.; Jin, Y.; Li, L.; Chang, B.; Zhang, B.; Li, K.; Li, Y.; Zhang, Q.; Wang, H.; Wang, J.; et al. A Selective Frequency Damping and Janus Adhesive Hydrogel as Bioelectronic Interfaces for Clinical Trials. *Nat. Commun.* **2024**, *15*, 8478.
(344) Gu, C.; Kong, F.; Liang, S.; Zhao, X.; Kong, B.; Jiang, T.; Yu, J.; Li, Q.; Lin, Y.; Bai, S.; et al. In Vivo Dynamic Tracking of Cerebral Chloride Regulation Using Molecularly Tailored Liquid/Liquid Interfacial Ultramicro Iontronics. *Science Advances* **2024**, *10* (49), No. eadr7218.
(345) Liu, Z.; Wang, Y.; Ren, Y.; Jin, G.; Zhang, C.; Chen, W.; Yan, F. Poly (Ionic Liquid) Hydrogel-Based Anti-Freezing Ionic Skin for a Soft Robotic Gripper. *Materials Horizons* **2020**, *7* (3), 919.
(346) Luo, J.; Xing, Y.; Sun, C.; Fan, L.; Shi, H.; Zhang, Q.; Li, Y.; Hou, C.; Wang, H. A Bio-Adhesive Ion-Conducting Organohydrogel as a High-Performance Non-Invasive Interface for Bioelectronics. *Chemical Engineering Journal* **2022**, *427*, 130886.
(347) Xia, J.; Luo, J.; Chang, B.; Sun, C.; Li, K.; Zhang, Q.; Li, Y.; Wang, H.; Hou, C. High-Performance Zwitterionic Organohydrogel Fiber in Bioelectronics for Monitoring Bioinformation. *Biosensors* **2023**, *13* (1), 115.
(348) Ling, Y.; Li, L.; Liu, J.; Li, K.; Hou, C.; Zhang, Q.; Li, Y.; Wang, H. Air-Working Electrochromic Artificial Muscles. *Adv. Mater.* **2024**, *36* (5), 2305914.
(349) Xu, R.; She, M.; Liu, J.; Zhao, S.; Zhao, J.; Zhang, X.; Qu, L.; Tian, M. Skin-Friendly and Wearable Iontronic Touch Panel for Virtual-Real Handwriting Interaction. *ACS Nano* **2023**, *17* (9), 8293.
(350) Peng, P.; Shen, P.; Qian, H.; Liu, J.; Lu, H.; Jiao, Y.; Yang, F.; Liu, H.; Ren, T.; Wang, Z.; et al. Photochemical Iontronics with Multitype Ionic Signal Transmission at Single Pixel for Self-Driven Color and Tridimensional Vision. *Device* **2025**, *3* (3), 100574.
(351) Ouyang, Y.; Li, X.; Li, S.; Peng, P.; Yang, F.; Wang, Z. L.; Wei, D. Opto-Iontronic Coupling in Triboelectric Nanogenerator. *Nano Energy* **2023**, *116*, 108796.
(352) Ouyang, Y.; Li, X.; Li, S.; Wang, Z. L.; Wei, D. Ionic Rectification by Dynamic Regulation of the Electric Double Layer at the Hydrogel Interface. *ACS Appl. Mater. Interfaces* **2024**, *16* (14), 18236.
(353) Lee, C. M.; Kim, Y.; Kim, W.; Lee, E.; Lee, E. K. High-Performance Synaptic Devices Based on Cross-Linked Organic Electrochemical Transistors with Dual Ion Gel. *Adv. Funct. Mater.* **2025**, *35* (12), 2417539.
(354) Xiong, T.; Li, C.; He, X.; Xie, B.; Zong, J.; Jiang, Y.; Ma, W.; Wu, F.; Fei, J.; Yu, P.; et al. Neuromorphic Functions with a Polyelectrolyte-Confined Fluidic Memristor. *Science* **2023**, *379* (6628), 156.
(355) Huang, Z.; Mei, T.; Zhu, X.; Xiao, K. Ionic Device: From Neuromorphic Computing to Interfacing with the Brain. *Chemistry−An Asian Journal* **2025**, *20* (7), No. e202401170.

https://doi.org/10.1021/acs.chemrev.5c00579
Chem. Rev. 2025, 125, 11840−11877

(356) Wei, X.; Wu, Z.; Gao, H.; Cao, S.; Meng, X.; Lan, Y.; Su, H.; Qin, Z.; Liu, H.; Du, W.; et al. Mechano-Gated Iontronic Piezomemristor for Temporal-Tactile Neuromorphic Plasticity. *Nat. Commun.* **2025**, *16* (1), 1060.
(357) Feng, P.; Du, P.; Wan, C.; Shi, Y.; Wan, Q. Proton Conducting Graphene Oxide/Chitosan Composite Electrolytes as Gate Dielectrics for New-Concept Devices. *Sci. Rep.* **2016**, *6* (1), 34065.
(358) Wang, S.; Chen, X.; Zhao, C.; Kong, Y.; Lin, B.; Wu, Y.; Bi, Z.; Xuan, Z.; Li, T.; Li, Y.; et al. An Organic Electrochemical Transistor for Multi-Modal Sensing, Memory and Processing. *Nature Electronics* **2023**, *6* (4), 281.
(359) Jang, H.; Lee, J.; Beak, C. J.; Biswas, S.; Lee, S. H.; Kim, H. Flexible Neuromorphic Electronics for Wearable near-Sensor and in-Sensor Computing Systems. *Adv. Mater.* **2025**, *37*, 2416073.
(360) Zhu, X.; Li, D.; Liang, X.; Lu, W. D. Ionic Modulation and Ionic Coupling Effects in Mos2 Devices for Neuromorphic Computing. *Nat. Mater.* **2019**, *18* (2), 141.
(361) Chen, S.; Zhou, Z.; Hou, K.; Wu, X.; He, Q.; Tang, C. G.; Li, T.; Zhang, X.; Jie, J.; Gao, Z.; et al. Artificial Organic Afferent Nerves Enable Closed-Loop Tactile Feedback for Intelligent Robot. *Nat. Commun.* **2024**, *15* (1), 7056.
(362) Kim, Y.; Chortos, A.; Xu, W.; Liu, Y.; Oh, J. Y.; Son, D.; Kang, J.; Foudeh, A. M.; Zhu, C.; Lee, Y.; et al. A Bioinspired Flexible Organic Artificial Afferent Nerve. *Science* **2018**, *360* (6392), 998.
(363) Goodenough, J. B. How We Made the Li-Ion Rechargeable Battery. *Nature Electronics* **2018**, *1* (3), 204.
(364) Konarov, A.; Voronina, N.; Jo, J. H.; Bakenov, Z.; Sun, Y.-K.; Myung, S.-T. Present and Future Perspective on Electrode Materials for Rechargeable Zinc-Ion Batteries. *ACS Energy Letters* **2018**, *3* (10), 2620.
(365) Stettner, T.; Balducci, A. Protic Ionic Liquids in Energy Storage Devices: Past, Present and Future Perspective. *Energy Storage Materials* **2021**, *40*, 402.
(366) Yuan, T.; Tan, Z.; Ma, C.; Yang, J.; Ma, Z. F.; Zheng, S. Challenges of Spinel Li4ti5o12 for Lithium-Ion Battery Industrial Applications. *Adv. Energy Mater.* **2017**, *7* (12), 1601625.
(367) He, C.; Sun, J.; Hou, C.; Zhang, Q.; Li, Y.; Li, K.; Wang, H. Sandwich-Structural Ionogel Electrolyte with Core−Shell Ionic-Conducting Nanocomposites for Stable Li Metal Battery. *Chemical Engineering Journal* **2023**, *451*, 138993.
(368) He, P.; Park, J. H.; Jiao, Y.; Ganguli, R.; Huang, Y.; Lee, A.; Ahn, C. H.; Wang, M.; Peng, Y.; Long, Y.; et al. High-Voltage Water-Scarce Hydrogel Electrolytes Enable Mechanically Safe Stretchable Li-Ion Batteries. *Science Advances* **2025**, *11* (15), No. eadu3711.
(369) Wang, W.; Kale, V. S.; Cao, Z.; Kandambeth, S.; Zhang, W.; Ming, J.; Parvatkar, P. T.; Abou-Hamad, E.; Shekhah, O.; Cavallo, L.; et al. Phenanthroline Covalent Organic Framework Electrodes for High-Performance Zinc-Ion Supercapattery. *ACS Energy Letters* **2020**, *5* (7), 2256.
(370) Fan, W.; Wang, F.; Xiong, X.; Song, B.; Wang, T.; Cheng, X.; Zhu, Z.; He, J.; Liu, Y.; Wu, Y. Recent Advances in Functional Materials and Devices for Zn-Ion Hybrid Supercapacitors. *NPG Asia Materials* **2024**, *16* (1), 18.
(371) Wang, Y.; Wang, X.; Li, X.; Bai, Y.; Xiao, H.; Liu, Y.; Liu, R.; Yuan, G. Engineering 3d Ion Transport Channels for Flexible Mxene Films with Superior Capacitive Performance. *Adv. Funct. Mater.* **2019**, *29* (14), 1900326.
(372) Ye, J.; Simon, P.; Zhu, Y. Designing Ionic Channels in Novel Carbons for Electrochemical Energy Storage. *National Science Review* **2020**, *7* (1), 191.
(373) Wei, D.; Yang, F.; Jiang, Z.; Wang, Z. Flexible Iontronics Based on 2d Nanofluidic Material. *Nat. Commun.* **2022**, *13* (1), 4965.
(374) Qian, H.; Peng, P.; Fan, H.; Yang, Z.; Yang, L.; Zhou, Y.; Tan, D.; Yang, F.; Willatzen, M.; Amaratunga, G.; et al. Horizontal Transport in Ti3c2tx Mxene for Highly Efficient Osmotic Energy Conversion from Saline-Alkali Environments. *Angew. Chem., Int. Ed.* **2024**, *63* (48), No. e202414984.
(375) Yang, F.; Peng, P.; Yan, Z.-Y.; Fan, H.; Li, X.; Li, S.; Liu, H.; Ren, T.-L.; Zhou, Y.; Wang, Z. L.; et al. Vertical Iontronic Energy Storage Based on Osmotic Effects and Electrode Redox Reactions. *Nature Energy* **2024**, *9* (3), 263.
(376) Yang, L.; Yang, F.; Liu, X.; Li, K.; Zhou, Y.; Wang, Y.; Yu, T.; Zhong, M.; Xu, X.; Zhang, L.; et al. A Moisture-Enabled Fully Printable Power Source Inspired by Electric Eels. *Proc. Natl. Acad. Sci. U. S. A.* **2021**, *118* (16), No. e2023164118.
(377) Park, T. H.; Kim, B.; Yu, S.; Park, Y.; Oh, J. W.; Kim, T.; Kim, N.; Kim, Y.; Zhao, D.; Khan, Z. U.; et al. Ionoelastomer Electrolytes for Stretchable Ionic Thermoelectric Supercapacitors. *Nano Energy* **2023**, *114*, 108643.
(378) Zhang, Y.; Zhou, Z.; Sun, L.; Liu, Z.; Xia, X.; Tao, T. H. "Genetically Engineered" Biofunctional Triboelectric Nanogenerators Using Recombinant Spider Silk. *Adv. Mater.* **2018**, *30* (50), 1805722.
(379) Huang, T.; Zhang, Y.; He, P.; Wang, G.; Xia, X.; Ding, G.; Tao, T. H. "Self-Matched" Tribo/Piezoelectric Nanogenerators Using Vapor-Induced Phase-Separated Poly(Vinylidene Fluoride) and Recombinant Spider Silk. *Adv. Mater.* **2020**, *32* (10), 1907336.
(380) Parida, K.; Kumar, V.; Jiangxin, W.; Bhavanasi, V.; Bendi, R.; Lee, P. S. Highly Transparent, Stretchable, and Self-Healing Ionic-Skin Triboelectric Nanogenerators for Energy Harvesting and Touch Applications. *Adv. Mater.* **2017**, *29* (37), 1702181.
(381) Xiao, K.; Chen, L.; Chen, R.; Heil, T.; Lemus, S. D. C.; Fan, F.; Wen, L.; Jiang, L.; Antonietti, M. Artificial Light-Driven Ion Pump for Photoelectric Energy Conversion. *Nat. Commun.* **2019**, *10* (1), 74.
(382) Sears, M. E.; Kerr, K. J.; Bray, R. I. Arsenic, Cadmium, Lead, and Mercury in Sweat: A Systematic Review. *Journal of environmental and public health* **2012**, *2012* (1), 184745.
(383) Roozbahani, G. M.; Chen, X.; Zhang, Y.; Wang, L.; Guan, X. Nanopore Detection of Metal Ions: Current Status and Future Directions. *Small Methods* **2020**, *4* (10), 2000266.
(384) Braha, O.; Gu, L.-Q.; Zhou, L.; Lu, X.; Cheley, S.; Bayley, H. Simultaneous Stochastic Sensing of Divalent Metal Ions. *Nat. Biotechnol.* **2000**, *18* (9), 1005.
(385) Roozbahani, G. M.; Chen, X.; Zhang, Y.; Juarez, O.; Li, D.; Guan, X. Computation-Assisted Nanopore Detection of Thorium Ions. *Analytical chemistry* **2018**, *90* (9), 5938.
(386) Dushyantha, N.; Batapola, N.; Ilankoon, I.; Rohitha, S.; Premasiri, R.; Abeysinghe, B.; Ratnayake, N.; Dissanayake, K. The Story of Rare Earth Elements (Rees): Occurrences, Global Distribution, Genesis, Geology, Mineralogy and Global Production. *Ore Geology Reviews* **2020**, *122*, 103521.
(387) Sun, W.; Xiao, Y.; Wang, K.; Zhang, S.; Yao, L.; Li, T.; Cheng, B.; Zhang, P.; Huang, S. Nanopore Discrimination of Rare Earth Elements. *Nat. Nanotechnol.* **2025**, *20* (4), 523.
(388) Aliasgharpour, M.; Rahnamaye Farzami, M. Trace Elements in Human Nutrition: A Review. *International Journal of Medical Investigation* **2013**, *2* (3), 115.
(389) Liu, Q.; Xiao, K.; Wen, L.; Dong, Y.; Xie, G.; Zhang, Z.; Bo, Z.; Jiang, L. A Fluoride-Driven Ionic Gate Based on a 4-Amino-phenylboronic Acid-Functionalized Asymmetric Single Nanochannel. *ACS Nano* **2014**, *8* (12), 12292.
(390) Wang, P.; Wang, M.; Liu, F.; Ding, S.; Wang, X.; Du, G.; Liu, J.; Apel, P.; Kluth, P.; Trautmann, C.; et al. Ultrafast Ion Sieving Using Nanoporous Polymeric Membranes. *Nat. Commun.* **2018**, *9* (1), 569.
(391) Tian, M.; Liu, Y.; Zhang, S.; Yu, C.; Ostrikov, K.; Zhang, Z. Overcoming the Permeability-Selectivity Challenge in Water Purification Using Two-Dimensional Cobalt-Functionalized Vermiculite Membrane. *Nat. Commun.* **2024**, *15* (1), 391.
(392) Tunuguntla, R. H.; Henley, R. Y.; Yao, Y.-C.; Pham, T. A.; Wanunu, M.; Noy, A. Enhanced Water Permeability and Tunable Ion Selectivity in Subnanometer Carbon Nanotube Porins. *Science* **2017**, *357* (6353), 792.
(393) Murata, K.; Mitsuoka, K.; Hirai, T.; Walz, T.; Agre, P.; Heymann, J. B.; Engel, A.; Fujiyoshi, Y. Structural Determinants of Water Permeation through Aquaporin-1. *Nature* **2000**, *407* (6804), 599.
(394) Zhao, C.; Zhang, Y.; Jia, Y.; Li, B.; Tang, W.; Shang, C.; Mo, R.; Li, P.; Liu, S.; Zhang, S. Polyamide Membranes with Nanoscale

Ordered Structures for Fast Permeation and Highly Selective Ion-Ion Separation. *Nat. Commun.* **2023**, *14* (1), 1112.
(395) Huang, J.; Zhang, Y.; Guo, J.; Yang, F.; Ma, J.; Bai, Y.; Shao, L.; Liu, S.; Wang, H. Polymeric Membranes with Highly Homogenized Nanopores for Ultrafast Water Purification. *Nature Sustainability* **2024**, *7* (7), 901.
(396) Hube, S.; Eskafi, M.; Hrafnkelsdóttir, K. F.; Bjarnadóttir, B.; Bjarnadóttir, M. Á.; Axelsdóttir, S.; Wu, B. Direct Membrane Filtration for Wastewater Treatment and Resource Recovery: A Review. *Sci. Total Environ.* **2020**, *710*, 136375.
(397) Yang, D.; Yang, Y.; Wong, T.; Iguodala, S.; Wang, A.; Lovell, L.; Foglia, F.; Fouquet, P.; Breakwell, C.; Fan, Z.; et al. Solution-Processable Polymer Membranes with Hydrophilic Subnanometre Pores for Sustainable Lithium Extraction. *Nature Water* **2025**, *3* (3), 319.
(398) Uliana, A. A.; Bui, N. T.; Kamcev, J.; Taylor, M. K.; Urban, J. J.; Long, J. R. Ion-Capture Electrodialysis Using Multifunctional Adsorptive Membranes. *Science* **2021**, *372* (6539), 296.
(399) Wang, S.; Song, W.; Liu, E.; Zhao, P.; Ng, H. Y.; Wang, X. Efficient, Facile and Recyclable Coating Strategy to Improve Heavy Metals Removal by Uf Membrane in Drinking Water Purification. *Sep. Purif. Technol.* **2025**, *363*, 131995.
(400) Mi, B. Graphene Oxide Membranes for Ionic and Molecular Sieving. *Science* **2014**, *343* (6172), 740.
(401) Kuehl, V. A.; Yin, J.; Duong, P. H.; Mastorovich, B.; Newell, B.; Li-Oakey, K. D.; Parkinson, B. A.; Hoberg, J. O. A Highly Ordered Nanoporous, Two-Dimensional Covalent Organic Framework with Modifiable Pores, and Its Application in Water Purification and Ion Sieving. *J. Am. Chem. Soc.* **2018**, *140* (51), 18200.
(402) Ding, L.; Li, L.; Liu, Y.; Wu, Y.; Lu, Z.; Deng, J.; Wei, Y.; Caro, J.; Wang, H. Effective Ion Sieving with Ti3c2t X Mxene Membranes for Production of Drinking Water from Seawater. *Nature Sustainability* **2020**, *3* (4), 296.
(403) Han, C.; Jiang, J.; Mu, L.; Zhao, W.; Liu, J.; Lan, J.; Hu, S.; Yang, H.; Gao, S.; Zhou, F.; et al. Quasi-Vertically Asymmetric Channels of Graphene Oxide Membrane for Ultrafast Ion Sieving. *Nat. Commun.* **2025**, *16* (1), 1020.
(404) Liu, S.-H.; Shi, W.; Hung, W.-S.; Shi, L.; Xue, B.; She, J.; Song, Z.; Lu, X.; Gray, S.; Lee, K.-R.; et al. Interfacial Self-Organization of Large-Area Mixed-Dimensional Polyamide Membranes for Rapid Aqueous Nanofiltration. *Nature Water* **2024**, *2* (12), 1238.
(405) Polachan, K.; Chatterjee, B.; Weigand, S.; Sen, S. Human Body−Electrode Interfaces for Wide-Frequency Sensing and Communication: A Review. *Nanomaterials* **2021**, *11* (8), 2152.
(406) Choi, C.; Ashby, D. S.; Butts, D. M.; DeBlock, R. H.; Wei, Q.; Lau, J.; Dunn, B. Achieving High Energy Density and High Power Density with Pseudocapacitive Materials. *Nature Reviews Materials* **2020**, *5* (1), 5.
(407) Liu, Y.; Wang, J.; Chen, J.; Yuan, Q.; Zhu, Y. Ultrasensitive Iontronic Pressure Sensor Based on Rose-Structured Ionogel Dielectric Layer and Compressively Porous Electrodes. *Advanced Composites and Hybrid Materials* **2023**, *6* (6), 210.
(408) Kwon, J. H.; Kim, Y. M.; Moon, H. C. Porous Ion Gel: A Versatile Ionotronic Sensory Platform for High-Performance, Wearable Ionoskins with Electrical and Optical Dual Output. *ACS Nano* **2021**, *15* (9), 15132.
(409) Li, F.; Wang, H.; Gu, J.; Zhu, G.; Wu, P.; Zhang, Q.; Ji, X.; Liang, J. An Iontronic Fiber Pressure Sensor with Hierarchical Porous Architecture Exhibiting High Sensitivity across a Broad Range. *Nano Lett.* **2025**, *25*, 10919.
(410) Shin, J. H.; Choi, J. Y.; June, K.; Choi, H.; Kim, T. i. Polymeric Conductive Adhesive-Based Ultrathin Epidermal Electrodes for Long-Term Monitoring of Electrophysiological Signals. *Adv. Mater.* **2024**, *36*, 2313157.
(411) Ricotti, L.; Trimmer, B.; Feinberg, A. W.; Raman, R.; Parker, K. K.; Bashir, R.; Sitti, M.; Martel, S.; Dario, P.; Menciassi, A. Biohybrid Actuators for Robotics: A Review of Devices Actuated by Living Cells. *Science Robotics* **2017**, *2* (12), No. eaaq0495.
(412) Jin, Y.; Mikhailova, E.; Lei, M.; Cowley, S. A.; Sun, T.; Yang, X.; Zhang, Y.; Liu, K.; Catarino da Silva, D.; Campos Soares, L.; et al. Integration of 3D-Printed Cerebral Cortical Tissue into an ex vivo Lesioned Brain Slice. *Nat. Commun.* **2023**, *14* (1), 5986.
(413) Rochford, A. E.; Carnicer-Lombarte, A.; Curto, V. F.; Malliaras, G. G.; Barone, D. G. When Bio Meets Technology: Biohybrid Neural Interfaces. *Adv. Mater.* **2020**, *32* (15), 1903182.

https://doi.org/10.1021/acs.chemrev.5c00579
Chem. Rev. 2025, 125, 11840−11877